2014-01-01

Characterization of NS1 SUMOylation and Its Effect on Influenza A Viral Infection

Katherine Anne Meraz
University of Texas at El Paso, kamaguire@miners.utep.edu

CHARACTERIZATION OF NS1 SUMOYLATION AND ITS EFFECT ON INFLUENZA A VIRAL INFECTION

KATHERINE ANNE MERAZ

Department of Biological Sciences

APPROVED:

German Rosas-Acosta, Ph.D., Chair

Kristine Garza, Ph.D.

Manuel Llano, Ph.D.

William Robertson, Ph.D.

Charles Ambler, Ph.D.
Dean of the Graduate School

DEDICATION

This dissertation is dedicated to my parents, husband, family and friends, and mentor who have continuously supported me.

CHARACTERIZATION OF NS1 SUMOYLATION AND ITS EFFECT ON INFLUENZA A VIRAL INFECTION

by

KATHERINE ANNE MERAZ, B.S.

DISSERTATION

Presented to the Faculty of the Graduate School of

The University of Texas at El Paso

in Partial Fulfillment

of the Requirements

for the Degree of

DOCTOR OF PHILOSOPHY

Department of Biological Sciences

THE UNIVERSITY OF TEXAS AT EL PASO

August 2014

ACKNOWLEDGEMENTS

To my mentor, Dr. German Rosas-Acosta, thank you for taking a chance on a stranger. You accepted me into your lab knowing only a little about me and now you have become more than a mentor, you have become my friend. I want to thank you for teaching me to be true to myself and stand up for myself and all that I have achieved. I would also like to thank my committee members, Dr. Kristine Garza, Dr. Manuel Llano, and Dr. William Robertson for pushing me to be better than I ever thought that I could be, and also to my advocate, Dr. Kyle L. Johnson, for not only introducing me into the fascinating world of viruses, but for supporting me throughout this amazing journey.

I am grateful to the faculty, staff, and students in the Department of Biological Sciences for helping me grow as a student and a researcher. I am very appreciative to the personnel of the core facilities and office staff for their assistance over the course of the last few years.

I would to thank Dr. Aaron Velasco, Dr. Vanessa Lougheed, Dr. William Robertson, and Mrs. Cynthia Ramirez for the opportunity to be a part of the GK-12 program and their continued support throughout my graduate career. To Mr. Walter Ray and Dr. Samuel Hogue, thank you for allowing me to become part of the Cotton Valley Early College High School family; it has been delightful to spend the last two years with you.

I would like to thank all of the members of the Rosas-Acosta lab, past and present, for paving the road that I was given the opportunity to follow. I am indebted to the members who directly contributed to this work: Jourdan Harper, Beu Oropeza, Reena

Beggs, David Quintanar, Theresa Rodriguez, Jeanette Gonzalez, Victoria Phillips, Isabel Lopez, Daniel Ramirez, and Jason Chacon. Thank you for giving me the honor to work with and learn from you. To Jeanette Gonzalez and Lorellie Frydenlund, I am greatly appreciative for the time that you have contributed to my overall well-being. Thank you for being great friends and always willing to help out. Additionally, I would like to thank Jessica Valles, Karla Prieto, Alejandra Navarro, and Andres Santos for their support.

Thank you to Griselda Melendez, Angelica Lopez, and Steven Martinez for being my cheering section over the last few years. You all have been there for me and become like family to me. I look forward to the many years and memories ahead of us.

I want to thank my parents, Richard and Rosemarie Labs, for their continued support and belief that I can achieve anything I set my mind to. You both have helped mold me into the person I am today and have always pushed me to prove to the world what I am truly capable of. Thank you to the rest of my family for your support and love. I am truly blessed to have you all in my life.

Foremost, I would like to thank my husband, Jesus Adrian Meraz, who has made all of this possible. You have provided me the opportunity to accomplish this dream. Thank you for your endless support, continued understanding, and unconditional love throughout this process.

ABSTRACT

Influenza virus is a contagious respiratory virus responsible for seasonal epidemics and several catastrophic pandemics in the last century. Its genome is comprised of negative sense, single-stranded RNA and, after entering the cell, it is capable of hijacking the host cellular machinery for reproducing its own genetic material. The activation of cellular defenses against influenza viral infection are triggered upon viral entry and help regulate the course of viral infection. This study focused on the interplay between the influenza A virus and the cellular SUMOylation system during viral infection. The first part of this dissertation deals with the relevance of NS1 SUMOylation during viral infection. We demonstrate that in studies performed in an animal model, infection with viruses containing a non-SUMOylatable NS1 resulted in increased clinical symptoms, morbidity, and mortality. Furthermore, the inhibition of NS1 SUMOylation enabled viral replication in a broad range of organs and increased pathology of influenza viral infection. Together, these results suggest that NS1 SUMOylation may be a factor contributing to the regulation of viral pathogenicity. The second part of this dissertation deals with NS1‘s role in triggering an increase in cellular SUMOylation. We show that the ability of NS1 to be SUMOylated directly correlates to its ability to trigger a global increase in cellular SUMOylation. Furthermore, we show that infection with vaccinia virus and lymphocyctic choriomeningitis virus are also able to trigger a less dramatic, but still detectable, increase in global cellular SUMOylation. Together, these results suggest that increases in cellular SUMOylation are frequently triggered by viral infection and may be a component of the cellular protective responses against viral infection. The last part of this dissertation deals with the evaluation of a novel fusion

protein capable of specifically increasing the SUMOylation of NS1 (known as $NS1_{(1-87)}$-Ubc9) as a potential therapeutic agent against influenza viral infection. Our results indicate that the two methods used to deliver the $NS1_{(1-87)}$-Ubc9 artificial SUMO ligase are effective. Overall, our results suggest that the global increase in cellular SUMOylation, which is associated with NS1 SUMOylation, may constitute a defense mechanism mounted by the host to inhibit the progression of influenza viral infection.

TABLE OF CONTENTS

LIST OF TABLES

LIST OF FIGURES

CHAPTER 1: INTRODUCTION

1.1 Influenza and its impact on human health

Influenza infections affect 5 to 20% of the population and causes an average of 52,000 deaths and 1.68 million hospitalizations each year in the United States alone with almost half of those cases being reported in children under the age of four and adults over the age of sixty-five (Lowen, Mubareka et al. 2007, Meunier and von Messling 2011, Pillet, Kobasa et al. 2011, Fauci and Collins 2012, Ortigoza, Dibben et al. 2012). Globally, there are an estimated 250,000 to 500,000 deaths due to influenza infection every year, with an increased number in pandemic years (Pillet, Kobasa et al. 2011, Fauci and Collins 2012, Maines, Belser et al. 2012).

In the last century, four pandemics have caused widespread morbidity and mortality, occurring in 1918, 1957, 1968, and the most recent, in 2009 (Maines, Belser et al. 2012). Emergence of influenza strains to which the human population has little or no pre-existing immunity can be associated with widespread and potentially severe disease pandemics (Kuchipudi, Dunham et al. 2011), as demonstrated by both the 1918 “Spanish Flu” and the H1N1 influenza pandemic of 2009. The 1918 “Spanish Flu” killed between 50 and 100 million people worldwide (Fauci and Collins 2012). The 2009 H1N1 influenza pandemic resulted in approximately 414,000 confirmed cases and 5,000 deaths worldwide (Kobinger, Meunier et al. 2010). It is likely that the actual numbers are substantially higher due to recent changes requiring that severe cases be confirmed by laboratory diagnosis (Kobinger, Meunier et al. 2010).

It has been shown that reassortment between the pandemic swine-origin strain of H1N1 influenza virus and the highly pathogenic avian-origin strain of H5N1 influenza virus could lead to the creation of highly pathogenic viruses capable of spreading efficiently among humans with deadly and pandemic potential (Neumann, Noda et al. 2009, Octaviani, Ozawa et al. 2010). The recent emergence of a novel influenza virus (subtype H7N9) in provinces of China is the product of a novel reassortment with clear pandemic potential (Guan, Farooqui et al. 2013, Kageyama, Fujisaki et al. 2013, Nicoll and Danielsson 2013).

The H7N9 subtype has shown increased transmission between poultry and humans and contains genetic markers that have been associated with improved replication in mammals resulting in severe respiratory illness and, in some cases, death (Guan, Farooqui et al. 2013, Kageyama, Fujisaki et al. 2013, Nicoll and Danielsson 2013). The H7N9 subtype influenza viruses contained mutations within one of the surface proteins and the ion channel that rendered current anti-viral treatments ineffective (Kageyama, Fujisaki et al. 2013). In addition, the surface proteins of the H7N9 subtype were found to contain several mutations within the receptor-binding site of the surface proteins that enabled systemic viral spread (Guan, Farooqui et al. 2013, Kageyama, Fujisaki et al. 2013). An additional mutation within one of the surface proteins of the H7N9 subtype contributed to increased binding to human-type receptors, while a specific lysine residue within one of the polymerase subunits was required for efficient viral replication (Kageyama, Fujisaki et al. 2013).

Furthermore, other factors, in addition to those identified in the H7N9 subtype, have been found to contribute to the pathogenicity of influenza viruses. Highly

pathogenic strains of influenza virus contain a consecutive group of basic amino acids in the cleavage site in one of the surface proteins and have been shown to play a role in viral spread (Bosch, Orlich et al. 1979, Bosch, Garten et al. 1981, Garten, Bosch et al. 1981). Similarly, the four C-terminal residues of the non-structural protein have been shown to contribute virulence and pathogenesis of avian influenza strains (Jackson, Hossain et al. 2008).

The genetic markers identified in influenza viruses play a significant role in determining the pattern of disease in the respiratory tract and the host range of influenza viral infection (Kuiken, van den Brand et al. 2010). For example, human influenza viruses infect the ciliated epithelial cells in the trachea and bronchi often resulting in mild inflammation of the upper respiratory tract (Ibricevic, Pekosz et al. 2006, Kuiken, van den Brand et al. 2010). In contrast, mouse adapted strains of influenza viruses infect the ciliated bronchiolar epithelial cells and alveoli of the lower respiratory tract resulting in virus-induced pneumonia (Ibricevic, Pekosz et al. 2006, Kuiken, van den Brand et al. 2010). The differences in human and mouse tropism of influenza infection are determined by the genetic markers encoded in viral proteins and their influence on host receptors (Ibricevic, Pekosz et al. 2006). Thus, understanding the interaction between host cellular factors and influenza viral proteins, and their relevance during infection, would allow for the development of novel, effective therapeutic interventions targeted against seasonal and pandemic strains of influenza.

1.2 General properties of influenza virus

Influenza belongs to the family *Orthomyxoviridae* and can be categorized into three groups: A, B, and C. Influenza C viruses cause mild respiratory illnesses and are not responsible for causing epidemics (Prevention 2012). Influenza A and B viruses are responsible for seasonal epidemics and pandemics, however, only influenza A can be further classified by antigenic variation based on the hemagglutinin (HA) and neuraminidase (NA) proteins, shortened to H and N respectively, when indicating the subtype of the virus (Steinhauer 2002, Herfst, Schrauwen et al. 2012, Prevention 2012, Angel, Kimble et al. 2013). Currently, there are 17 H variants and 10 N variants which can give rise to hundreds of combinations of virus subtypes, (Herfst, Schrauwen et al. 2012, Rahim, Selman et al. 2013). Virus subtypes H1 to H4, H6, and H8 to H17 are associated with low pathogenic influenza viruses (Herfst, Schrauwen et al. 2012). Most viruses comprised of subtypes H5 and H7 are considered low pathogenic influenza viruses in poultry, however some of these subtypes can be high pathogenic viruses once domestic birds are infected and undergo reassortment with other influenza strains (Herfst, Schrauwen et al. 2012, Prevention 2013).

1.3 Composition of the viral particle

The influenza A genome is comprised of eight segments of single-stranded, negative-sense RNA that encode at least 11 viral proteins, including two non-structural proteins, NS1 and NEP (also known as NS2), and nine structural proteins, as listed in Table 1 (Steinhauer 2002, Chan, Lin et al. 2006, Lowen, Mubareka et al. 2007, Hale, Randall et al. 2008, Ozawa and Kawaoka 2011, Arranz, Coloma et al. 2012, Backstrom Winquist, Abdurahman et al. 2012, Herfst, Schrauwen et al. 2012, Ortigoza, Dibben et al. 2012, Rahim, Selman et al. 2013, Santos, Pal et al. 2013). Most of the RNA segments encode a single protein, with the exception of segments 7 and 8, and in some viral strains, segment 2, which encode two proteins (Hale, Randall et al. 2008, Backstrom Winquist, Abdurahman et al. 2012, Herfst, Schrauwen et al. 2012, Chua, Schmid et al. 2013). Nine influenza viral proteins have been identified to make up the influenza virion (Shaw, Stone et al. 2008). The viral particle is surrounded by a lipid membrane acquired from the host and that is heavily populated with the viral proteins HA and NA. The ion channel protein, M2, is also embedded within the membrane, but at much lower levels as compared to HA and NA (Shaw, Stone et al. 2008). The most abundant viral protein in the virion is M1 which forms a brick-like membrane matrix that lies just below the membrane and is responsible for supporting and connecting the internal viral ribonucleoprotein (vRNP) core and external membrane proteins (Shaw, Stone et al. 2008, Ran, Chen et al. 2013). The vRNPs are comprised of viral RNA coated by the viral nucleoprotein, NP, and bound in a closed conformation in which each end of the viral RNA interacts with a single copy of the trimeric polymerase complex (PB2, PB1, PA) similar to a hairpin structure (Shaw, Stone et al. 2008, Arranz, Coloma

et al. 2012). The final viral protein found within the virion is the nuclear export protein, NEP, which is responsible for the nuclear export of vRNPs through its association with M1 and critical to the virus life cycle (Chua, Schmid et al. 2013).

Table 1.1 Proteins encoded by viral RNA segments

RNA Segment	Viral Protein	Function	Gene Size (bp)
1	PB2	Basic polymerase 2; polymerase component; host cap binding	2341
2	PB1	Basic polymerase 1; polymerase component; catalytic subunit	2341
	PB1-F2	Apoptosis induction; interferon antagonist; modulate polymerase activity	
3	PA	Acidic polymerase; cap snatching endonuclease; replication of viral genome	2233
4	HA	Hemagglutinin; antigenic determinant; surface glycoprotein; binds host receptors on cell membrane; fusion with endosomal membrane	1778
5	NP	Nucleoprotein; viral ribonucleoprotein (vRNP) complex component; viral assembly; RNA synthesis	1565
6	NA	Neuraminidase; antigenic determinant; surface glycoprotein; release of new viral particles by cleaving sialic acids	1413
7	M1	Matrix protein; viral assembly	1027
	M2	Transmembrane ion-channel; viral disassembly upon infection	
8	NS1	Non-structural protein; interferon antagonist; suppresses host gene expression; modulates mRNA splicing and translation	890
	NEP	Nuclear export protein; trafficking of vRNPs for viral assembly	

1.4 Influenza viral life cycle

Viral infection occurs when viral particles bind to sialic acid receptors on the host cell via receptor binding sites in an uncleaved form of hemagglutinin (HA), HA0 (Skehel and Wiley 2000). Upon binding, receptor-mediated endocytosis is activated allowing the virus to enter the cell in an endocytic vesicle (Skehel and Wiley 2000, Samji 2009, Das, Aramini et al. 2010). The low pH of the endosome causes a conformational change and cleavage event of HA0 resulting in the exposure of its two subunits, HA1 and HA2, which contain the receptor binding domain and the fusion peptide, respectively. The HA2 fusion peptides bring the viral and endosomal membranes into close proximity resulting in the fusion of the two membranes (Samji 2009, Das, Aramini et al. 2010). The low pH also causes an influx of protons to enter the viral particle through the M2 ion channel thus causing the vRNPs to dissociate from the M1 matrix (Samji 2009, Das, Aramini et al. 2010).

Influenza is distinct from other RNA viruses in that it is able to replicate and transcribe its vRNAs in the nucleus (Ozawa and Kawaoka 2011). Once the vRNPs dissociate from M1, the vRNPs are released into the cytoplasm and transported into the nucleus (Das, Aramini et al. 2010). The viral RNA (vRNA) segments contain a region of approximately 12 to 13 terminal nucleotides at the 3’ and 5’ ends that are highly conserved among each of the eight RNA segments which may serve as key elements in transcription and replication events (Ozawa and Kawaoka 2011). Once inside the nucleus, the viral polymerase activates transcription by a 5’-“cap snatching” mechanism from nascent mRNA strands (Dias, Bouvier et al. 2009). This occurs when the PB2 subunit binds the mRNA strand at the 5’ cap and PA cleaves 10-15 nucleotides

downstream from the cap (Das, Aramini et al. 2010). The cap structure is then used to prime viral mRNA transcripts, thus initiating transcription of the viral mRNAs by PB1 and replication of full-length cRNAs (Samji 2009, Das, Aramini et al. 2010, Scull and Rice 2010). The cRNAs will serve as the template for progeny vRNAs (Scull and Rice 2010). Following transcription of the viral mRNAs, they are shuttled out of the nucleus into the cytoplasm for translation. Transcription of the viral genome is separated into two phases, early, in which viral proteins necessary for replication are synthesized, and late, in which all other viral proteins needed for viral assembly are synthesized. After translation, the early viral proteins, PB2/PB1/PA (RdRp), NP, NS1, and NEP, are shuttled back to the nucleus to facilitate the transcription of late viral genes, mainly the ones coding for the surface proteins, HA, NA, M1, and M2, and replication of the cRNA into progeny vRNA. In addition, translation of the surface membrane proteins, HA, NA, and M2, occurs at the rough Endoplasmic Reticulum (rER) thus allowing them to enter the secretory pathway where they undergo extensive processing (Ran, Chen et al. 2013). In the rER, the surface proteins are glycosylated, transported to the Golgi, and targeted to the apical domain of the cell membrane (Das, Aramini et al. 2010). The newly synthesized progeny vRNAs, are transported out of the nucleus to the cell membrane, mediated by the M1-NS2 complex, where they are incorporated into new viral particles (Ran, Chen et al. 2013). Once at the plasma membrane, vRNPs are incorporated into new viral particles (Ran, Chen et al. 2013) that bud out and are released when sialic acid residues are cleaved by NA (Das, Aramini et al. 2010). **Figure 1.1** illustrates the life cycle of influenza virus.

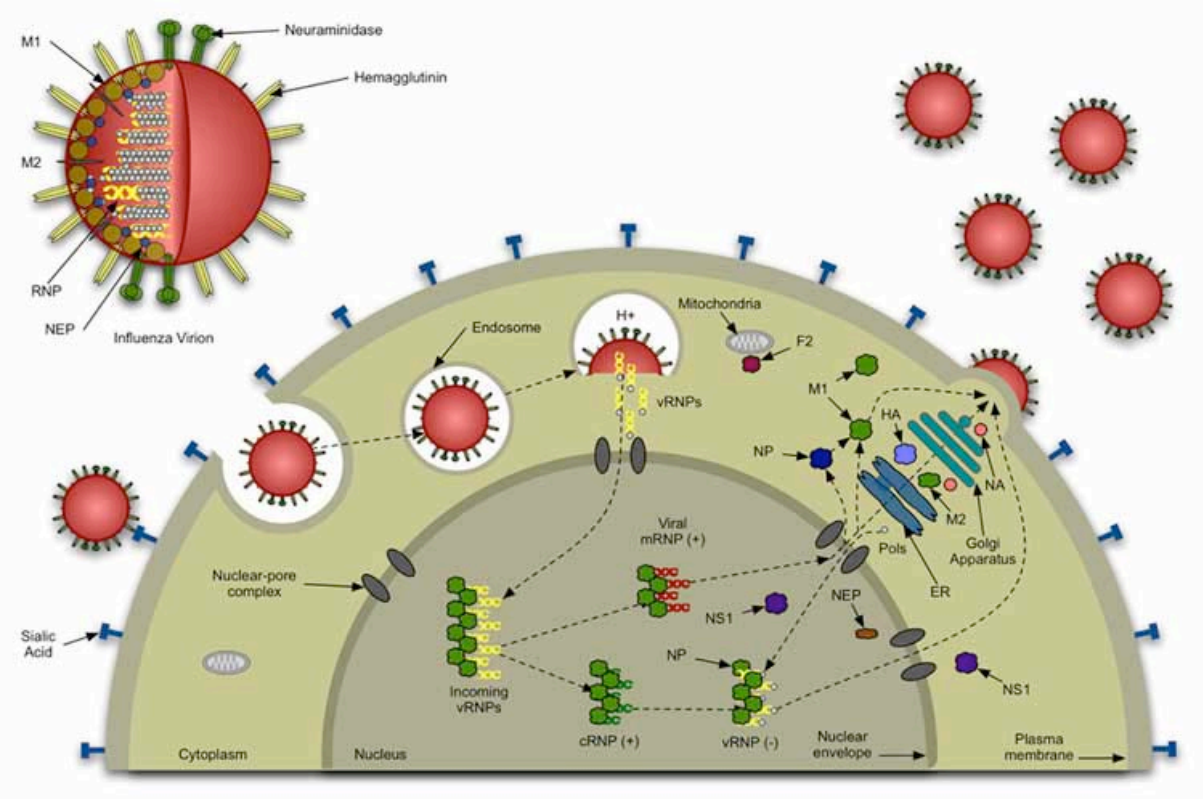

Figure 1.1 Diagram of influenza viral replication. The virus binds to sialic acid residues on the host cell membrane and enters the cell via endocytosis. Fusion of the viral membrane with the endosome membrane causes the release of the viral RNPs into the cytoplasm for export into the nucleus. Viral proteins are produced. New vRNAs are synthesized and shuttled to the membrane for budding. Viral particles are released from the infected cells.

Image from P Palese, ML Shaw, "Orthomyxoviridae: The Viruses and Their Replication", Fields Virology, 5th edition D.M. Knipe and P.M. Howley, Editors. 2006, Lippencott Williams and Wilkins: Philadelphia ISBN-10: 0-7817-6060-7, 2001, 1647-1689.

1.5 Immune response to influenza infection

The first line of defense for a host against viral infection is the recognition of various pathogen-associated molecular patterns (PAMPs) that lead to the activation of cellular innate immune responses, including the interferon (IFN)-response (Ehrhardt and Ludwig 2009, McKinstry, Strutt et al. 2011). PAMPs are short sequences within pathogens and are recognized by pathogen recognition receptors (PRRs) (Kumar, Kawai et al. 2011). There are several families of PRRs including toll-like receptors (TLRs), which are considered to be the primary sensors of pathogens, and RIG-I-like receptors (RLRs) such as RIG-I, MDA5, and LGP2 (Kumar, Kawai et al. 2011). The recognition of PAMPs by TLRs and RLRs leads to the activation of signaling pathways of the innate immune response (Akira and Hemmi 2003). Several factors contribute to the immune response to viral infection including the nature of the pathogen itself, the route of infection, whether it is a chronic persisting or acute infection, and how the virus is presented to specific T cells for the adaptive response (Brown, Roman et al. 2004). Moderate increases of immune activation in virus-infected individuals may favor viral clearance; however a hyper-activated immune response may lead to detrimental effects for the host (Jiang, Zhang et al. 2010). The balance between the key players during immune activation ultimately determines the extent and progression of infection (Gannage and Munz 2009, Rossman and Lamb 2009).

CD4 T cells have been shown to act as helper cells to regulate innate immunity and as direct effectors of cell-mediated protection (McKinstry, Strutt et al. 2011). CD4 T cells regulate innate immunity early after influenza infection, which has been shown to decrease viral titers (Brown, Dilzer et al. 2006, McKinstry, Strutt et al. 2011). The

secretion of antiviral cytokines and cell-mediated cytotoxic activity by CD4 T cells has also been shown to control viral titers (Brown, Dilzer et al. 2006, Brown 2010, Nayak, Richards et al. 2010) while orchestrating the host immune response (Jiang, Zhang et al. 2010). The main family of cytokine mediators responsible for initiating a cellular immune response to viral infection are IFNs (Le Page, Genin et al. 2000). IFNs are crucial for controlling viral replication and limiting the spread of the virus (Meunier and von Messling 2011). Upon viral infection, viral PAMPs are recognized by the TLRs or RLRs stimulating the production of IFNs, via activation of interferon regulatory transcription factors, IRF3 and IRF7 (Kumar, Kawai et al. 2011). IFN production results in the upregulation of several hundred genes that produce an antiviral state (Randall and Goodbourn 2008). Some of the upregulated genes encode enzymes endowed with antiviral activity, as exemplified by protein kinase R (PKR) and 2', 5'-oligoadenylate synthetase (OAS), two key factors activated upon IFN stimulation. PKR is responsible for phosphorylating the alpha subunit of the eukaryotic translational initiation factor 2 (eIF2 alpha), which inhibits translation and activates autophagy, resulting in degradation of the cell (Randall and Goodbourn 2008). Additionally, OAS binds and activates RNase L leading to the degradation of cellular and viral RNAs (Randall and Goodbourn 2008). Distinct cytokine secretion patterns are used to separate CD4 T cells into subsets, which provide insights on their functional diversity and their contribution to an immune response (Strutt, McKinstry et al. 2009). The development of each subset is controlled by a unique transcription factor and once the developmental program is established, the genes that promote the other subsets are silenced (Brown 2010). For example, the secretion of the primary cytokine IFN-gamma upon viral infection leads to the

differentiation of CD4 T cells into T helper 1 cells while suppressing T helper 2 cell differentiation (Schoenborn and Wilson 2007).

It has been shown that CD4 T cell responses are not determined, to a significant extent, by the localization of the viral proteins within the infected cell, but by the strength of the immunodominant epitopes that are presented by these viral proteins (Nayak, Richards et al. 2010). Earlier studies had identified T cell epitopes to influenza in which HA was the major antigen for CD4 T cells (Lamb and Green 1983). However, recently it has been shown that M1 and PB1 are the major antigens for CD4 T cells (Ge, Tan et al. 2010). Although the other viral proteins elicit an immune response, it is significantly lower than the response elicited by M1 and PB1 (Ge, Tan et al. 2010).

The HA envelope protein plays a major role in viral entry into the cells, thus playing a critical role in virulence (Surls, Nazarov-Stoica et al. 2010); however, both capsid proteins, HA and NA, are highly variable (McKinstry, Strutt et al. 2011). It has been suggested that the ability of viral proteins HA and NA to induce cytotoxic activity has been severely underestimated (Rahim, Selman et al. 2013). In a study by Subbramanian et al. (Subbramanian, Basha et al. 2010), the variable and conserved regions of HA were investigated in order to determine their contribution to the CD4 T cell response from the pandemic 2009 H1N1 and seasonal H1N1 influenza viruses. It was found that the variable regions of the 2009 pandemic virus induced a highly diverse HA-specific T cell response with a significant subset of individuals that demonstrated higher levels of several proinflammatory cytokines and chemokines compared to the responses induced by the seasonal influenza virus (Hale, Steel et al. 2010, Subbramanian, Basha et al. 2010). It was also found that the conserved regions of both

the pandemic 2009 H1N1 virus and seasonal H1N1 influenza virus induced comparable levels of HA-specific T cell responses, suggesting that CD4 T cells preferentially respond to variable regions of HA viral proteins, more than conserved regions (Subbramanian, Basha et al. 2010). In addition, the 2009 H1N1 pandemic virus was also able to replicate more efficiently thus causing increased levels of morbidity and mortality as compared to the seasonal influenza virus (Hale, Steel et al. 2010).

CD4 T cells have been shown to act as helpers by driving optimal CD8 T cell responses (McKinstry, Strutt et al. 2011). Earlier studies also identified T cell epitopes to influenza in which NP and M1 were the major antigens for CD8 T cells (Lamb and Green 1983, Yewdell, Bennink et al. 1985, Gotch, Rothbard et al. 1987). It is important to note that it is not surprising that M1 is a major antigen for both CD4 and CD8 T cells. M1 is the most highly conserved viral protein across many strains of influenza. Other influenza viral proteins, including PB1, PB2, PA, and NP, have also been shown to be highly conserved across many strains of influenza, most likely due to their highly regulated functional constraints and different selection pressures, supporting that virulence is a polygenic trait (Hale, Steel et al. 2010, McKinstry, Strutt et al. 2011). It has been shown that immune cytotoxic CD8 T cells are directed predominantly against the internal viral proteins, which are commonly shared and highly conserved among many strains of influenza virus (Furuya, Chan et al. 2010).

Influenza-specific CD8 T cells proliferate and promote the elimination of the virus and host recovery via the production of pro-inflammatory cytokines, which are elicited by highly activated dendritic cells, which are essential for an efficient immune response (McKinstry, Strutt et al. 2011, Meunier and von Messling 2011). Viral infection causes an

robust upregulation of IFN-stimulated genes related to antigen presentation leading to the stimulation of dendritic cells (Tisoncik, Billharz et al. 2011). This stimulation causes a release of proinflammatory cytokines and chemokines that migrate to lymph nodes where they present pathogen-specific antigens to T helper and cytotoxic cells, thus accelerating T-cell responses and initiating the destruction of virus infected cells through cytotoxic mechanisms (Hale, Randall et al. 2008, Hatta, Hershberger et al. 2010, Tisoncik, Billharz et al. 2011, Valkenburg, Rutigliano et al. 2011). Cell-mediated cytotoxic activity occurs via two major mechanisms including cell surface receptor binding of Fas with Fas ligand, and granule exocytosis, in which T cells secrete perforin and granzyme B after recognition of an antigen. Both of these mechanisms result in the activation of caspases, which in turn, induce apoptosis in target cells (Brown, Dilzer et al. 2006). Highly pathogenic influenza virus triggers CD8 T cells to induce the production of proinflammatory cytokines interleukin (IL)-6 and tumor necrosis factor (TNF)-alpha thus inducing cellular apoptosis through the TNF-related apoptosis-inducing ligand (TRAIL)/ TRAIL receptor-dependent mechanism (Brincks, Kucaba et al. 2008, Hatta, Hershberger et al. 2010, Meunier, Embury-Hyatt et al. 2012). It has been shown that the lack of CD8 T cells leads to increased viral replication and eventual morbidity, which suggests that CD8 T cells are required for viral clearance (Brown, Roman et al. 2004).

1.6 Role of NS1 in influenza viral infection

Viruses have evolved numerous strategies in order to evade the host defense responses mounted upon viral infection. For influenza virus, the non-structural 1 (NS1) protein is the virally encoded antagonist responsible for neutralizing cellular innate immune responses (Garcia-Sastre, Egorov et al. 1998, Meunier and von Messling 2011, Backstrom Winquist, Abdurahman et al. 2012, Ortigoza, Dibben et al. 2012). The NS gene segment is the smallest gene segment of the influenza genome and encodes at least two viral proteins, an unspliced product, NS1, and a spliced product, nuclear export protein, NEP (Hale, Randall et al. 2008, Backstrom Winquist, Abdurahman et al. 2012, Chua, Schmid et al. 2013). NS1 is a 26 kDa protein that ranges in length from 219 to 237 amino acids (Rahim, Selman et al. 2013) and is expressed early during viral infection (Thomas, Kranjec et al. 2011). Viruses lacking NS1 are able to efficiently replicate in interferon-deficient cell lines, however, are attenuated and do not cause disease, implicating NS1 as a factor responsible for pathogenicity (Meunier and von Messling 2011, Backstrom Winquist, Abdurahman et al. 2012, Ortigoza, Dibben et al. 2012). NS1 is predominantly localized in the nucleus which allows for exerting its multiple functions associated to regulating viral infection and circumventing host immune defenses (Li, Yamakita et al. 1998).

NS1 exhibits two distinct globular domains linked by a flexible, unstructured linker sequence. Each globular domain acts as a functional domain with the N-terminal (amino acids 1-73) acting as an RNA binding domain (RBD) and the C-terminal (amino acids 74-230) acting as an effector domain (ED), mediating the interactions with host-cellular proteins and stabilizing the RNA binding domain (Wang and Krug 1996, Hale, Randall et

al. 2008). The RNA-binding domain is required for counteracting the IFN response (Dundon and Capua 2009). This domain functions by sequestering double stranded RNA (dsRNA) preventing the activity of the OAS and PKR, two key regulators of the antiviral response (Talon, Horvath et al. 2000, Salvatore, Basler et al. 2002, Kochs, Garcia-Sastre et al. 2007, de Vries, Haasnoot et al. 2009). The RBD of NS1 is responsible for out-competing with OAS for dsRNA preventing the activation of the RNase L pathway contributing to the suppression of IFN-beta synthesis (Hale, Randall et al. 2008). NS1 blocks the activation of PKR by preventing a conformational change that is normally required for the activation of transcription factors, such as eIF2-alpha, and, ultimately, the inhibition of protein synthesis (Wang and Krug 1996, Talon, Horvath et al. 2000, Salvatore, Basler et al. 2002, Kochs, Garcia-Sastre et al. 2007, Jackson, Hossain et al. 2008). NS1 has been shown co-precipitate with the retinoic acid-inducible gene product I, RIG-I, suggesting a potential protein-protein interaction which is stabilized by the presence of 5’-triphosphorylated single stranded RNA (ssRNA) (Hale, Randall et al. 2008, Jackson, Hossain et al. 2008, Meunier and von Messling 2011). Furthermore, the interaction between NS1 and RIG-I inhibits activation of transcription factors IRF3, IRF7, NF-κB and c-Jun/ATF, which are critical for the expression of IFN-beta and an effective immune response (Kochs, Garcia-Sastre et al. 2007, Hale, Randall et al. 2008, Jackson, Hossain et al. 2008, de Vries, Haasnoot et al. 2009, Tisoncik, Billharz et al. 2011). Additionally, NS1 has been implicated in G0/G1 cell cycle arrest in an IFN-dependent manner (Jiang, Wang et al. 2013). This is achieved either by directly binding the Ras homolog gene family member A (RhoA), a small GTPase that controls many cell cellular functions, or by downregulating the transcription factor NF-κB

(Jiang, Wang et al. 2013). Additionally, NS1‘s ability to bind dsRNA has been shown to interfere with the RNA-silencing antiviral response (RSAR) in an NS1-ED dependent manner as another measure to counteract host antiviral mechanisms (Li, Li et al. 2004). This demonstrates that the ED is responsible for enhancing the antagonistic properties of NS1 by stabilizing its dimeric structure, which is required for RNA binding (Dundon and Capua 2009).

The ED of NS1 is also responsible for mediating interactions with a number of host cellular proteins and contains the nuclear export and import sequences as well as a nucleolar localization signal (Dundon and Capua 2009). The ED of NS1 has been shown to play a role in disrupting the activation of RIG-I by targeting TRIM25, a RING E3 ubiquitin ligase and antiviral molecule critical for RIG-I mediated induction of the type-1 IFN response and activation of dendritic cells (Jackson, Hossain et al. 2008, Hale, Steel et al. 2010, Tisoncik, Billharz et al. 2011, Di Pietro, Kajaste-Rudnitski et al. 2013). NS1 binds TRIM25 via its ED preventing the formation of protein complexes and multimerization (Di Pietro, Kajaste-Rudnitski et al. 2013). The C-terminal four residues of NS1 encode a potential PDZ-binding motif involved in protein-protein interactions that can modulate a range of cell-signaling pathways, including transport, localization, complex formation, and cell polarity organization among others (Hale, Randall et al. 2008, Jackson, Hossain et al. 2008, Dundon and Capua 2009). The EPEV and ESEV C-terminal residues have been shown to play a role in binding PDZ-domain containing proteins interfering with cell-signaling (Krug 2006, Jackson, Hossain et al. 2008, Thomas, Kranjec et al. 2011) and disrupting cellular tight junctions through binding of Scribble and DlgI, factors involved in the induction of apoptosis, thus leading to an

overall increase in lung pathology (Thomas, Kranjec et al. 2011, Soubies, Hoffmann et al. 2013). NS1 proteins containing C-terminus extensions that alter the PDZ-binding motif have been associated with attenuated virulence implicating the C-terminus of NS1 as an indicator of pathogenicity (Thomas, Kranjec et al. 2011, Meunier, Embury-Hyatt et al. 2012, Soubies, Hoffmann et al. 2013).

NS1 contains several other protein interaction sites including SH2 and SH3 domains, as well as recognition sites for the kinases CK2 and MAPK (Dundon and Capua 2009, Thomas, Kranjec et al. 2011). SH3 domains are responsible for mediating protein-protein interactions and are commonly found in proteins involved in the regulation of cell signaling pathways, cytoskeletal organization, and membrane trafficking (Dundon and Capua 2009). One of the cell signaling components targeted by NS1 is phosphatidylinositol-3-kinase (PI3K) (Kochs, Garcia-Sastre et al. 2007, Li, Anderson et al. 2008, Ehrhardt and Ludwig 2009, Thomas, Kranjec et al. 2011). The activation of PI3K supports viral replication in two phases: 1) early phase, regulating viral attachment or uptake, and 2) intermediate phase, following expression of NS1 (Ehrhardt and Ludwig 2009). The SH3 domain of NS1 binds the inter-SH2 domain of the p85-beta subunit of PI3K, thus leading to its activation and regulation of kinase phosphorylation events, including the phosphorylation of the serine/threonine kinase, Akt (Hale, Randall et al. 2008, Li, Anderson et al. 2008, Ehrhardt and Ludwig 2009, Thomas, Kranjec et al. 2011). These phosphorylation events lead to the induction of downstream signaling pathways responsible for cell proliferation, migration, differentiation, and the suppression of cellular apoptosis (Li, Anderson et al. 2008). Furthermore, the ability of NS1 to bind adapter proteins Crk and CrkL has been

associated with enhanced PI3K signaling supporting the role of PI3K/Akt signaling in the regulation of viral infection (Li, Anderson et al. 2008).

Another function associated to the ED of NS1 is the ability to regulate viral and cellular processing of mRNAs (Backstrom Winquist, Abdurahman et al. 2012). Many NS1 proteins are able to inhibit mRNA splicing and nuclear export of host-cellular proteins by preventing polyadenylation of mRNAs and through binding of the zinc-finger regions in the 30 kDa subunit of the cleavage and polyadenylation specificity factor (CPSF30) and the poly-A binding protein II (PABPII) (Kochs, Garcia-Sastre et al. 2007, Dundon and Capua 2009, Hale, Steel et al. 2010, Meunier and von Messling 2011, Tisoncik, Billharz et al. 2011, Backstrom Winquist, Abdurahman et al. 2012, Selman 2012). These interactions prevent the splicing, polyadenylation, and transport of the cellular mRNAs into the cytoplasm, thus inhibiting translation, and have been suggested to be the major reason for the shutoff of host cellular protein synthesis observed during influenza infections (Salvatore, Basler et al. 2002, Hale, Randall et al. 2008, Dundon and Capua 2009, Backstrom Winquist, Abdurahman et al. 2012). Furthermore, the ability of NS1 to form inhibitory complexes with other components of the nuclear export machinery, including NXF2, p15, Rael, E1B-AP5, and Nup98, support NS1's role in regulating the export of cellular mRNAs (Hale, Randall et al. 2008). NS1 also has the ability to modulate expression levels of proteins via its ability to act as a general translational enhancer (Salvatore, Basler et al. 2002). NS1 is able to recruit translation factors, such as eIF4G1, eIF4F, hStaufen, and PABPI, to the 5'-untranslated region (UTR) of viral mRNAs in order to form multi-protein translation complexes to preferentially increase viral translation (Hale, Randall et al. 2008, Pal 2010).

1.7 Limitations of anti-influenza measures

There are two current measures against the influenza virus: 1) vaccines and 2) antiviral drugs. Vaccines are a widely accepted weapon against viral infection due to their ability to elicit a strong immune response to circulating strains of the virus. Each year the vaccine has to be modified so that it will protect against influenza viruses that research indicates will be most prevalent during the upcoming season. However, vaccines are limited in their ability to protect against new strains that are generated through antigenic drift or antigenic shift. Viruses can undergo antigenic drift in which small changes are accumulated over time, thus producing viruses that may be unrecognizable to the body's immune system (Prevention 2012). Antigenic shift is a sudden, major change in the virus composition resulting in a virus that most people have little or no immune response against (Brooke, Ince et al. 2013). In 1957, two strains of influenza, an avian H2N2 and a circulating H1N1, exchanged gene segments thus generating an H2N2 viral strain that triggered an H2N2 pandemic (Masurel 1969). Subsequently, in 1968, the H2N2 pandemic strain combined with an avian H3 strain to produce the H3N2 pandemic (Scholtissek, Rohde et al. 1978, Kawaoka, Krauss et al. 1989). Thus, due to the continually changing genetic composition of the virus, caused by both, genetic drift and genetic shift, vaccines lose effectiveness approximately after every influenza season and are likely to not be readily available in the event of new pandemics (Angel, Kimble et al. 2013).

Current FDA-approved anti-viral drugs belong to three main groups: 1) neuraminidase inhibitors, 2) M2 ion-channel inhibitors, and, 3) the most recent, a viral RNA synthesis inhibitor (Ortigoza, Dibben et al. 2012). The neuraminidase inhibitors,

Oseltamivir and Zanamivir, act by binding neuraminidase proteins thus blocking its enzymatic activity and preventing the release of newly formed viral particles. The M2 ion-channel inhibitors, Amantidine and Rimantidine, act by blocking the activity of the M2 ion-channel, thus preventing the release of vRNPs into the cytoplasm (Krug and Aramini 2009). The viral RNA synthesis inhibitor, Favipiravir (T-705), acts as a purine analogue thus inhibiting the synthesis of viral RNA (Ortigoza, Dibben et al. 2012). The available anti-viral drugs function by inhibiting structural components of the virus which are subject to mutations introduced by the error-prone viral RdRp. In a study by Moscona (Moscona 2009), a single mutation, H274Y, in the NA viral protein target, rendered the anti-viral drug Oseltamivir fully ineffective against influenza viral infection. Currently, 98.6% and 100% of circulating 2009 H1N1 and H3N2 strains of influenza virus are susceptible to the neuraminidase inhibitors, Oseltamivir and Zanamivir, respectively, while all of the 2009 H1N1 and H3N2 strains of influenza are resistant to the M2 ion-channel inhibitors, Amantidine and Rimantidine (Moscona 2009, Prevention 2012).

Despite current influenza treatments, it is critical to develop novel treatments that are effective against influenza virus independent of the subtype, strain, or antigenic properties. One alternative is the development of therapies targeting cellular mechanisms utilized for viral propagation, which will be less likely to be affected by genomic mutations or reassortment. One such cellular mechanism is the cellular SUMOylation system, in which the Small Ubiquitin-like MOdifier (SUMO) protein is conjugated to target proteins, a modification that has been reported to modulate protein function (Pal, Santos et al. 2011).

1.8 SUMO: the Small Ubiquitin-like MOdifier

SUMOylation is a reversible, post-translational modification in which a SUMO protein is covalently attached to a lysine residue within the target protein. SUMO was discovered by numerous investigators independently of one another; thus, it was initially known under several different names including PIC1 (Boddy, Howe et al. 1996), UBL1 (Shen, Pardington-Purtymun et al. 1996), Sentrin (Gong, Kamitani et al. 1997), and hSMT3C (Lapenta, Chiurazzi et al. 1997, Wilson and Rangasamy 2001). Matunis et al. (Matunis, Coutavas et al. 1996) reported the first protein target of SUMO (then referred to as GMP1), a nuclear transport component, RanGAP1. In humans, SUMO, an 11 kDa protein, has four distinct homologs: SUMO 1 through 4. SUMO homologs 1 through 3 are ubiquitously expressed, while the SUMO 4 is mainly expressed in the kidneys, lymph nodes, and spleen. SUMO 2 and 3 are 97% identical and are commonly referred to as SUMO2/3, while SUMO 1 only shares 50% identity with SUMO 2/3 (Geiss-Friedlander and Melchior 2007). SUMO 2 and 3 are able to form poly-SUMO chains, an ability conferred by their extended N-terminal tail (Song, Durrin et al. 2004). In contrast, SUMO 1 is not able to form poly-SUMO chains; however, it is able to serve as a poly-SUMO chain terminator (Hannoun, Greenhough et al. 2010). Recent studies have proposed a potential mechanism that explains why some proteins are preferentially modified by SUMO 2/3 over SUMO1 (Meulmeester, Kunze et al. 2008, Sarge and Park-Sarge 2009). This mechanism involves an interaction between SUMO and SUMO-interaction motifs (SIMs), in an manner analogous to the mechanism in which ubiquitin is able to interact with ubiquitin-interaction motifs (UIMs) (Meulmeester, Kunze et al. 2008, Sarge and Park-Sarge 2009). SUMO interacting motifs are generally short

sequences of hydrophobic residues that are surrounded by acidic ones and contribute to the SUMOylation of a protein thanks to their ability to bring into close-proximity Ubc9-associated SUMO molecules hence leading to an enhanced SUMOylation (Song, Durrin et al. 2004, Hecker, Rabiller et al. 2006, Song, Bhattacharya et al. 2006, Geiss-Friedlander and Melchior 2007, Merrill, Melhuish et al. 2010). Similar to the ubiquitin-interaction motif, defined as L-A-L-A-L, SUMO-interacting motifs are defined as V/I/L-X-V/I-V/I or the inversion (Swanson, Kang et al. 2003, Song, Durrin et al. 2004, Hecker, Rabiller et al. 2006, Song, Bhattacharya et al. 2006, Geiss-Friedlander and Melchior 2007, Merrill, Melhuish et al. 2010).

1.9 Protein modification by SUMOylation

As illustrated in Figure 2, SUMO proteins are expressed as immature precursor proteins. In order for SUMO proteins to be conjugated to target proteins, a stretch of amino acids on the C-terminus must be cleaved by a SUMO-specific protease, SENP, to reveal a di-glycine motif that indicates the C-terminus of the mature protein (Wilson and Rangasamy 2001, Geiss-Friedlander and Melchior 2007, Drag and Salvesen 2008, Bekes and Drag 2012). Once SUMO has been cleaved into its mature form, the E1 activating enzyme, SAE1/2, activates SUMO in an ATP-dependent manner in which a thioester bond is formed between the C-terminal carboxy group of SUMO and the catalytic cysteine residue of SAE2 (Geiss-Friedlander and Melchior 2007, Hannoun, Greenhough et al. 2010).

SUMO is then transferred from SAE2 to the E2 conjugating enzyme, Ubc9, an 18 kDa monomeric enzyme that is specific for SUMO conjugation (Wilson and Rangasamy 2001, Geiss-Friedlander and Melchior 2007, Hannoun, Greenhough et al. 2010). A thioester bond is then formed between the C-terminal carboxy group of SUMO and the catalytic cysteine residue, C93, of Ubc9 (Wilson and Rangasamy 2001, Geiss-Friedlander and Melchior 2007, Hannoun, Greenhough et al. 2010). SUMO is then transferred from Ubc9 to the target protein, in which an isopeptide bond is formed between the carboxy group of SUMO and the ε-amino group on a lysine residue in the target protein. The target lysine residues are usually located with in a consensus sequence, Ψ-K-X-E, in which the Ψ represents a large hydrophobic amino acid, followed by a lysine residue (K), any amino acid (X) and a glutamic acid (E) residue. Numerous SUMO target proteins contain only one target lysine residue, however, a few,

such as the cytomegalovirus (CMV) IE2 protein, contain multiple target residues (Wilson and Rangasamy 2001). Approximately 40% of known SUMOylated proteins are SUMOylated at lysine residues that are not located within a SUMO consensus sequence (Hannoun, Greenhough et al. 2010). This process may occur with or without the participation of a SUMO E3 ligase, which are enzymes that catalyze the transfer of SUMO from Ubc9 to the target protein either by activation of Ubc9 or by bringing Ubc9 and the target protein into close proximity with each other (Rosas-Acosta, Langereis et al. 2005, Geiss-Friedlander and Melchior 2007, Sarge and Park-Sarge 2009, Hannoun, Greenhough et al. 2010).

SUMO can be removed from the target protein by proteolytic cleavage, thus making SUMOylation a reversible modification. The SUMO released upon cleavage can be used for conjugation with another target protein (Geiss-Friedlander and Melchior 2007, Drag and Salvesen 2008, Bekes and Drag 2012). The main family of SUMO proteases is the sentrin-specific proteases (SENPs) (Drag and Salvesen 2008). There are seven different isoforms of SENP, including SENPs 1-3, SENP6 and SENP7. Each of the SENP isoforms contain a Ulp domain at the C-terminus, which is responsible for cleaving the isopeptide bond between SUMO and the target protein (Hannoun, Greenhough et al. 2010). The hydrolase activity at the C-terminus of each of the SENPs varies, suggesting that each SENP may differentially regulate the maturation and activity of the different SUMO homologs (Wilson and Rangasamy 2001, Hannoun, Greenhough et al. 2010). SENPs tightly regulate the levels of SUMOylation of target proteins and are thought to regulate the levels of free SUMO in the cell (Hannoun, Greenhough et al. 2010, Ribet and Cossart 2010).

Post-translational modifications, such as glycosylation, phosphorylation, methylation, acetylation, and SUMOylation, are highly conserved processes that have been shown to affect protein activity, cellular localization, homeostasis maintenance, signal transduction, and protein-protein interactions, either by creating or masking existing binding sites (Geiss-Friedlander and Melchior 2007, Bekes and Drag 2012). Most of the targets for SUMOylation are nuclear proteins with critical roles in biological processes and SUMOylation has been associated with regulating functions such as transcription, ribosome biogenesis, receptor function, cell cycle control, and DNA repair (Rosas-Acosta, Langereis et al. 2005, Drag and Salvesen 2008, Bekes and Drag 2012). Previous studies have shown that various diseases and pathogens are using these post-translational mechanisms to their advantage, suggesting a potential role that may be relevant for influenza viral infection (Ehrhardt and Ludwig 2009, Bekes and Drag 2012).

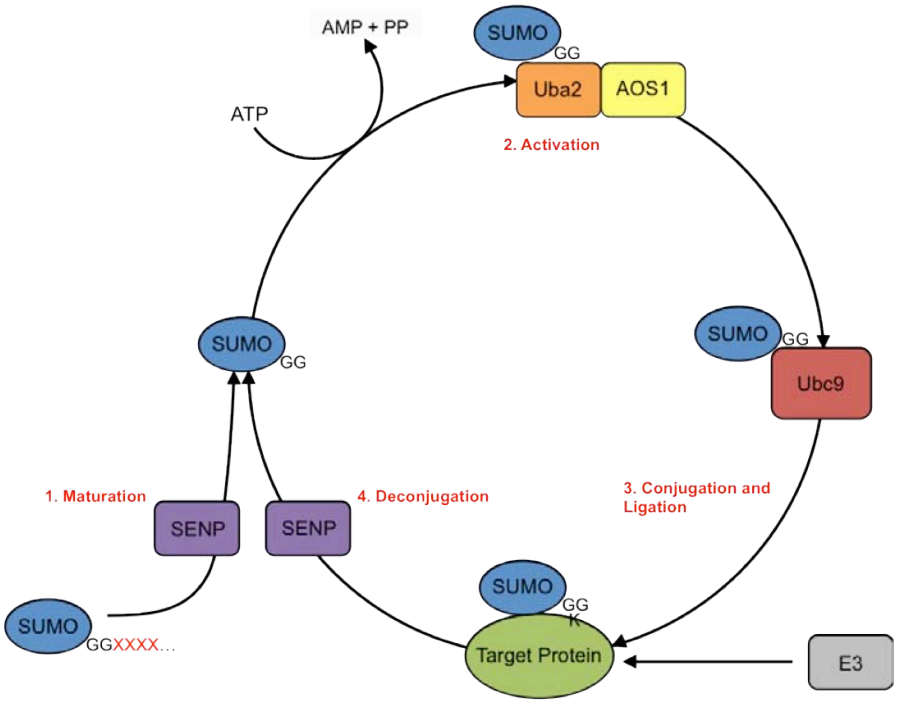

Figure 1.2. The SUMOylation pathway. 1) SUMO is generated as an immature precursor protein requiring cleavage by a SUMO protease. 2) In an ATP dependent manner, SUMO is activated by the heterodimeric E1 protein. 3) SUMO is then transferred to the E2 conjugating enzyme, Ubc9. SUMO is conjugated to its target protein at a lysine residue. This reaction may be facilitated by an E3 ligase, but ligases are not required. 4) SUMO can then be cleaved from the target protein and re-enter the pathway.

1.10 The cellular SUMOylation system and disease

The discovery that a pathogen could modulate the post-translational modification machinery occurred almost 50 years ago when the diphtheria toxin from *Corynebacterium diphtheriae* was discovered to be able to ribosylate ADP leading to the inhibition of the host elongation factor 2 (EF-2) (Ribet and Cossart 2010). Since then, other post-translational modifications have been reported to be modulated, induced, or counteracted by pathogen-associated virulence factors (Ribet and Cossart 2010). Besides its role in mediating critical processes within the cell, recent studies have implicated the SUMOylation system as a target for pathogen-associated virulence factors (Sarge and Park-Sarge 2009, Ribet and Cossart 2010). Proteins involved in human diseases, such as huntingtin (Huntington's disease), ataxin-1 (Spinocerebellar ataxia type 1), tau, α-synuclein, DJ-1 (Alzheimer's and Parkinson's disease), and superoxide dismutase 1 (Amyotrophic lateral sclerosis), have all been identified as protein targets of the cellular SUMOylation system (Sarge and Park-Sarge 2009). Other proteins, including amyloid precursor protein (Alzheimer's) and lamin A (Hutchison-Gilford Progeria Syndrome, among others), have also been identified as SUMO targets, and the loss of SUMO modification of these proteins have been associated with elevated amyloid-β levels and cardiomyophathies, respectively (Sarge and Park-Sarge 2009). Increased levels of the E2 conjugating enzyme, Ubc9, and the deconjugating enzyme, SENP, have also been linked to several human cancers, including prostate and thyroid cancer, and can lead to increased cancer growth (Sarge and Park-Sarge 2009).

1.11 The cellular SUMOylation system and bacterial pathogens

Bacterial pathogens have been known to interfere with may different post-translational modifications in order to promote their own survival (Ribet and Cossart 2010). For example, the protein YopJ/P from the Yersenia species and the XopD and AvrXv4 proteins from *Xanthomonas campestris* have been shown to enhance SUMO deconjugation from host proteins (Ribet and Cossart 2010, Ribet and Cossart 2010, Wimmer, Schreiner et al. 2012). Similarly, listeriolysin O (LLO) from *Listeria monocytogenes*, in addition to perfringolysin (PFO) from *Clostridium perfringens* and pneumolysin (PLO) from *Streptococcus pneumoniae*, directly impair the SUMOylation pathway by enhancing the degradation of Ubc9, which results in increased infection (Citro and Chiocca 2010, Ribet and Cossart 2010, Wimmer, Schreiner et al. 2012). However, when SUMO was overexpressed within the cell, there was a decrease in *Listeria* infection, suggesting an important role for the regulation of the cellular SUMOylation system during bacterial infection (Ribet and Cossart 2010). The SUMOylation pathway has also been suggested in modifying rhoptry proteins in *Toxoplasma gondii*, which may play a role in host cell invasion, cyst development and maintenance, and pathogenesis (Braun, Cannella et al. 2009).

1.12 The cellular SUMOylation system and viral pathogens

In addition to bacterial pathogens, viruses are also able to interfere with the host SUMOylation system through either inhibiting *de novo* SUMOylation or enhancing deconjugation of SUMO from target proteins (Boggio and Chiocca 2006). Viruses may also extort the host SUMOylation system in order to create an environment that is favorable for viral replication, which may require SUMO modification for transcriptional regulation or the nuclear localization of proteins (Boggio and Chiocca 2006). Most SUMOylated viral proteins are either intermediate-early or early nuclear proteins and are preferentially modified by SUMO1 (Rosas-Acosta, Langereis et al. 2005, Boggio and Chiocca 2006). The viral immediate-early proteins that have been shown to be SUMOylated include IE1 and IE2 from human cytomegalovirus (HCMV); Zta, Rta, and BZLF1 from Epstein-Barr virus (EBV); and IE1 from human herpes virus 6 (HHV6) (Wilson and Rangasamy 2001, Boggio and Chiocca 2006). The first viral proteins observed to interact with the cellular SUMOylation system were the herpes simplex virus (HSV) immediate-early protein ICP0 (infected cell protein 0) and the HCMV-immediate early 1 protein (IE1), the first viral protein found to be SUMOylated (Wilson and Rangasamy 2001, Boggio and Chiocca 2006, Wimmer, Schreiner et al. 2012). Both the ICP0 protein from HSV and the IE1 protein from HCMV are responsible for regulating early events during the lytic cycle and induce dispersion of promyleocytic leukemia nuclear bodies (PML NBs), sub-nuclear structures associated with transcriptionally active regions (Boggio and Chiocca 2006, Wimmer, Schreiner et al. 2012). Though both ICP0 and IE1 have the ability to interact with PMLs and to deSUMOylate them, the mechanism in which this is executed is unique to each protein

(Boggio and Chiocca 2006, Wimmer, Schreiner et al. 2012). An orthologue of ICP0, ORF61, from varicella-zoster virus (VSV) contains SUMO interacting motifs which may facilitate the reduction of PML NBs (Wimmer, Schreiner et al. 2012). The function of IE1 is not dependent upon being SUMOylated, but this modification does contribute to its full activity and overall viral replication by promoting the expression of IE2, the transcriptional activator of the HCMV lytic cycle (Boggio and Chiocca 2006). In addition, the IE2 protein contains a SUMO interacting motif that necessary for its modification by SUMO (Wimmer, Schreiner et al. 2012). Another protein from HCMV, pp71, induces the SUMOylation of a cellular transcription co-repressor, Daxx (Hwang and Kalejta 2011). This SUMOylation event is required for the interaction between pp71 and Daxx (Hwang and Kalejta 2011). The Zta (BZLF1) and Rta viral proteins from EBV are early proteins that are responsible for activating early genes allowing the virus to enter the lytic cycle (Wilson and Rangasamy 2001, Boggio and Chiocca 2006, Hagemeier, Dickerson et al. 2010, Wimmer, Schreiner et al. 2012). When SUMOylated, Zta and Rta have been shown to induce the dispersion of PML NBs by out-competing PMLs for free SUMO and by increasing its trans-activation activity, respectively (Boggio and Chiocca 2006, Hagemeier, Dickerson et al. 2010, Wimmer, Schreiner et al. 2012). The K-bZIP (KSHV-basic leucine zipper) viral protein of Kaposi's sarcoma associated herpesvirus (KSHV) also has the ability to be SUMOylated thus allowing for exertion of its transcriptional repression activity by recruiting Ubc9 to specific viral target promoters in an E3 ligase-like manner (Boggio and Chiocca 2006, Ribet and Cossart 2010, Wimmer, Schreiner et al. 2012). The avian adenoviral protein, Gam1, inhibits the SUMOylation pathway by binding to the E1 heterodimer preventing its function (Boggio and Chiocca 2006, Citro

and Chiocca 2010, Ribet and Cossart 2010, Ribet and Cossart 2010, Wimmer, Schreiner et al. 2012).

Other viral proteins that are SUMOylated during infection are the papillomavirus (PV) E1 and E2 proteins, in which SUMOylation plays a role in the nuclear localization of these proteins (Wilson and Rangasamy 2001, Rosas-Acosta, Langereis et al. 2005, Boggio and Chiocca 2006, Wu, Roark et al. 2008, Wu, Bian et al. 2009, Wimmer, Schreiner et al. 2012). The SUMOylation of PV-E1 is enhanced by the protein inhibitor of activated STAT (signal transducer and activator of transcription) (PIAS) family of E3 ligases, in particular, Miz1 (PIASχβ) (Rosas-Acosta, Langereis et al. 2005). Two retroviruses, Moloney murine leukemia virus (MuLV) and human immunodeficiency virus type 1 (HIV-1) contain viral proteins that have been shown to be targets of the cellular SUMOylation system (Boggio and Chiocca 2006). The viral Gag genes in both viruses, which encode the Gag capsid proteins responsible for the formation of the nuclear viral DNA forms and viral propagation, have been shown to be modified by SUMO (Boggio and Chiocca 2006). Although SUMOylation is not required for the functionality of these proteins, the overexpression of SUMO within the cell caused a decrease in infectivity, suggesting that SUMOylation plays an important regulatory role during infection (Boggio and Chiocca 2006). Other regulatory proteins expressed by HIV-1, Tat and Rev, have also been associated with the cellular SUMOylation system. The SUMO modification of Tat is required for stabilization, allowing for the penetration of lymphocytes, while SUMO modification of Rev exhibits inhibition of function (Boggio and Chiocca 2006). Other viral regulatory proteins that are known to be SUMOylated include the E3L and A40R proteins from poxvirus vaccinia virus (VV) and the Tax protein from human T-cell

leukemia virus type 1 (HTLV-1) (Boggio and Chiocca 2006, Wimmer, Schreiner et al. 2012).

1.13 The cellular SUMOylation system and RNA viruses

In terms of RNA viruses, our knowledge of the mechanistic role of the SUMOylation pathway during viral infection is very limited (Wimmer, Schreiner et al. 2012). In the family *Bunyaviridae*, several different species of the genus *Hantavirus*, including Hantaan virus (HTNV), Tula virus (TULV) and Seoul virus (SEOV), were investigated for potential targets of SUMOylation. Studies of these different species identified the nucleocapsid protein (NP) as a target for the SUMOylation pathway. Although there is no evidence that this protein is SUMOylated during viral infection, it is able to directly interact with the SUMO pathway components, SUMO 1, Ubc9 and certain E3 ligases (Wimmer, Schreiner et al. 2012). The nucleocapsid (N) protein from the *Coronaviridae* family, SARS (severe acute respiratory syndrome) coronavirus (SARS-CoV), has been identified as a SUMO modified protein target (Wimmer, Schreiner et al. 2012). The N protein is able to directly bind Ubc9, and may regulate its E2 conjugating activity. Data suggests that SUMOylation of the N protein plays a role in the induction of viral ribonucleoprotein complex formation and nucleocapsid assembly (Wimmer, Schreiner et al. 2012). Two other viral proteins, the VP35 from Ebola Zaire virus (*Filviridae* family) and the envelope protein (env) from Dengue virus (*Flaviviridae* family), have been shown to directly interact with members of the SUMOylation pathway (Wimmer, Schreiner et al. 2012). The VP35 protein is able to directly bind PIAS1 inducing the SUMOylation of IFN-regulatory factor 7 (IFN7) thus decreasing its transcription activating function upon the promoter (Wimmer, Schreiner et al. 2012). The Dengue env protein is able to directly interact with Ubc9 in a SUMOylation independent

manner, however the functional relevance for this interaction has yet to be elucidated (Wimmer, Schreiner et al. 2012).

1.14 The cellular SUMOylation system and influenza virus

Influenza virus is one of the few RNA viruses that are able to replicate within the nucleus of host cells making it a potential target for the host cellular SUMOylation system. The viral protein, NS1, has been shown to be modified by ISGylation, a member of ubiquitin-like modifier family, in which its major downstream effectors are members of the host antiviral response (Tang, Zhong et al. 2010, Pal, Santos et al. 2011). In a study by Wu et al. (Wu, Jeng et al. 2011), M1 was found to be SUMOylated at residue 242. In addition, SUMOylation of M1 was shown to be relevant for viral replication and for the formation of the M1/NEP-vRNP complex, which is required for the nuclear export of vRNPs (Wu, Jeng et al. 2011). Recent studies have also demonstrated that NS1 is an authentic SUMO target and that it is modified by the SUMOylation system at lysine residues 70 and 219 during viral infection (Pal 2010, Pal, Santos et al. 2011, Xu, Klenk et al. 2011, Santos, Pal et al. 2013). In addition, influenza viral infection causes an increase in cellular SUMOylation and the appearance of novel SUMOylated bands in a viral-replication dependent manner (Pal, Santos et al. 2011). Furthermore, four other influenza viral proteins, PB1, NP, M1, and NEP, were shown to be SUMOylated upon viral infection, with NS1 being the most effectively SUMOylated protein (Pal, Santos et al. 2011, Wu, Jeng et al. 2011). Altogether, the interaction between the viral proteins, M1 and NS1, with the SUMOylation pathway serves as a mechanism facilitating the progression of influenza infection, further supporting the relevance for influenza viral infection.

1.15 Significance and Aims

Influenza virus is the etiologic agent responsible for the contagious respiratory illness that afflicts millions of people worldwide during seasonal winter epidemics. Current treatments against influenza A virus, such as vaccines and anti-viral drugs, target structural components of the virus and are becoming largely ineffective due to accumulation of mutations either through antigenic drift or antigenic shift. The sporadic occurrence of pandemics, to which a population has little or no pre-existing immunity, can lead to severe and even deadly respiratory infections, highlighting the need to develop new therapeutics against influenza virus that are independent of virus strain or subtype by targeting cellular components necessary for viral replication.

Viruses exploit host cellular systems in order to efficiently and effectively replicate to produce new viral progeny. One of the cellular systems shown to be exploited during viral infections is the cellular SUMOylation system. Although an interaction between the cellular SUMOylation system and influenza virus has been identified, it is not understood how influenza virus specifically utilizes this system during viral infection. Elucidating the relevance of this interaction could lead to a better understanding of the mechanisms regulating influenza viral infection and, ultimately, the development of novel treatments to combat influenza virus.

There are three **aims** of this dissertation: 1) the assessment of NS1 SUMOylation and its role during viral infection; 2) the investigation of the interplay between the increase in cellular SUMOylation and viral infection; and 3) the evaluation of a novel protein that could potentially act as a therapeutic agent against influenza viral infection.

Previous studies identified eight influenza viral proteins that are SUMOylated *in vitro*, of which five have been shown to be SUMOylated during viral infection (Pal, Santos et al. 2011). Of the influenza viral proteins SUMOylated during viral infection, it was shown that NS1 is the most effectively SUMOylated viral protein, suggesting that SUMOylation may be playing a role in modulating NS1 function (Pal 2010). Currently, the relevance of NS1 SUMOylation during viral infections has yet to be characterized. Therefore, the focus of **Chapter 2** is to assess the relevance of NS1 SUMOylation during influenza viral infection in both tissue culture and animal models. Moreover, we evaluate how mutations affecting NS1 SUMOylation affect viral fitness, clinical signs and symptoms, and pathogenicity.

Furthermore, we have demonstrated that influenza viral infection causes an increase in cellular SUMOylation that is neither cell specific nor strain specific (Pal, Santos et al. 2011). Molecular studies have shown that the influenza viral protein NS1 is the main factor responsible for this increase in cellular SUMOylation (data not published). However, increases in cellular SUMOylation have not been characterized for other viruses nor whether it occurs in animal infections. Therefore, the goal of **Chapter 3** is to investigate whether the increase in cellular SUMOylation occurs in animal infections or as an artifact of tissue culture infections. Moreover, whether the increase in cellular SUMOylation is specific to influenza virus or shared among other viruses is assessed.

Previous studies have shown that cells over expressing components of the SUMOylation pathway, including SUMO or the conjugating enzyme, Ubc9, are less likely to become infected with influenza virus. In addition, studies have shown that

modulation of NS1 SUMOylation decreases NS1‘s ability to neutralize the host IFN response. Although the development of the artificial SUMO ligase specifically enhances the SUMOylation of NS1, its effects have yet to be tested during influenza viral infection. Therefore, the objective of **Chapter 4** is to evaluate the artificial SUMO ligase (ASL) for its use as a novel therapeutic treatment against influenza infection.

Together, these studies provide the first conclusive evidence for the existence of an interaction between the cellular SUMOylation system and a viral infection in an animal model. They also show how an increase in general levels of cellular protein SUMOylation is a phenomenon associated to infection with all viral agents tested and, therefore, may represent a cellular response to viral infection. Importantly, for influenza virus this is a phenomenon observed during infection in both tissue culture and animal models. In addition, they demonstrate that the use of the artificial SUMO ligase could potentially be an effective therapeutic against influenza viral infection.

CHAPTER 2: MUTATIONS AFFECTING NS1 SUMOYLATION DURING INFLUENZA VIRAL INFECTION ALTER VIRAL GROWTH AND PATHOGENICITY

2.1 Introduction:

Influenza virus is a contagious respiratory virus responsible for seasonal epidemics and continues to be a global threat to public health. It is estimated that influenza infections affect 5 to 20 percent of the population resulting in approximately 50,000 deaths and 2 million hospitalizations in the United States alone (Lowen, Mubareka et al. 2007, Pillet, Kobasa et al. 2011, Fauci and Collins 2012, Maines, Belser et al. 2012). Influenza virus can be transmitted via direct contact with infected individuals, contact with virus-infected objects, and inhalation of infectious aerosols (Mubareka, Lowen et al. 2009).

Upon viral infection, the virus is recognized by PRRs which will initiate a robust host antiviral response. Viruses, as well as other pathogens, have evolved strategies to antagonize host antiviral mechanisms (Ploegh 1998). The non-structural protein of influenza A virus, NS1, is a multifunctional protein and acts as the main antagonist of host immune response allowing for effective propagation of the virus (Hale, Randall et al. 2008). The first mechanism by which NS1 subverts the immune response is by preventing the virus-mediated activation of RIG-I, which senses double-stranded RNA (dsRNA) within the cytoplasm (Hale, Randall et al. 2008, Meunier and von Messling 2011). NS1 sequesters dsRNA by binding RNA through residues arginine 38 and lysine 41 within the N-terminal RNA binding domain, thus preventing RIG-I activation (Hale,

Randall et al. 2008). In addition, NS1 is able to directly interact with RIG-I through complex formation that is stabilized by the presence of 5'-triphosphorylated single stranded RNA (Garcia-Sastre 2011, Goubau, Deddouche et al. 2013). NS1 is also able to block the function of two cytoplasmic antiviral proteins, PKR and OAS, which are involved in IFN production and cellular apoptosis, respectively, by out-competing these proteins for binding of dsRNA (Hayman, Comely et al. 2006, Kochs, Garcia-Sastre et al. 2007). Similarly, binding of dsRNA by NS1 prevents the activation of the IRF3 and 7, NF-kB, and c-Jun/ATF-2, transcription factors responsible for the expression of type I IFNs, (Kawai and Akira 2006, Hale, Randall et al. 2008) and interferes with the RNA-silencing antiviral response (Li, Li et al. 2004).

NS1 is also able to form an inhibitory complex with components of the cellular mRNA nuclear export machinery, including NXF1, p15, RaeI, E1B-AP5 and Nup98 (Satterly, Tsai et al. 2007). A majority of these interactions, such as PABPI, nucleolin, E1B-AP5, and importin-alpha occur in close proximity to NS1 residue K70. Interactions with CrkL, PABPII, PDZ, hStaufen, and p15 occur in close proximity to K219 (Hale, Randall et al. 2008). Studies have shown that viruses that cannot form these interactions, contain truncated forms of NS1, or do not contain NS1, induce large amounts of IFN during viral infection and are attenuated in IFN-competent and IFN-deficient systems (Garcia-Sastre, Durbin et al. 1998, Hale, Randall et al. 2008). We have demonstrated, through transfection studies, that lysine to alanine mutations at residues 70 and 219, which also results in the loss of NS1 SUMOylation, dramatically decreases NS1's ability to neutralize the IFN response (Santos, Pal et al. 2013).

In addition, *in vitro* and *in vivo* methods have shown that out of all the proteins produced by influenza virus during infection, NS1 is the most effectively SUMOylated (Pal, Santos et al. 2011). Two SUMOylation sites have been characterized within the influenza A/Puerto Rico/8/1934 NS1, located at lysine residues K70 and K219 (Santos, Pal et al. 2013). The SUMOylation of NS1 is highly conserved at residues K70 and K219 in H1N1 and H3N2 human, or low pathogenic, strains of influenza virus (Santos, Pal et al. 2013). These same residues are not present in avian, or high pathogenic, strains of influenza, including H5N1, H9N2, and the new H7N9 (Santos, Pal et al. 2013). The objective of this chapter is to determine the relevance of NS1 SUMOylation and how it contributes to the pathogenicity during influenza viral infection.

For these studies, recombinant viruses were synthesized from plasmids encoding the influenza viral genome using an 12-plasmid based reverse genetics system as shown in **Figure 2.1** (Pekosz, He et al. 1999, Neumann and Kawaoka 2002, Neumann, Fujii et al. 2005). In the 12-plasmid system, four of the plasmids, each carrying one of the genes for the structural components of the viral polymerase (PB2, PB1, PA, and NP), have an RNA polymerase II promoter, thus allowing for the production of messenger RNA coding for those genes and the subsequent synthesis of the encoded proteins. The remaining eight plasmids, each carrying one of the influenza viral gene segments, under a RNA polymerase I promoter, allow for the production of viral RNA. The viral polymerase, produced by the four RNA polymerase II plasmids, will then initiate viral replication and transcription of the vRNA produced by the RNA polymerase I plasmids. In the 8-plasmid system, each of the plasmids carries one influenza viral gene segment flanked by both RNA polymerase I and RNA polymerase II

promoters, which allow for the production of viral RNA and messenger RNA from the same template (Neumann, Fujii et al. 2005).

Plasmids were generated containing the NS1 from Puerto Rico (PR8) influenza strain within the A/Wilson Smith Neurotropic/1933 (WSN) gene constellation. This substitution was made due to the strong interferon blocking ability of the PR8 NS1 (Hayman, Comely et al. 2006, Kochs, Garcia-Sastre et al. 2007, Kuo, Zhao et al. 2010). The main SUMOylation sites within the NS1 from A/Puerto Rico/8 1934 have been identified as lysine residues K70 and K219 (Santos, Pal et al. 2013), the latter of which is not a SUMOylation site within WSN NS1. **Table 2.1** describes each of the recombinant viruses that were developed and the modifications that were introduced into the plasmid that encodes the PR8 NS gene segment. A complete list of all the plasmids developed is shown in Appendix A.

The shifted mutants were developed in order to prevent introducing an asparagine to histidine substitution at amino acid residue 62 within NS2 when the K219A mutation is introduced. The shifted constructs were constructed by mutating the splicing acceptor site within the NS gene segment, followed by the introduction of a copy of the second exon for NS2, including a functional splicing acceptor site, downstream from the stop codon for NS1 (**Figure 2.2**). This construct encoded the shifted wild-type NS gene segment used to develop the WSN/T7T7[NS1~NS2] recombinant virus. To develop the shifted double mutant construct, two lysine to alanine mutations were inserted at positions 70 and 219 within the NS gene segment (**Figure 2.2**). This construct encoded the shifted double-mutant NS gene segment used to develop the WSN/T7T7[NS1K70AK219A~NS2] recombinant virus.

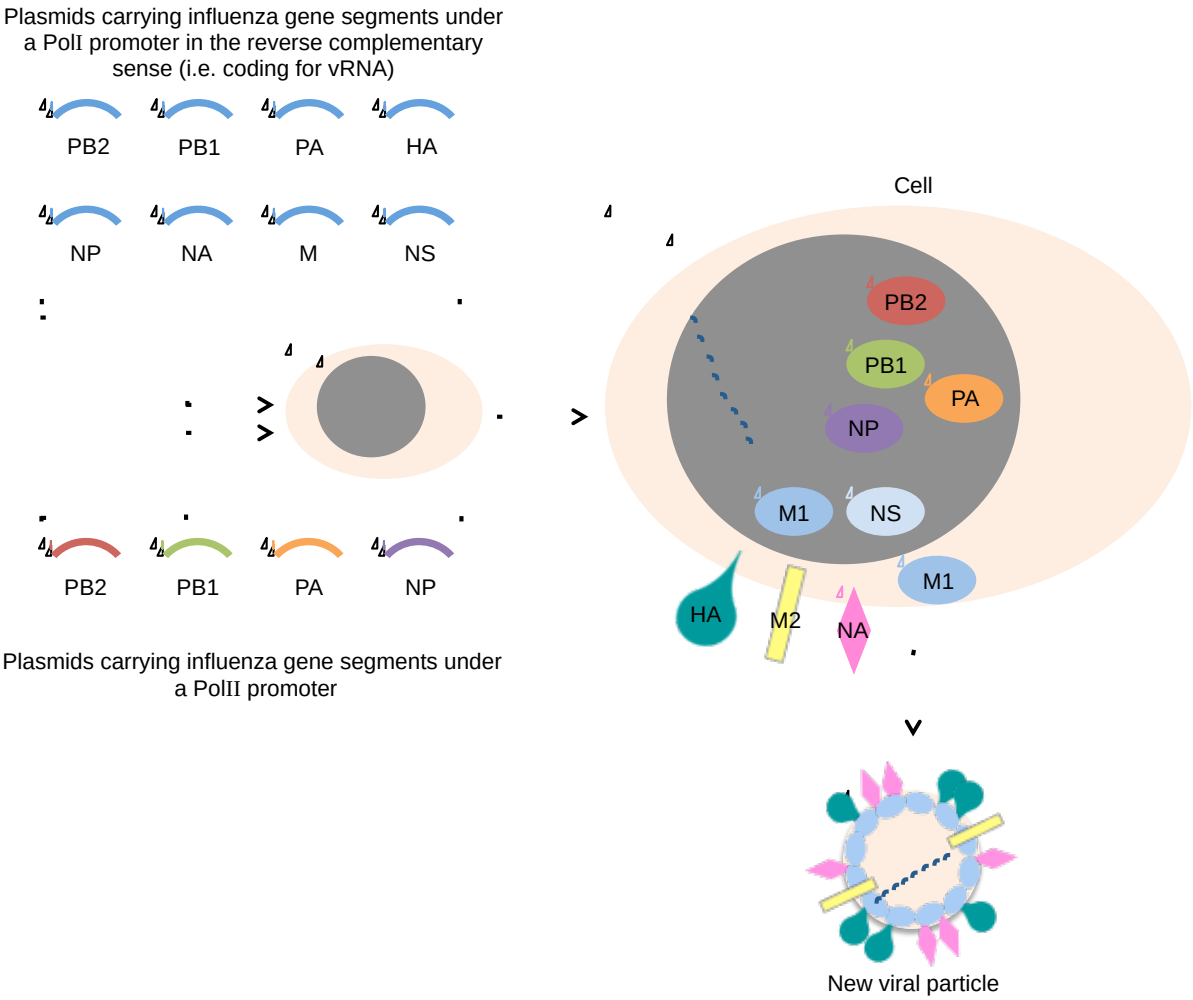

Figure 2.1. Diagram of the 12-plasmid based reverse genetics system. Full length cDNAs of the eight gene segments were cloned into RNA polymerase I (Pol I) based plasmids. In addition, full length cDNAs expressing PA, PB1, PB2 and NP gene segments, which are required for transcription and replication of vRNAs, were cloned into Pol II based plasmids. The 12 plasmids are then co-transfected allowing for the production of replication competent viral particles.

Table 2.1 Properties of the recombinant viruses developed and their modifications

Recombinant viruses	Gene constellation	NS gene segment	T7T7 tag	Other modifications
1. WSN/NS	WSN	WSN	No	none
2. WSN/T7T7NS	WSN	PR8	Yes	none
3. WSN/T7T7[NS1K70AK219A]	WSN	PR8	Yes	SUMOylation deficient
4. WSN/T7T7[NS1~NS2]	WSN	PR8	Yes	Shifted NS2
5. WSN/T7T7[NS1K70AK219A~NS2]	WSN	PR8	Yes	Shifted NS2; SUMOylation deficient

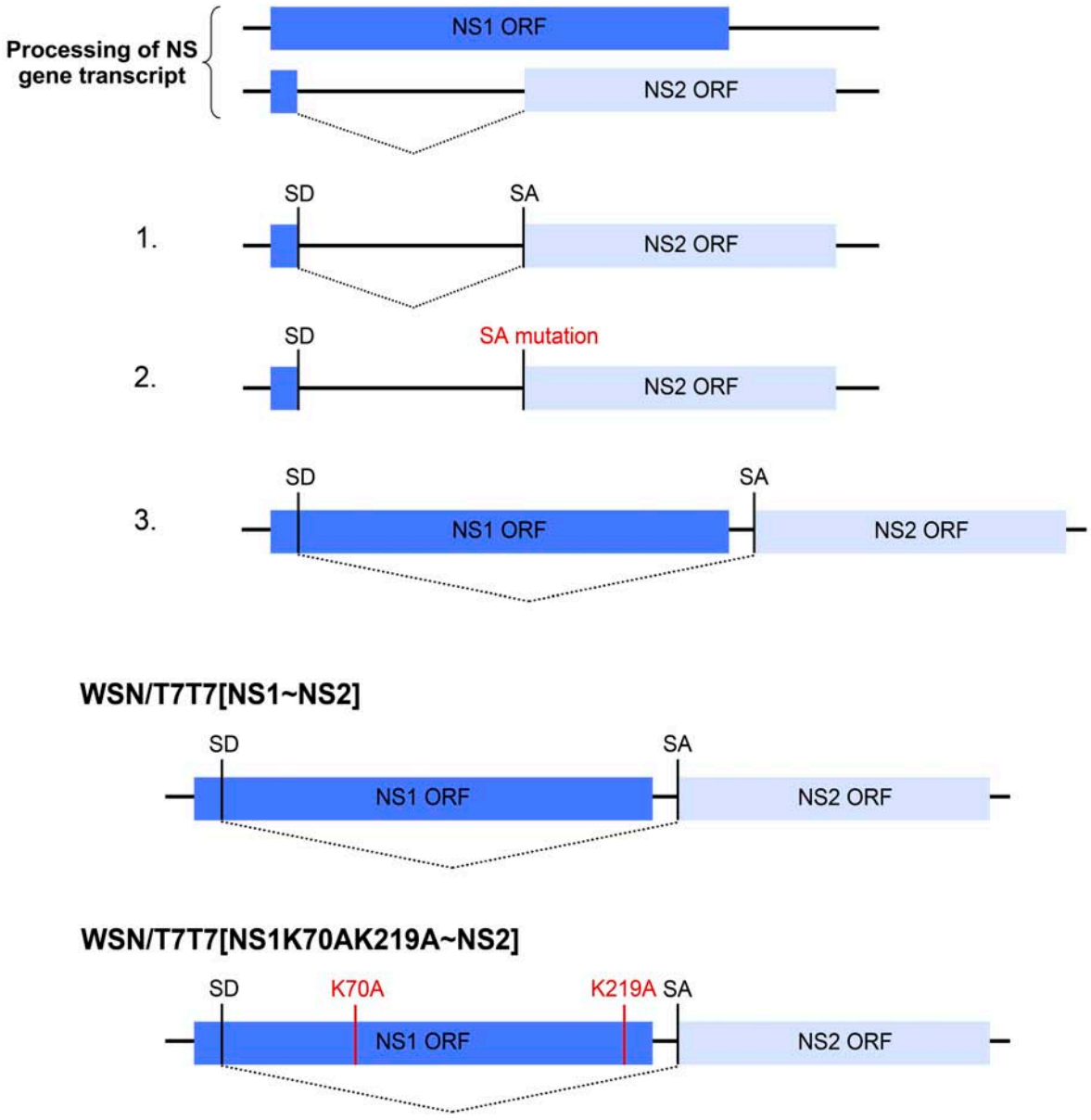

Figure 2.2. Generation of shifted NS constructs. The shifted constructs were developed: 1) identification of the splicing donor (SD) and splicing acceptor (SA) sites for NS2; 2) mutation of the splicing acceptor site alleviating the overlap of the NS1 and NS2 ORFs and preventing NS2 production; and 3) cloning of the NS2 ORF downstream of the NS1 stop codon, including the splicing acceptor site. ORF: open reading frame.

2.2 Materials and Methods:

Cells and viruses

HEK293FT cells (Invitrogen Corp., Carlsbad, CA), MDCK cells (ATCC, Manassas, VA) and VERO cells (ATCC) were maintained in complete medium consisting of 1x Dulbecco's modified eagle medium (DMEM) supplemented with high glucose, L-glutamine, sodium pyruvate (Corning Incorporated Life Sciences, Corning, NY), and 10% fetal bovine serum (Atlanta Biologicals, Inc., Flowery Branch, GA). For HEK293FT cells, Geneticin (Invitrogen Corp.) was added to the complete medium at a final concentration of 500 µg/mL. All cell lines were maintained at 37°C incubator at 5% CO_2. Influenza A/Puerto Rico/8/1934 H1N1 (referred to as PR8) was a gift from John M. Quarles (Department of Microbial and Molecular Pathogenesis, College of Medicine, Texas A&M Health Sciences Center). PR8 virus was propagated in MDCK cells at a multiplicity of infection (MOI) of 0.001 by using 1x DMEM supplemented with 0.2% bovine serum albumin (BSA) and 2 µg/mL tosyl-phenylalanyl-chloromethyl-ketone (TPCK)-treated trypsin (Worthington Biochemical Corp., Lakewood, NJ).

Plasmids

The recombinant influenza viruses used in this study were generated as previously described (Santos, Pal et al. 2013). In brief, the A/WSN/1933 [H1N1] 12-plasmid reverse genetics system (Neumann, Watanabe et al. 1999) was provided by Yoshihiro Kawaoka (Department of Pathobiological Sciences, School of Veterinary Medicine, University of Wisconsin-Madison, Madison, WI). A double T7-tag insert was inserted at the N-terminus of the NS1 open reading frame of our laboratory strain of A/Puerto Rico/

8/1934 [H1N1] by using the Phusion site-directed mutagenesis kit (Finnzymes, Woburn, MA) according to the manufacturer's protocol. Specific mutations in the sequence of NS1 were inserted by using the same site-directed mutagenesis approach, resulting in the expression constructs for T7T7[NS1K70A], T7T7[NS1K219A], and the double mutant T7T7[NS1K70AK219A]. To generate the pPol1/WSN/T7T7NS1 construct, the pPol1/WSN/NS construct from the 12-plasmid reverse genetics system (Neumann, Watanabe et al. 1999) was PCR amplified using primers complementary to the 5' untranslated region (UTR) and the 3' UTR of the WSN NS gene segment, producing a PCR product containing the backbone of the original plasmid, and the 5' and 3' UTRs of the NS gene segment from our PR8 strain. This PCR product was ligated with the PCR-amplified coding region of the NS gene segment from the PR8 strain. Similar overall approaches were used to mutate the splicing acceptor site in the NS gene segment and generate the splicing-deficient pPol1/WSN/T7T7NS1-derived mutants, pPol1/WSN/T7T7[NS1-SplAccptMut] and pPol1/WSN/T7T7[NS1K70AK219A-SplAccptMut], and their NS2-shifted derivative constructs pPol1/WSN/T7T7[NS1~NS2] and pPol1/WSN/T7T7[NS1K70AK219A~NS2].

Transient transfections and generation of recombinant viruses by reverse genetics

HEK293FT cells (Invitrogen Corp.) were seeded at a density of 5 x 10^5 cells/well into 6 well plates. The following day, cells were transfected by liposome-mediated transfection using 13 µg of CsCl-purified plasmids and 26 µL of TransIT-LT1 (Mirus Bio LLC, Madison, WI) per well, according to the manufacturer's recommendations. Cells were incubated at 37ºC in 5% CO_2 for 24 hours. The culture supernatant was then discarded

and replaced with 1x DMEM supplemented with 0.2% BSA and 2 µg/mL TPCK-treated trypsin. The cells were further incubated for another 48 hours at 37ºC in 5% CO_2, and the culture supernatants were subsequently collected and used for plaque assays.

Plaque assays

MDCK cells were plated into 6-well plates at a density of 1 x 10^6 cells/well in 1x DMEM supplemented with 10% fetal bovine serum (Atlanta Biologicals) and incubated at 37°C in 5% CO_2 until the cells formed a confluent monolayer. The cells were then washed twice with 1x DMEM, and a virus dilution prepared in 1ml of 1x DMEM supplemented with 0.2% BSA was added to the cells and incubated with the cells at 35°C for 1 hour. The supernatant was removed and a 3-mL overlay of 1x DMEM supplemented with TPCK-treated trypsin (at a final concentration of 1%) and 0.6% SeaKem ME agarose (Lonza, Rockland, ME), maintained at 39.5°C using a bench-top heater-shaker, was poured over the cells and allowed to solidify for 20 minutes at room temperature. The cells were subsequently incubated at 35°C in 5% CO_2, and starting at 24 hours post-infection, the cells were visually screened for the presence of plaques. When the size of the plaques observed reached 1 to 2 mm in diameter, the overlay was removed, and the cells were fixed and stained with a solution containing 0.12% crystal violet in 20% ethanol.

Alternatively, for plaque purification of recombinant viruses, the overlay was left in place, and well-isolated plaques were transferred into a vial containing 1x DMEM plus 0.2% BSA by using a sterile 1-mL pipette. All of the viruses produced were purified by two consecutive rounds of plaque purification. During the second round of purification,

plaques of identical diameter (as measured under a microscope) were selected as a method to initiate the experiment with similar virus numbers. The plaques selected were incubated in 1 mL of 1x DMEM plus 0.2% BSA at 4ºC for 4 hours to allow the virus to diffuse out of the the agarose plug. Subsequently, the whole volume of 1x DMEM plus 0.2% BSA, including the agarose plug, was added to a confluent monolayer of MDCK cells or Vero cells plated onto 10 cm^3 petri dishes in 1x DMEM supplemented with 0.2% BSA and TPCK-treated trypsin at a final concentration of 1%. At 24 and 48 hours post-infection, the culture supernatants were removed, and their virus titers were analyzed by plaque assay.

Animal infections

All animal experiments were approved by the institutional animal care and use committee of the University of Maryland-College Park, Department of Veterinary Medicine. Female, 6-week-old DBA/2J mice (The Jackson Laboratory, Bar Harbor, ME) were used for viral pathogenicity experiments. Mice were anesthetized in groups of five by isoflurane inhalation and infected intranasally with $1x10^5$ PFU of the respective virus in 50 µL of PBS. To determine differences between clinical signs of disease, a 0-1-2-3 scoring scale was used, with 0 and 3 representing normal and severe, respectively (Koudstaal, Koldijk et al. 2009). Animals were observed for 6 days for clinical signs of infection. Viral pathogenicity (viral titers and gross and histopathology) was studied in two groups of twenty mice over 6 days. Four mice from each group were sacrificed on days 0, 1, 2, 4, and 6 after inoculation and lungs, trachea, nasal turbinates, kidney, and brain were removed from each mouse and immediately stored at -80°C in PBS.

$TCID_{50}$ to determine viral titers

MDCK cells were plated into 96-well plates at a density of 1.6 x 10^5 cells/well in 1x DMEM supplemented with 10% FBS and incubated at 37°C in 5% CO_2 until the cells formed a confluent monolayer. The cells were then washed once with 1x DMEM, and a virus dilution prepared in 1ml of 1x DMEM supplemented with 0.2% BSA was added to the cells and incubated with the cells at 37°C in 5% CO_2 for 3 days until cytopathic effects (CPE) were observed. 50 µL of the supernantants from $TCID_{50}$ plates were transferred to a 96-well V-bottom plate (Corning Incorporated Life Sciences). 50 µL of 0.5% turkey red blood cells (Lampire Biological Laboratories, Pipersville, PA) suspended in 1x PBS, were added to the V-bottom plate and gently tapped to mix. Plates were incubated at room temperature for 45 minutes. Plates were scored and viral titers were determined using the Reed-Muench method.

Histology

A portion corresponding to approximately 10% of lung tissue from mice at days 4 and 6 post-inoculation were dissected, washed in sterile PBS, and fixed in 10% neutral phosphate buffered formalin (NBF). Tissue samples were embedded in paraffin, cut into 5-µm-thick sections, and stained with hematoxylin and eosin (H&E) for histopathological examination or were processed for analysis by immunohistochemistry.

Viral titration and viral RNA sequencing

A confluent 96-well tissue culture plate of MDCK cells was prepared one day before the virus titration. Virus was titrated in lungs, trachea, nasal turbinates, kidney, and brain.

Tissues were homogenized in PBS using a bead mill homogenizer (Tissue Lyser, Qiagen, Valencia, CA). Cell debris was pelleted by centrifugation and supernatant was titrated on MDCK cells. Cells were washed once with PBS and serial dilutions were performed (from 1 $\log_{10}$ to 10 $\log_{10}$ dilutions) in serum-free 1x DMEM medium supplemented with 1% penicillin/streptomycin (Corning Incorporated Life Sciences) and 1% TPCK-treated trypsin (Sigma, Oakville, ON). Viral dilutions were added onto the plates and at 72 hours post-infection the plates were scored for cytopathic effect. 50 µL of the supernantants from $TCID_{50}$ plates were transferred to a 96-well V-bottom plate (Corning Incorporated Life Sciences). 50 µL of 0.5% turkey red blood cells (Lampire Biological Laboratories) suspended in 1x PBS, were added to the V-bottom plate and gently tapped to mix. Plates were incubated at room temperature for 45 minutes. Titers were expressed as 50% tissue culture infectious dose ($TCID_{50}$) per mL using the Reed-Muench Method.

Total RNA was extracted using the RNeasy Mini Kit (Qiagen). A reverse transcription product of the viral RNA was generated using the M-MLV Reverse Transcriptase (Promega, Madison, WI) and using the previously described UNI-12 primer (Hoffmann, Stech et al. 2001) targeting the 12 conserved nucleotides at the 3' end of all viral RNA gene segments. A secondary set of primers were used to target the amplification of the NS gene segment through the generation of two overlapping read-outs.

Immunoblot analyses

Prior to SDS-PAGE analyses, all cell extracts generate were passed several times through a 29½ gauge needle to break down the genomic DNA released and to decrease the viscosity of the samples. β-mercaptoethanol was added up to a final concentration of 10%, and the samples were boiled in a water bath for 3 minutes. The samples were resolved by 10% SDS-PAGE gels made in-house and, subsequently, the proteins were transferred to Immobilon-FL (Millipore Corp., Bedford, MA) for use with IRDye-conjugated secondary antibodies (LI-COR Biosciences Inc., Lincoln, NE) and infrared fluorescence imaging.

Infrared fluorescence imaging

Immobilon-FL membranes (Millipore Corp.) were washed four times in 1x PBS, blocked with Odyssey Blocking Buffer (LI-COR Biosciences Inc.) for a minimum of 1 hour at room temperature, and incubated in Odyssey Blocking Buffer at 4°C overnight with the primary antibody at the indicated dilution. The membranes were then washed four times with 1x PBS, supplemented with 0.1% polysorbate 20 (Tween 20), and incubated with Odyssey Blocking Buffer with the appropriate highly cross-absorbed IRDye 800 CW- and IRDye 680 LT-conjugated secondary antibodies (LI-COR Biosciences Inc.) at the indicated dilution. The membranes were then washed four times with 1x PBS, supplemented with 0.1% Tween 20 and twice again with 1x PBS and scanned on an Odyssey CLx infrared imaging system (LI-COR Biosciences Inc.). Quantitative analyses of the images obtained was performed by using Odyssey Infrared Imaging System Application software version 3.0.29 (LI-COR Biosciences Inc.). Statistical analyses and

graphics of the data generated were performed by using GraphPad Prism version 5.04 for Windows (GraphPad Software Inc., San Diego, CA).

Immunohistochemistry

Approximately 10% of lung tissue from mice at days 4 and 6 post-inoculation were dissected, washed in sterile PBS, and fixed in 10% NBF. Tissue sample were embedded in paraffin, cut into 5-um-thick sections, and mounted onto glass slides. Paraffin was removed using two washes of xylene followed by ethanol gradient (100%, 95%, and 80%) washes. A 70% ethanol wash was supplemented with 0.25% ammonia and incubated for 1 hour at room temperature. Slides were incubated in 50% ethanol followed by two washes in 1x PBS to rehydrate the tissues. Antigens within the tissues were unmasked by incubating in 1 mM ethylenediaminetetraacetic acid (EDTA) and heated in a microwave on full power until the buffer began to boil. The tissues were let cool for 20 minutes and washed three times with 1x PBS, the last of which was supplemented with sodium borohydride (Sigma Aldrich, St. Louis, MO) at a concentration of 10 mg/mL, to minimize the autofluorescence of the tissues, and followed by four washes with 1x PBS.

Tissue sections were drained and a hydrophobic barrier was drawn around each tissue using an ImmEdge Pen (Vector Laboratories, Burlingame, CA). In order to permeabilize the tissues, the sections were washed twice with 1x PBS, the second of which was supplemented with 0.2% Triton X-100 (MP Biomedicals, Santa Ana, CA), and followed by three washes with 1x PBS. Sections were blocked with 1x PBS with 1% goat serum for 1 hour at room temperature and incubated in 1x PBS with 1% goat

serum at 4C overnight with the primary antibody at the indicated dilution. The sections were then washed four times with 1x PBS and incubated with 1x PBS with 1% goat serum supplemented with the appropriate highly cross-absorbed AlexaFluor 594 and 488 fluorophore conjugated secondary antibodies (Life Technologies Inc.) at the indicated dilution. Sections were washed three times in 1x PBS followed by one wash with 1x PBS supplemented with 4',6-diamidino-2-phenylindole, dihydrochloride (DAPI) (Thermo Scientific) at a final concentration of 0.5 ug/mL. Sections were washed in 1x PBS, glycerol and glass cover slips were added, and slides were sealed with clear nail polish.

Statistical analysis and computer software.

All statistical analyses and graphics presented were performed by using GraphPad Prism version 5.04 for Windows (GraphPad Software Inc.). All figures were created by using Adobe Photoshop CS5 extended version 12.0.3 X64 (Adobe Systems Inc., San Jose, CA).

2.3 Results:

NS1 SUMOylation affects viral growth in IFN-competent and IFN-deficient host cells. Previous studies had shown that out of all the viral proteins produced during influenza viral infections, the NS1 protein was the most extensively SUMOylated protein **(Pal, Santos et al. 2011)**. To determine the effect of NS1 SUMOylation on viral infection, recombinant viruses containing either a SUMOylatable NS1 (referred to as WSN/T7T7[NS1~NS2]) or a non-SUMOylatable NS1 (referred to as WSN/T7T7[NS1 K70AK219A~NS2]) were used to infect MDCK cells. Infection with the WSN/ T7T7[NS1~NS2] virus produced viral titers in the 1-3 x 10^7 PFU/mL range in MDCK cells 24 hours post-infection (hpi). Infection with the WSN/T7T7[NS1K70AK219A~NS2] virus produced significantly lower viral titers of 3.5 x 10^3 PFU/mL, approximately 2.5-logs lower than titers obtained after infection with the WSN/T7T7[NS1~NS2] virus (**Figure 2.3A)**. At 48 hpi, infection with the WSN/T7T7[NS1K70AK219A~NS2] virus resulted in slightly lower titers than infection with the WSN/T7T7[NS1~NS2] virus. To determine if this difference was due to an alteration of NS1‘s ability to neutralize the IFN response, we used the same recombinant viruses to infect Vero cells, which are incapable of producing type-1 IFN (**Figure 2.3B**). Infection with the WSN/ T7T7[NS1~NS2] virus produced viral titers in the 2-5 x 10^4 PFU/mL range 24 hpi and 0.7-1.1 x 10^6 PFU/mL at 48 hpi. Infection with the WSN/T7T7[NS1K70A K219A~NS2] virus resulted in significantly lower viral titers of 2.3 x 10^2 PFU/mL at 24 hpi, and appeared to have stopped growing, as the titers appear similar at 48 hpi (**Figure 2.3B**). In addition, during the plaque purification steps we observed that plaque formation by the WSN/T7T7[NS1K70AK219A~NS2] virus resulted in dramatically smaller plaques

than plaques produced by the WSN/T7T7[NS1~NS2] virus (**Figure 2.3C**). When the differences were quantified, plaques resulting from infection with the WSN/T7T7[NS1 K70AK219A~NS2] virus were approximately 2.5 times smaller than those that formed from infection with the WSN/T7T7[NS1~NS2] virus (**Figure 2.3D**).

Infection with an influenza viral mutant expressing a non-SUMOylatable PR8 NS1 results in an increase in clinical symptoms, morbidity, and mortality in the mouse model. Due to the differences in viral titers between viruses containing a SUMOylatable and non-SUMOylatable NS1, we sought to determine the effect of NS1 SUMOylation in an animal model. The overall approach for this experiment is shown in **Figure 2.4**. Each infected mouse was assigned an average clinical score associated to viral infection ranging from 0 to 3, with 0 being normal and 3 being the lethal endpoint required by the IACUC protocol. At days 0, 1, and 2 all mice were assigned a clinical score of 0 indicating no signs of infection and/or normality (**Figure 2.5A**). At day 4 post-infection, mice infected with the either virus showed an increase of average clinical score to 1, characterized by weight loss and lack of grooming. By day 6 post-infection, the mice infected with the WSN/T7T7[NS1~NS2] virus were assigned an average clinical score of 2, characterized by further weight loss, between 10-20%, rough coat, and reduced motility. Mice infected with the WSN/T7T7[NS1K70AK219A~NS2] virus were assigned an average clinical score of 3, characterized by even further weight loss, a very rough coat, immobility, and abnormal posture (**Figure 2.5A**). In addition to exacerbated clinical symptoms, infection with the WSN/T7T7[NS1K70AK219A~NS2] virus was also associated with increased average weight loss beginning 2 days post-

infection (p.i.) (**Figure 2.5B**). Interestingly, mice infected with the WSN/T7T7[NS1~NS2] recombinant virus gained weight at day 2 post-infection, followed by significant weight loss by day 4 post-infection (**Figure 2.5B**). On the contrary, mice infected with the WSN/T7T7[NS1K70AK219A~NS2] recombinant virus showed consistent weight loss over the 6 days post-infection (**Figure 2.5B**). The mortality rate was also slightly higher in the WSN/T7T7[NS1K70AK219A~NS2] infected mice, resulting in three deaths, and the WSN/T7T7[NS1~NS2] infection resulting in only one death (**Figure 2.5B**).

Infection with an influenza viral mutant expressing a non-SUMOylatable PR8 NS1 also results in viral detection in a broader range of organs. To determine differences in viral replication in an animal model, we assessed viral titers at day 1, 2, 4, and 6 post-infection. The recombinant virus containing a non-SUMOylatable form of NS1 produced viral titers similar to the recombinant viruses containing a SUMOylatable form of NS1 in the lungs, trachea and nasal turbinates at days 1, 2, 4, and 6 post-infection (**Figure 2.6A-C**). Viruses were detected in the kidney (**Figure 2.6D**) and brain (**Figure 2.6E**) day 6 post-infection, with viral titers of 8.4×10^2 and 1.0×10^2 $TCID_{50}$/mL, respectively, in mice infected with the WSN/T7T7[NS1K70AK219A~NS2] virus, while no viruses were detected in those organs in mice infected with the WSN/T7T7[NS1~NS2] virus.

In order to verify that the data collected during viral infection could be attributed to the presence of the indicated mutations known to prevent NS1 SUMOylation, total RNA was isolated from the lungs collected at days 1, 2, 4, and 6 post-infection from four mice per group. The NS gene segment was amplified by RT-PCR and the resulting

cDNA was sequenced using a series of sequencing primers designed to generate overlapping read outs. The chromatograms obtained indicated that some of the samples analyzed consisted of a diverse population of viruses that frequently carried mutations different from these initially introduced at codons 70 and 219 of NS1, as indicated by the overlapping peaks shown for the sequences derived around codons 70 and 219 for all the WSN/T7T7[NS1K70AK219A~NS2] infected animals (**Figure 2.7**). Although the viral population was mixed, the predominant peaks in the chromatogram represent nucleotides that would encode for either an alanine or a glutamic acid at residues 70 and 219 (**Figure 2.7**), two amino acid substitutions that still render NS1 non-SUMOylatable.

Infection with a recombinant virus expressing a non-SUMOylatable PR8 NS1 results in increased gross pathology and enhanced histopathological changes in the lung. Since the severity of influenza infection is frequently associated to the degree of lung damage produced, lungs harvested from WSN/T7T7[NS1~NS2] and WSN/T7T7[NS1K70AK219A~NS2] infected mice were evaluated for gross pathology and histopathology. In the first two days of infection, there was no change in the overall activity of the mice or the gross pathology of the lungs (data not shown). Beginning at day 4 post-infection, we observed that lungs harvested from both groups of infected mice displayed lung enlargement and the development of pulmonary hemorrhages (**Figure 2.8A**). More evident pathological changes were observed at day 6 post-infection in both groups of infected mice with the development of plum-colored pulmonary lesions, which sharply contrasted with the pink-colored lungs of non-infected

(healthy) mice (**Figure 2.9A**). Remarkably, the lesions observed in mice infected with the WSN/T7T7[NS1K70AK219A~NS2] virus were substantially more severe than those observed for mice infected with the WSN/T7T7[NS1~NS2] virus (**Figure 2.9A**), with lungs of WSN/T7T7[NS1K70AK219A~NS2] infected mice exhibiting complete hemorrhaging of the lungs and little to no visible pink-colored tissue.

To further examine the significance of NS1 SUMOylation on influenza viral infection, we evaluated histopathological changes in lung tissue from infected mice at days 4 and 6 post-infection (**Figure 2.8B and Figure 2.9B**). Viral infection with either WSN/T7T7[NS1~NS2] or WSN/T7T7[NS1K70AK219A~NS2] resulted in significant changes in lung architecture as compared to lung tissue from day 0 post-infection (**Figure 2.8B and 2.9B**). Infected lung tissue from WSN/T7T7[NS1~NS2] infected mice displayed severe bronchiolar hyperplasia 6 days post-infection (**Figure 2.9B**). In addition to bronchiolar hyperplasia, the WSN/T7T7[NS1K70AK219A~NS2] infected lung tissue also displayed epithelial necrosis with a complete loss of the epithelium (**Figure 2.9B**).

Microscopically, histopathological changes in all infected animals were characterized by moderate to severe bronchiolar lesions including necrosis, infiltration of cell debris, and epithelial hyperplasia (**Table 3**). Mice infected with the WSN/T7T7[NS1~NS2] virus exhibited mild to moderate alveolar lesions caused by the infiltration of inflammatory cells (**Table 3**). In contrast, mice infected with the WSN/T7T7[NS1K70AK219A~NS2] virus produced moderate to severe lesions which were further characterized by diffuse alveolar damage and the development of hyaline membranes. Mild vascular lesions were observed in both groups and were attributed to

perivascular cuffing with lymphocytes and occasional vasculitis (**Table 3**). The total lung scores for mice infected with the WSN/T7T7[NS1K70AK219A~NS2] virus were slightly higher than those from mice infected with the WSN/T7T7[NS1~NS2] virus.

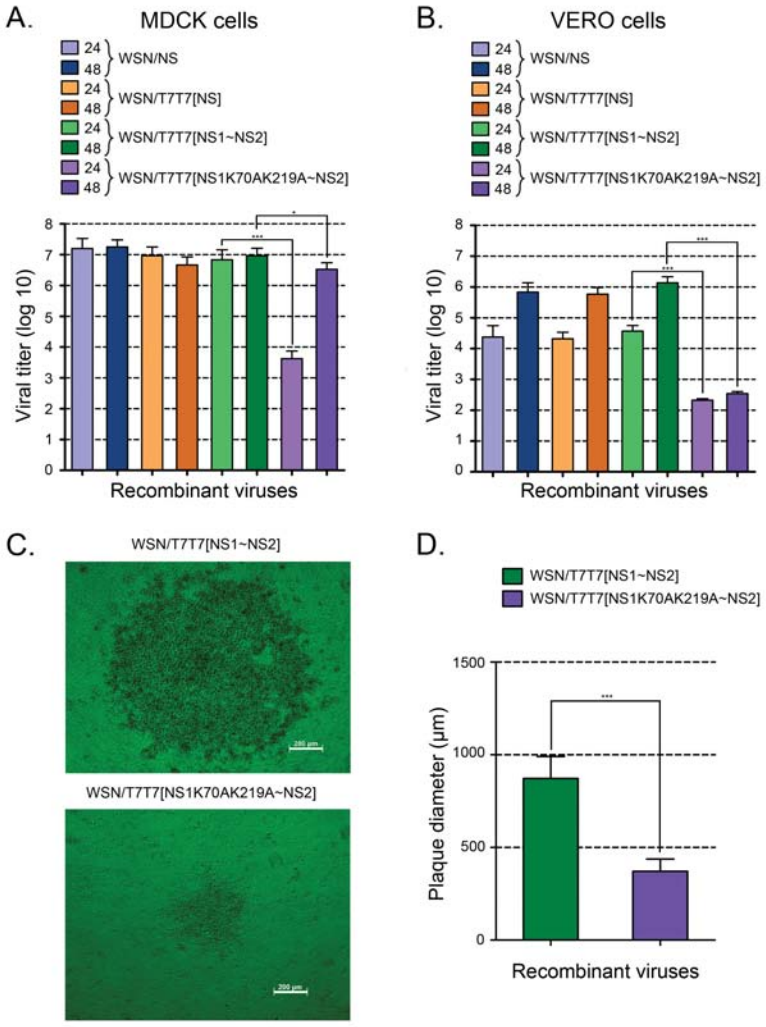

Figure 2.3. Mutations affecting NS1 SUMOylation decreases viral fitness in tissue culture. Viral growth of the recombinant viruses developed with the various pPolI/WSN/NS gene segments. All recombinant viruses generated by reverse genetics, including WSN/T7T7[NS1~NS2] and WSN/T7T7[NS1K70AK219A~NS2], were purified by two consecutive rounds of plaque purification. Plaques of identical diameter produced during the second round of plaque purification were inoculated over a confluent monolayer of either MDCK cells or Vero cells plated on 10 cm petri dishes. Twenty four and forty-eight hours post-infection the culture supernatants were removed and their viral titers analyzed by plaque assay. (A) Viral titers obtained with the supernatants collected from MDCK cells. (B) Viral titers obtained with the supernatants collected from Vero cells. (C) Representative plaques showing resulting plaque morphology. (D) Diameter of resulting plaques. The values presented in B correspond to the data obtained from the random sampling of 10 plaques. The values presented in C and D corresponds to the data obtained in 3 independent experiments. Error bars indicate standard deviation. *, $P < 0.05$. ***, $P < 0.0001$.

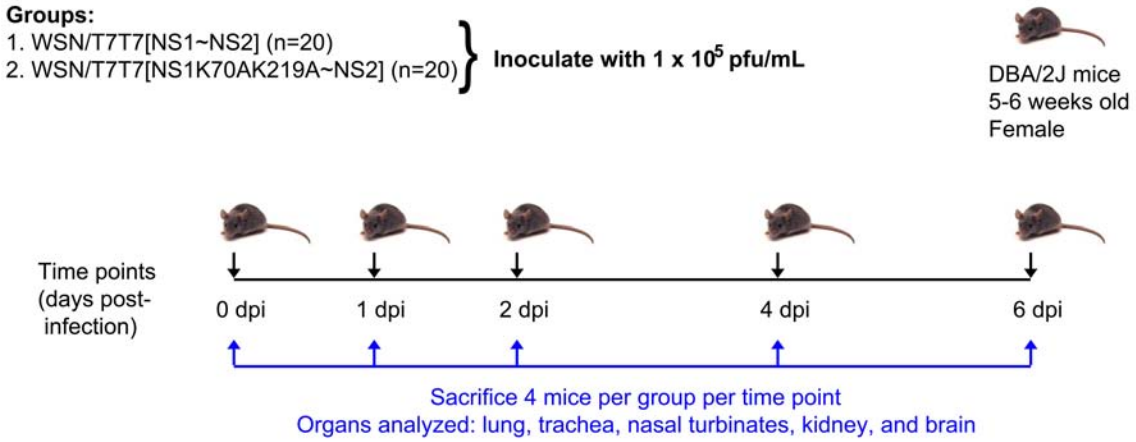

Figure 2.4. Overall experimental approach. 5-6 week old female DBA/2J mice were inoculated with one of the viruses indicated. At the indicated times post-infection, four animals per inoculation group were sacrificed and the organs were harvested for viral multiplication analysis and vRNA sequencing.

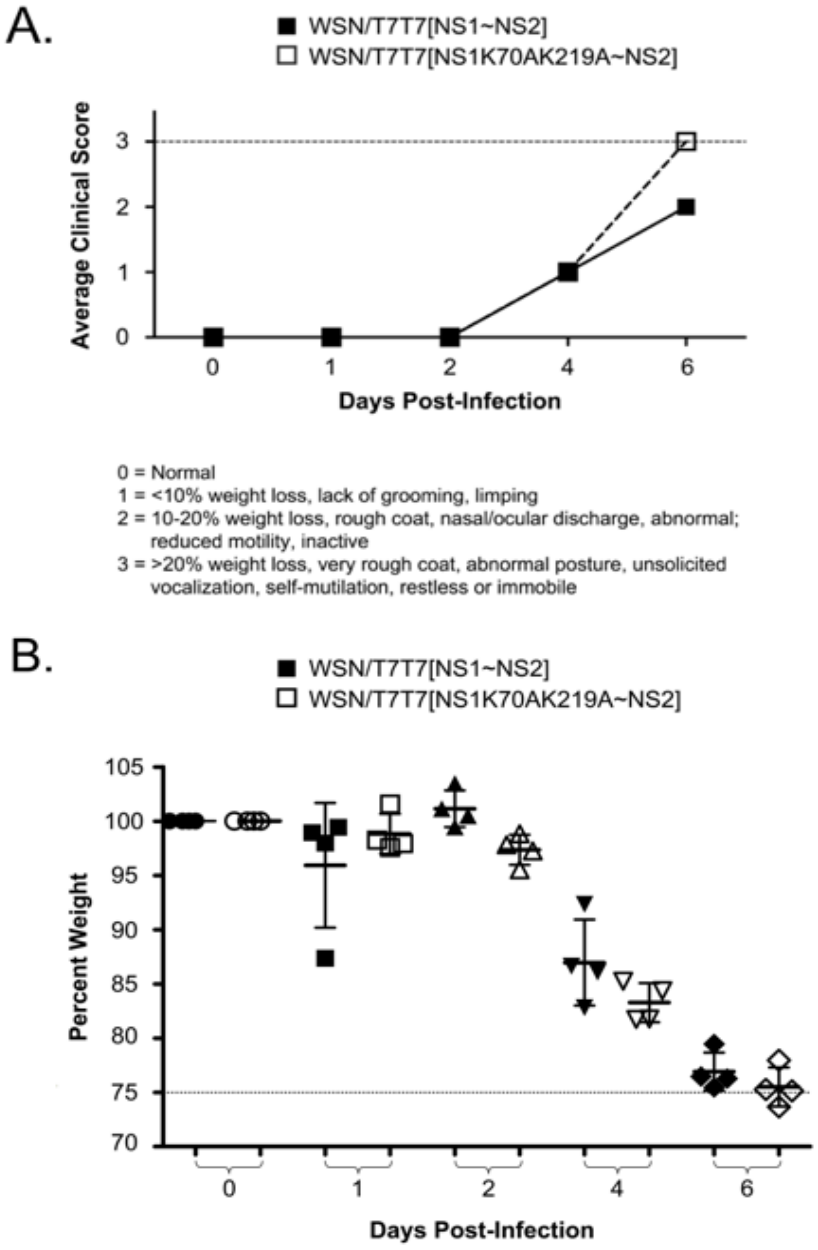

Figure 2.5. Impairment of NS1 SUMOylation does not affect survival but causes increased weight loss during viral infection in vivo. (A) Average clinical score of animals infected with either WSN/T7T7[NS1~NS2] or WSN/T7T7[NS1K70A K219A~ NS2]. (B) Average weight loss of animals infected with either WSN/T7T7[NS1~NS2] or WSN/T7T7[NS1K70AK219A]~NS2.

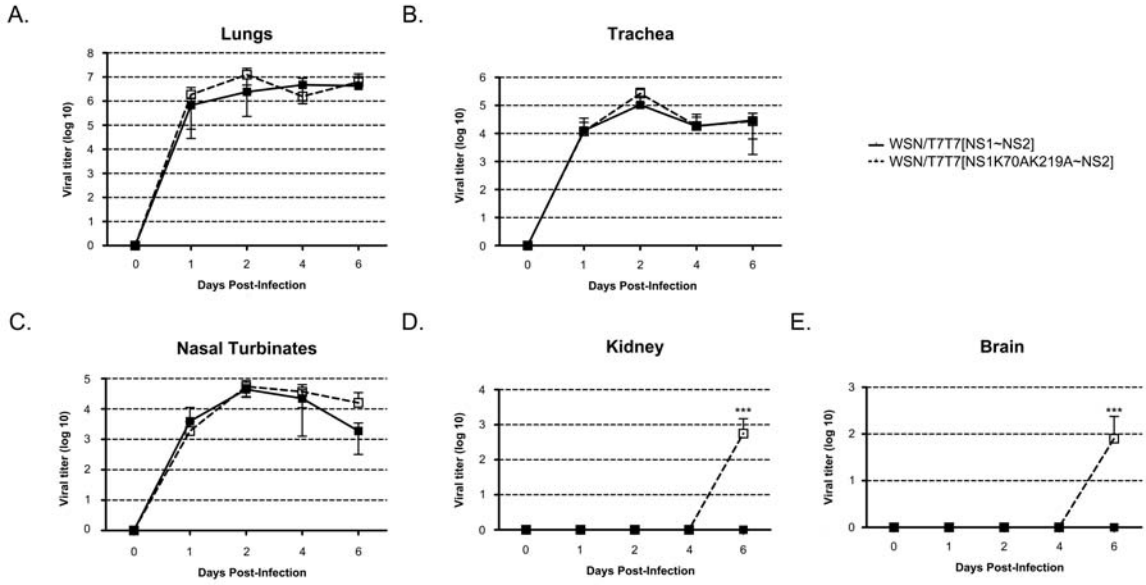

Figure 2.6. Impairment of NS1 SUMOylation results in viral detection in a broad range of organs. Viral titers of tissues from mice infected with either WSN/T7T7[NS1~NS2] or WSN/T7T7[NS1K70AK219A]~NS2. (A) Viral titers in lungs. (B) Viral titers in trachea. (C) Viral titers in nasal turbinates. (D) Viral titers in kidney. (E) Viral titers in brain. Error bars indicate standard deviation. ***, P<0.0001.

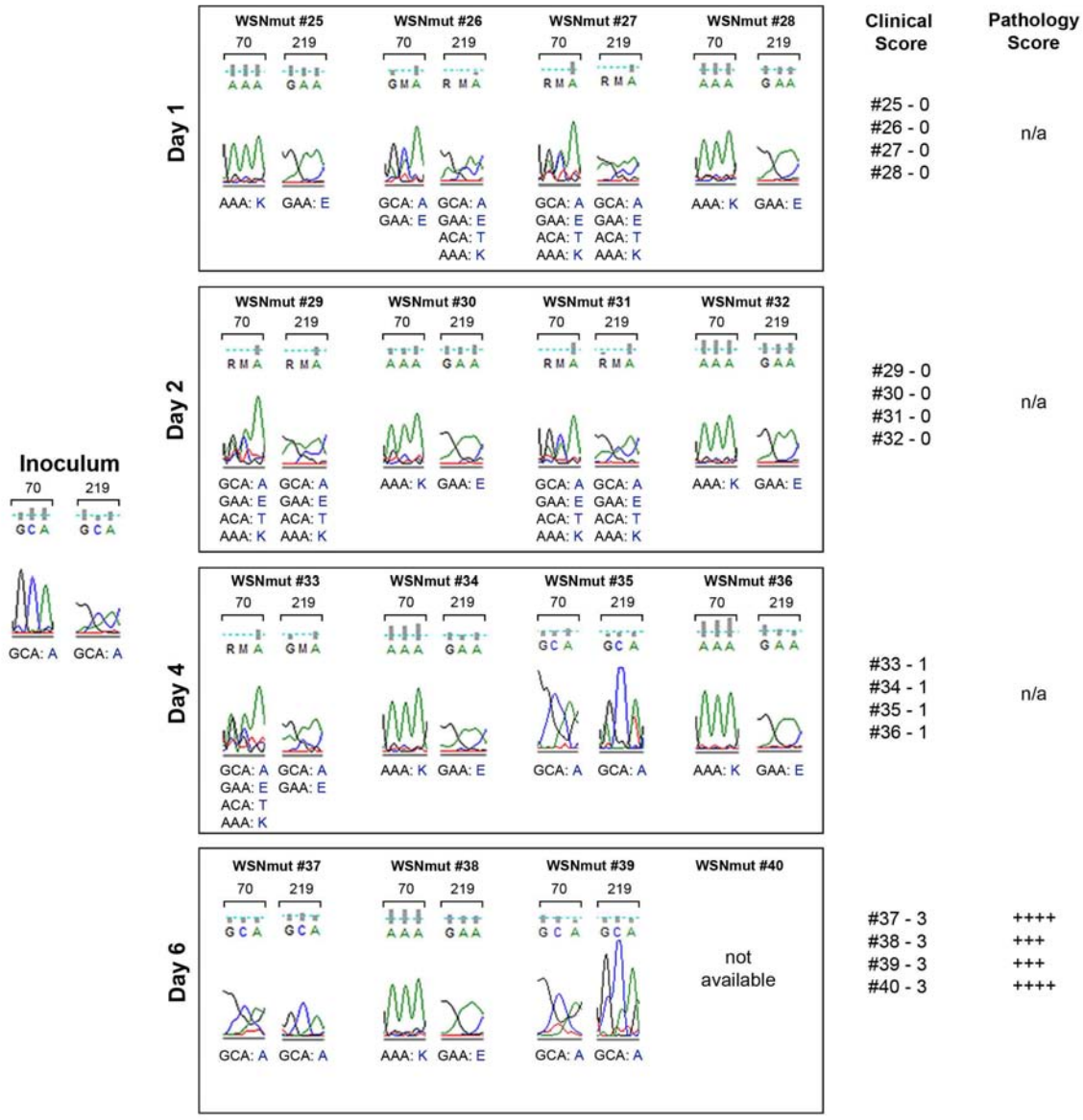

Figure 2.7. Viral replication *in vivo* results in a mixed population of viruses. Sequencing results of WSN/T7T7[NS1K70AK219A~NS2] viruses collected at 1, 2, 4, and 6 days post-infection.

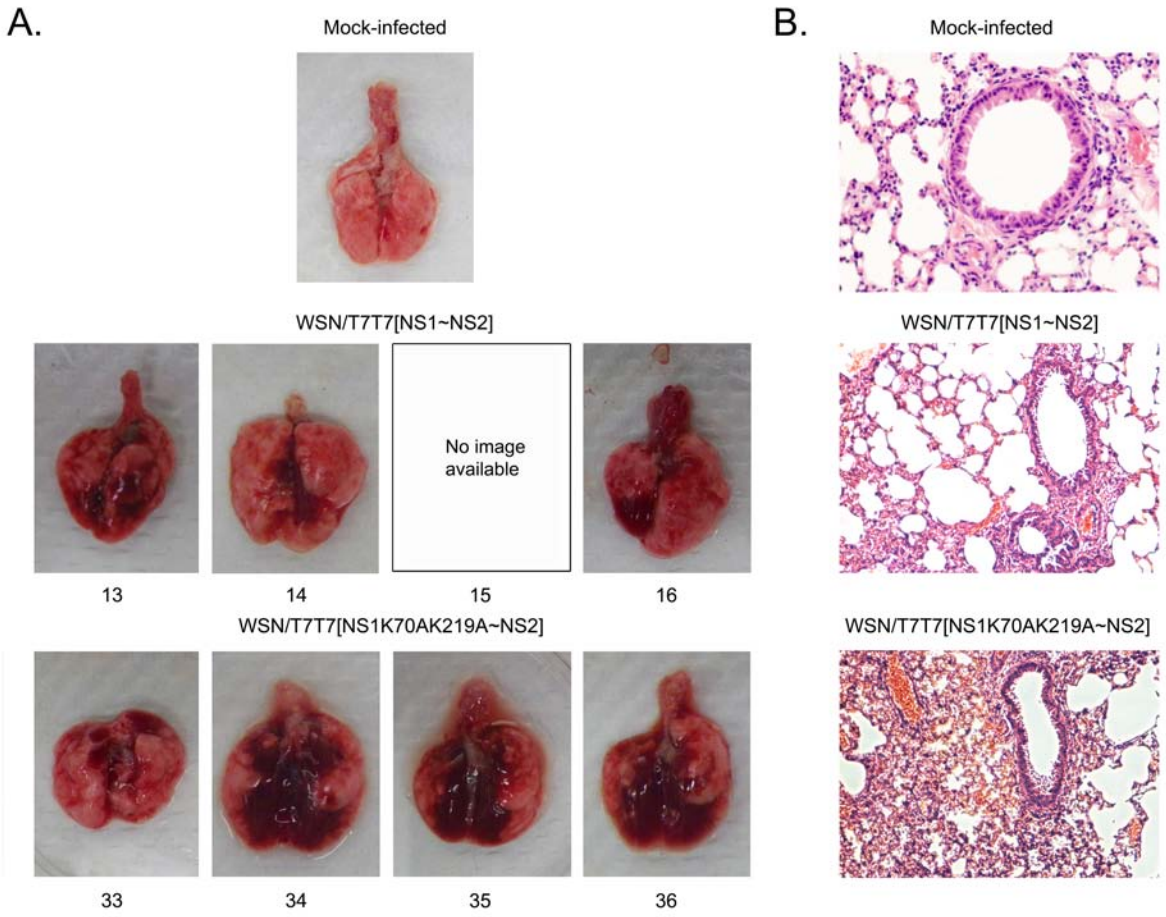

Figure 2.8. Viruses containing a non-SUMOylatable NS1 significantly enhance changes in gross pathology and histopathology in lungs from infected mice at 4 days post-infection. (A) Gross pathology of the lung after infection in a mock-infected control (top) or after infection with WSN/T7T7[NS1~NS2] (middle) or WSNT7T7[NS1K70AK219A ~NS2] (bottom) viruses. Mice were inoculated as described in Figure 1 legend and lungs harvested at day 4 post-infection. (B) Lungs were fixed in formalin, embedded in paraffin, sectioned, and mounted onto glass slides. Haematoxylin and eosin-stained sections of lung tissue from mice infected with recombinant viruses and sacrificed at day 4 post-infection. Images are shown at 200x magnification.

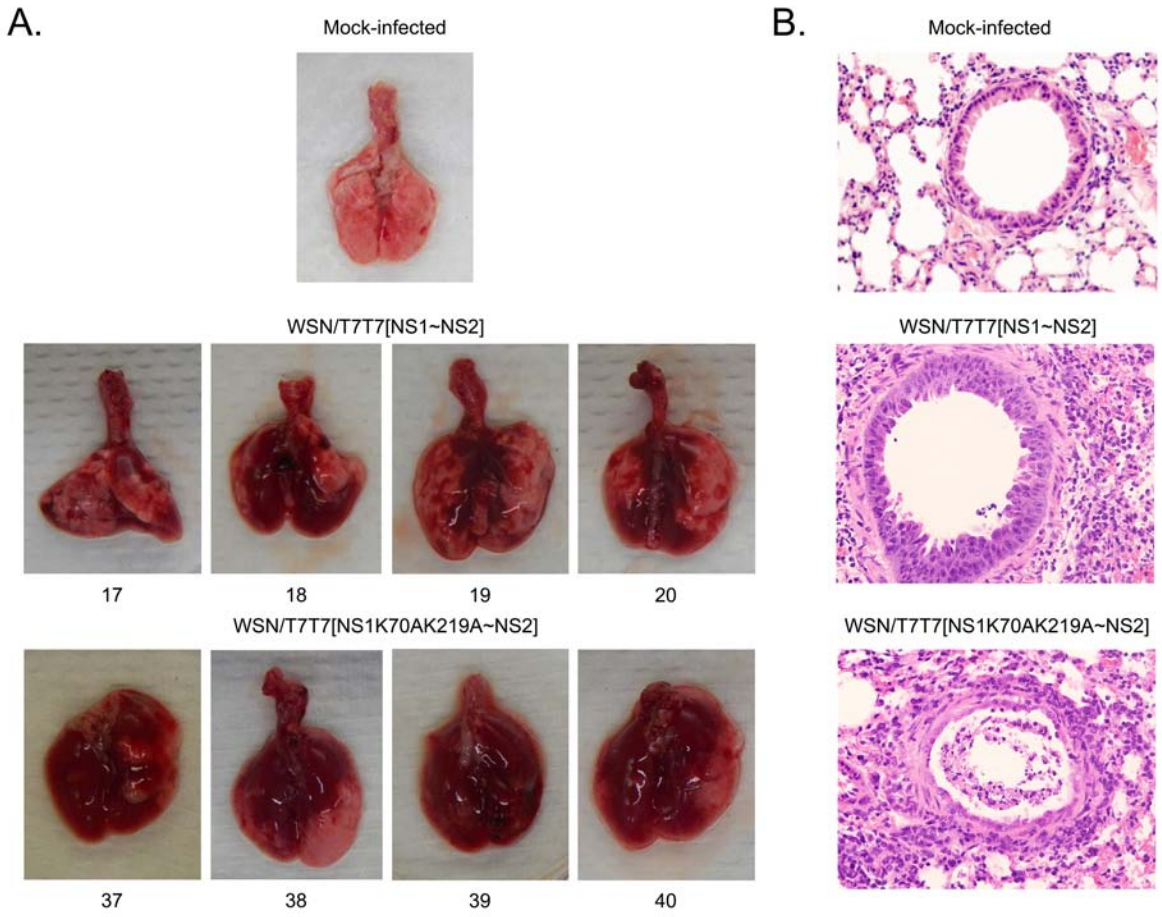

Figure 2.9. Viruses containing a non-SUMOylatable NS1 significantly enhance changes in gross pathology and histopathology in lungs from infected mice at 6 days post-infection. (A) Gross pathology of the lung after infection in a mock-infected control (top) or after infection with WSN/T7T7[NS1~NS2] (middle) or WSNT7T7[NS1K70AK219A~NS2] (bottom) viruses. Mice were inoculated as described in Figure 1 legend and lungs harvested at day 6 post-infection. (B) Lungs were fixed in formalin, embedded in paraffin, sectioned, and mounted onto glass slides. Haematoxylin and eosin-stained sections of lung tissue from mice infected with recombinant viruses and sacrificed at day 6 post-infection. Images are shown at 400x magnification.

Table 2.2 Pathology report from influenza infected lungs

Virus/ Animal #	Tissue	Lesion	Brochi/ Bronchioles	Alveoli	Vascular	Total Lung Score	Both Mutations?
WSN/T7T7[NS1~NS2]							
17	Lung	Bronchiolar-necrosis, hyperplasia	+++	+++	++	+++	n/a
18	Lung	Bronchiolar-necrosis, hyperplasia	+++	+++	++	+++	n/a
19	Lung	Bronchiolar-necrosis, hyperplasia	+++	+++	++	+++	n/a
20	Lung	Bronchiolar-necrosis, hyperplasia	+++	++	++	+++	n/a
WSN/T7T7[NS1K70AK219A~NS2]							
37	Lung	Alveoli-inflammation, edema/hyaline membranes**	+++	++++	++	++++	Yes
38	Lung	Bronchiolar-necrosis, hyperplasia, alveoli-edema	+++	+++	++	+++	No
39	Lung	Bronchiolar-necrosis, hyperplasia	++++	+++	++	+++	Yes
40	Lung	Bronchiolar-necrosis, hyperplasia	+++	+++	++	++++	n/a

- = no lesions; + = minimal lesions; ++ = mild lesions; +++ = moderate lesions; ++++ = severe lesions
** Most severely involved lung

2.4 Discussion:

Previous studies relating to the role of SUMOylation for the influenza virus non-structural protein NS1 had suggested a role for regulating the function of NS1 through the modulation of protein-protein interactions, thus limiting its ability to neutralize the host antiviral response (Santos, Pal et al. 2013). Despite the ongoing research related to the role of NS1 SUMOylation in tissue culture, this is the first and only study that investigates the role of SUMOylation of a viral protein in an animal model. Here, we evaluated the effects of mutations affecting NS1‘s ability to become SUMOylated in a mouse model of influenza infection. We demonstrated that compared with a virus carrying a SUMOylatable NS1 protein, infection with viruses containing a non-SUMOylatable NS1 resulted in increased clinical symptoms, morbidity, and mortality. Furthermore, the inhibition of NS1 SUMOylation enabled viral detection in a broad range of organs and increased the pathology of influenza viral infection. Overall, our results indicate that a non-SUMOylatable PR8 NS1 exhibits increased pathogenicity as compared to its SUMOylated counterpart.

In addition to the viral proteins HA, NA, PB2, and PB1-F2, NS1 has also been implicated as a pathogenicity factor for influenza viral infections (Hale, Randall et al. 2008, Tscherne and Garcia-Sastre 2011). Certain characteristics within NS1, such as glycine residue 184 (Steidle, Martinez-Sobrido et al. 2010) and the four C-terminal residues (Jackson, Hossain et al. 2008) have been identified as determinants for influenza virulence. Due to the increase in pathogenicity observed with the mutant virus, this study provides the first insight on whether the ability of NS1 to be SUMOylated may act as a good predictor of viral pathogenicity. Further studies would need to be

performed to determine whether these findings would be applicable to other influenza viral strains. Similar to the results using viruses containing a non-SUMOylatable M1 obtained by Wu, et al. (Wu, Jeng et al. 2011), tissue culture studies using viruses containing a non-SUMOylatable NS1 showed impaired viral growth (Santos, Pal et al. 2013). However, in these animal studies, there was no significant difference in viral titers between the wild-type and mutant virus in the lung, trachea or nasal turbinates over the course of viral infection.

Furthermore, in a study by Xu, et al. (Xu, Zhong et al. 2013), lysine residue 70 has been found to form hydrogen bonds with RNA, directly and indirectly, via water suggesting that K70 may play a role in RNA-dependent interactions. It is possible that the non-SUMOylatable NS1 may be able to bind double-stranded RNA more effectively, which has been shown to lead to a strong, prolonged activation of inflammatory cytokines and the innate immune response, as well as, an increase in the rate of viral replication (Kurokawa, Koyama et al. 1999). The sustained increase in the immune response, along with enhanced viral replication, leads to more severe pathology as observed in infections with highly pathogenic strains of influenza virus (Baskin, Bielefeldt-Ohmann et al. 2009). However, the SUMOylation of NS1 may alter its ability to bind double-stranded RNA resulting in the activation and induction of genes relevant to the IFN response and the innate immune and stress pathways in order to overcome viral infection. SUMOylation of NS1 may also serve as a docking site for additional protein-protein interactions regulating these responses. The balance between the immune response and stress response allows for the slower replication of the viruses resulting in lower pathogenicity and less severe pathology.

In contrast to studies performed in tissue culture showing that viruses containing a non-SUMOylatable NS1 had decreased viral growth as compared to viruses containing a SUMOylatable NS1, studies performed in an animal model showed that viruses containing a non-SUMOylatable NS1 developed more severe pathology associated to viral infection. These contrasting results may be attributed to differences in the viruses ability to overcome the cellular immune and stress responses. It is likely that SUMOylation of NS1 is required for other functions associated to viral infection in tissue culture, however are dispensable during infections in an animal model. Furthermore, a previous study found that influenza A virus grows at a slower rate in Vero cells as compared to MDCK cells (Youil, Su et al. 2004), so these differences may have been exacerbated during viral infection in Vero cells resulting in lower titers.

Overall, these studies suggest that SUMOylation of viral proteins may serve as another antiviral strategy exerted by the host in order to combat viral infection. Further studies would be required to determine the relevance of SUMOylation for other viral proteins and the role of SUMOylation on NS1 proteins from different strains of influenza.

2.5 Acknowledgements:

I want to thank Dr. Daniel R. Perez and Ms. Johanna Lavigne (Department of Veterinary Medicine, University of Maryland-College Park, College Park, MD) for providing the mice, materials, and time necessary to complete the animal infections. I would also like to thank Dr. John M. Quarles (Department of Microbial and Molecular Pathogenesis, College of Medicine, Texas A&M Health Sciences Center, College Station, TX) for providing the A/Puerto Rico/8/1934 [H1N1] influenza virus, and Dr. Yoshihiro Kawaoka (Department of Pathobiological Sciences, School of Veterinary Medicine, University of Wisconsin-Madison, Madison, WI) for providing the A/WSN/1933 [H1N1] 12-plasmid reverse genetics system. I would also like to thank Dr. Jerrold M. Ward (Histoserv, Inc., Germantown, MD) for providing the histological analysis and images of the infected lung tissue. This project was funded by grants from the National Institutes of General Medicine Sciences (NIH grant #1SC1AI098976 to GRA), Border Biomedical Research Center at UTEP (NIH-HIMHD-RCMI grant #8G12MD007592), Center for Research on Influenza Pathogenesis (CRIP grant #HHSN266200700010C to DP). Katherine A. Meraz was supported by Graduate STEM Fellows in K-12 Education (GK-12) (NSF grant #NSF0947992).

CHAPTER 3: SUMOYLATION OF VIRAL PROTEINS RESULTS IN AN INCREASE IN CELLULAR SUMOYLATION OF INFECTED CELLS

3.1 Introduction:

Our lab has shown that NS1 is a major contributor to the global increase in cellular SUMOylation observed during viral infection (Chacon et al., manuscript in preparation). In addition, the increase has been characterized to occur in cells that surround infected cells (unpublished data), and not limited to infected cells. Previous studies by others had demonstrated that various conditions known to produce cellular stress led to a simultaneous global increase in cellular SUMOylation in order to protect the cell from the effects of various types of stress, including heat shock (Flotho and Melchior 2013) and oxidative stress (Yang, Sheng et al. 2008). The upregulation of these pathways can lead to the enhancement of SUMO-dependent protein-protein interactions and the competitive conjugation, between SUMO and Ubc9, at specific lysine residues (Wilson 2012).

It has been shown that both, RIG-I and MDA-5, are SUMOylated thus enhancing their interactions with VISA, an adapter protein required for IFN signaling (Xu, Wang et al. 2005, Wilson 2012, Liu, Wang et al. 2013). The SUMOylation of RIG-I and MDA-5 acts as a positive regulator increasing the IFN levels within the cell (Wilson 2012). Viral infection results in the activation of TLR and RIG-I signaling pathways leading to the phosphorylation, and subsequent SUMOylation, of IRF3 and IRF7 in a TLR/RIG-I activation-dependent manner, however, not an IFN-dependent manner (Kubota,

Matsuoka et al. 2008, Wilson 2012, Liu, Wang et al. 2013). The SUMOylation of IRF3 has negative effects on IFN transcription and may function by recruiting histone deacetylases (HDACs) to the IFN promoter (Kubota, Matsuoka et al. 2008). Similarly, the SUMOylation of IRF7 acts to repress transcription, while ubquitination of IRF7 acts to activate transcription (Kubota, Matsuoka et al. 2008). SUMOylated transcription factors, such as Elk1, act as transcriptional repressors by binding HDAC2 and reducing the acetylation of chromatin (Gill 2005, Kubota, Matsuoka et al. 2008).

In addition, p300 is SUMOylated through the CRD1 domain and binds HDAC6 resulting in transcriptional repression (Gill 2005, Kubota, Matsuoka et al. 2008). Components of the AP-1 transcription complex are targets for SUMOylation (Kubota, Matsuoka et al. 2008). Two proteins belonging to the AP-1 complex, c-Jun and c-Fos, are SUMOylated resulting in diminished transcriptional activity (Yang, Sheng et al. 2008). SUMOylation competes for the modification of both c-Fos and p53 (Kubota, Matsuoka et al. 2008). The post-translational modification of p53 promotes its nuclear export and regulates its transcriptional activity leading to G1 cell cycle arrest (Shen, Wang et al. 2009, Bennett, Pan et al. 2012, Santiago, Li et al. 2013). Furthermore, SUMOylation can alter through the transcriptional repression caused by the subnuclear localization of transcription factors Sp3 and SATB2 (Kubota, Matsuoka et al. 2008). Together, SUMOylation leads to transcriptional repression and the induction of IFN pathways to protect the cell against stress-mediated effects.

Viral infection also leads to the activation of SUMO E3 ligases which regulate innate immunity pathways, including JAK/STAT and NF-kB dependent transcription (Kubota, Matsuoka et al. 2008). For example, the transcription factor, IRF1, is

SUMOylated through induction by the E3 ligase PIAS3 (Kubota, Matsuoka et al. 2008). The SUMOylation of STAT1 protects cells from hyper-responsiveness to IFN-gamma thus preventing apoptosis (Song, Bhattacharya et al. 2006, Begitt, Droescher et al. 2011). PIAS3 is also responsible for the SUMOylation of the progesterone receptor isoform B which promotes its nuclear export (Man, Li et al. 2006). Competitive SUMOylation of IkB-alpha blocks its ubiquitination and degradation, thus preventing activation of NF-kB (Kubota, Matsuoka et al. 2008, Yang, Sheng et al. 2008, Liu, Wang et al. 2013). Other target proteins, such as HSF1, HSF4b, and GATA-1, must be phosphorylated in order for them to be SUMOylated (Kubota, Matsuoka et al. 2008, Flotho and Melchior 2013).

Many viruses use the SUMOylation system to regulate transcriptional activity, PML-NB dispersion, cell cycle regulation and apoptosis, reactivation of latent infections, IFN inhibition, and viral assembly (Mattoscio, Segre et al. 2013). The localization of Sp100 and Daxx require SUMOylation for the localization and assembly in PML-NBs in response to IFN stimulation and viral infection (Everett, Boutell et al. 2013, Glass and Everett 2013, Mattoscio, Segre et al. 2013). Influenza infection induces activation of PKR and IFN resulting in the accumulation of viral RNA-induced stress granules (Onomoto, Jogi et al. 2012). In turn, the induction in IFN increases the levels of dsRNA-dependent PKR within the cell (Onomoto, Jogi et al. 2012). The stress granules are formed in a PKR-dependent manner and are comprised of viral ribonucleoprotein complexes in which RLRs, MDA5, and LGP2 are recruited (Onomoto, Jogi et al. 2012). The stress granules are generated from stress response and are translationally-stalled, however, are still able to interact directly with the mitochondria (Onomoto, Jogi et al.

2012). These stress granules could not be recreated by polyI:C treatment (Onomoto, Jogi et al. 2012).

SUMOylation, in particular SUMO-2/3 conjugation, has been shown to play an important role in ischemia (Li, Santockyte et al. 2006, Yang, Sheng et al. 2008, Flotho and Melchior 2013). Transient ischemia induces a massive increase in protein SUMOylation within 10 min of onset (Yang, Sheng et al. 2008, Flotho and Melchior 2013). SUMO-2/3 conjugation to p53 and retinoblastoma protein may play a role in premature senescence and the stress response (Li, Santockyte et al. 2006). Levels of the Cdk inhibitor, p21, have been shown to be enhanced in cells that over-express SUMO-2/3 (Li, Santockyte et al. 2006). Although, SUMO-1 conjugation is important, it is more prominent in a non-stressed cells (Yang, Sheng et al. 2008). Arsenite, a respiratory poison, induces oxidative stress similar to viral infection and functions to suppress protein synthesis by phosphorylation of eIF2-alpha, and to activate heat-shock proteins (Yang, Sheng et al. 2008). Interestingly, western blots of tissues that were treated with arsenite led to SUMO-1 and SUMO-2/3 profiles with molecular weight bands of approximately 40, 52, and 70 kDa (Yang, Sheng et al. 2008). These findings suggest that viral infection or chemical treatments can leads to an increase in SUMOylation to protect the cell from stress-related effects. The objective of this chapter is to investigate the interplay between viral infection and the increase in cellular SUMOylation.

As stated previously, we have determined that SUMOylation of NS1 is required for viral fitness and that it is the major contributor to the global increase in cellular SUMOylation. Previously our lab has shown that SUMOylation of NS1 affects NS1's

ability to neutralize the host IFN response as well as viral growth (Santos, Pal et al. 2013). Most notably, viruses containing a non-SUMOylatable form of NS1 are able to cause infection, however, viral titers are 3-logs lower than viruses containing a SUMOylatable form of NS1 both in interferon-competent and interferon-deficient cell lines which indicates that the interaction with SUMO is important to the replicative ability of the virus in tissue culture (Santos, Pal et al. 2013). In this section, we aimed at investigating whether the ability of NS1 to be SUMOylated has an effect on its ability to trigger an increase in cellular SUMOylation and whether this increase in cellular SUMOylation occurs during infection with other viruses.

3.2 Materials and Methods:

TNT coupled transcription/translation reaction

The TNT coupled transcription/translation reaction was performed according to manufacturers instructions (Promega). A quick mix containing a rabbit reticulocyte lysate, TNT reaction buffer, RNA polymerase, amino acid mixture (minus methionine), an energy source (ATP/GTP), and a ribonuclease inhibitor, is mixed with plasmid, ^{35}S-Methionine, and MG132 to stabilize the reaction. The reaction was incubated at 30C for 90 minutes and either stored at -80°C or on ice until analyzed by SDS-PAGE or used for *in-vitro* SUMOylation reactions. Increasing amount of SUMO1 protein was added to the samples and incubated at 4°C for 1 hour.

In-vitro SUMOylation reaction

A quick mix containing the SUMO activating enzymes (SAE1/2), GST-Ubc9, SUMO1 protein, 5x SUMOylation reaction buffer, and the TNT sample were mixed and incubated at 37°C for 90 minutes. Following the incubation, 4x sample buffer and β-mercaptoethanol was added up to a final concentration of 10%, and the samples were boiled in a water bath for 3 minutes.

GST-pulldown

A GST pulldown, using either GST-SUMO1 or GST-SUMO3, was performed in which glutathione-sepharose beads were used to capture GST fused proteins of interest. Glutathione-sepharose beads were centrifuged twice at 3,000 rpm for 1 minute, once with water and once with cold 1x PBS. The beads were then equilibrated with 1x PBS

supplemented with either GST or GST-NS1 to make a 50% slurry. The reaction was then incubated at 4°C for 1 hour. The beads were washed with 1x PBS supplemented with 0.1% Tween 20 in the HulaMixer® Sample Mixer (Life Technologies) for 3 minutes. Samples were centrifuged at 3,000 rpm for 1 minute and the supernatant removed by the vacuum system. Samples were mixed with 4x sample buffer and analyzed by immunoblot.

Transient transfections

HEK293FT cells (Invitrogen Corp.) were seeded at a density of 5 x 10^5 cells/well into 6 well plates. The following day, cells were transfected by liposome-mediated transfection using 5 ug of CsCl-purified plasmids and 10 uL of TransIT-LT1 (Mirus Bio LLC) per well, according to the manufacturer's recommendations. Cells were incubated at 37ºC in 5% CO_2 for 24 hours. Cell extracts were collected at 1 and 24 hours post-transfection and analyzed by SDS-PAGE followed by immunoblotting to determine transfection efficiency of the ASL. Culture supernatant was then discarded and 4x sample buffer and β-mercaptoethanol was added up to a final concentration of 10%, and the samples were boiled in a water bath for 3 minutes.

Immunoblot analyses

Prior to SDS-PAGE analyses, all cell extracts generate were passed several times through a 29½ gauge needle to break down the genomic DNA released and to decrease the viscosity of the samples. β-mercaptoethanol was added up to a final concentration of 10%, and the samples were boiled in a water bath for 3 minutes. The samples were

resolved by 10% SDS-PAGE gels made in-house and, subsequently, the proteins were transferred to Immobilon-FL (Millipore Corp., Bedford, MA) for use with IRDye-conjugated secondary antibodies (LI-COR Biosciences Inc., Lincoln, NE) and infrared fluorescence imaging and analysis by autoradiography and phosphordensitometry.

Autoradiography

The Immobilon-FL membrane was dried and exposed to film (Sigma Aldrich) for 10 minutes, 1 hour, and 18 hours. The image was quantified using Quantity One Software (Bio-Rad Laboratories, Hercules, CA).

Phosphodensitometry

The Immobilon-FL membrane was dried and exposed to the phosphor screen for 6 hours. The screen was developed 6 hours and quantified using Quantity One Software (Bio-Rad Laboratories).

Infrared fluorescence imaging

Immobilon-FL membranes (Millipore Corp.) were washed four times in 1x PBS, blocked with Odyssey Blocking Buffer (LI-COR Biosciences Inc.) for a minimum of 1 hour at room temperature, and incubated in Odyssey Blocking Buffer at 4°C overnight with the primary antibody at the indicated dilution. The membranes were then washed four times with 1x PBS, supplemented with 0.1% polysorbate 20 (Tween 20), and incubated with Odyssey Blocking Buffer with the appropriate highly cross-absorbed IRDye 800 CW- and IRDye 680 LT-conjugated secondary antibodies (LI-COR Biosciences Inc.) at the

indicated dilution. The membranes were then washed four times with 1x PBS, supplemented with 0.1% Tween 20 and twice again with 1x PBS and scanned on an Odyssey CLx infrared imaging system (LI-COR Biosciences Inc.). Quantitative analyses of the images obtained was performed by using Odyssey Infrared Imaging System Application software version 3.0.29 (LI-COR Biosciences Inc.). Statistical analyses and graphics of the data generated were performed by using GraphPad Prism version 5.04 for Windows (GraphPad Software Inc., San Diego, CA).

Isolation and infection of bone marrow derived dendritic cells

Bone marrow derived dendritic cells were isolated from female C57BL/6 mice. On day 8 post-isolation, cells were enriched through magnetic bead sorting for CD11c (AutoMACS® Pro Separator, Miltenyi Biotec Inc., Auburn, CA). Dendritic cells were seeded at a density of 3.7 x 10^6 cells/well in complete medium consisting of 1x Roswell Park Memorial Institute medium (1x RPMI) supplemented with 10% fetal bovine serum (Atlanta Biologicals), 1% Penicillin-Streptomycin Solution (Thermo Scientific, Waltham, MA), and 1% GlutaMAX (Life Technologies Inc., Carlsbad, CA). Cells were maintained in a 37ºC incubator in 5% CO_2. Four hours after plating, the cells were washed twice with 1 x RPMI, and a viral dilution prepared in 3 mL of 1 x RPMI supplemented with 0.2% BSA was added to the cells and incubated with the cells at 35ºC for 1 hour. The cells were washed again with 1 x RPMI and the total volume was removed and placed into a 15 mL conical tube. Tubes were centrifuged at 1000 rpm for 5 minutes to collect the cells. The supernatant was removed by vacuum and cells were resuspended in 9 mL of 1 x RPMI. Cells were re-plated 3 mL/well and incubated at 35ºC in 5% CO_2. At 12

hours post-infection, the cells were washed with 1 x RPMI and the total volume was removed and placed into a 15 mL conical tube. Tubes were centrifuged at 1000 rpm for 5 minutes to collect the cells. The supernatant was removed by vacuum and cell extracts were collected by adding boiling 2x sample buffer (25 mM Tris pH 6.8, 5% glycerol, 2% SDS, 0.01% bromophenol blue) for SDS-PAGE and immunoblotting analyses.

Animal infections

All animal experiments were approved by the institutional animal care and use committee of the University of Maryland-College Park, Department of Veterinary Medicine. Female, 6-week-old DBA/2J mice (The Jackson Laboratory) were used for viral pathogenicity experiments. Mice were anesthetized in groups of five by isoflurane inhalation and infected intranasally with $1x10^6$ PFU of the respective virus in 50 uL of PBS. To determine differences between clinical signs of disease, a 0-1-2-3 scoring scale was used, with 0 and 3 representing normal and severe, respectively. Animals were observed for 2 days for clinical signs of infection. Viral infection was studied in 5 groups of twenty mice over 6 days. Four mice from each group were sacrificed on hours 0, 6, 12, 24, and 48 after inoculation and lungs and trachea were removed from each mouse and immediately placed in 10% NBF.

Immunohistochemistry

Approximately 10% of lung tissue from mice at days 4 and 6 post-inoculation were isolated, washed in sterile PBS, and fixed in 10% NBF. Tissue sample were embedded

in paraffin, cut into 5-um-thick sections, and mounted onto glass slides. Paraffin was removed using two washes of xylene followed by ethanol gradient (100%, 95%, and 80%) washes. A 70% ethanol wash was supplemented with 0.25% ammonia and incubated for 1 hour at room temperature. Slides were incubated in 50% ethanol followed by two washes in 1x PBS to rehydrate the tissues. Antigens within the tissues were unmasked by incubating in 1 mM EDTA and heated in a microwave on full power until the buffer began to boil. The tissues were let cool for 20 minutes and washed three times with 1x PBS, the last of which was supplemented with sodium borohydride (Sigma Aldrich) at a concentration of 10 mg/mL, and followed by four washes with 1x PBS.

Tissue sections were drained and a hydrophobic barrier was drawn around each tissue using an ImmEdge Pen (Vector Laboratories). In order to permeabilize the tissues, the sections were washed twice with 1x PBS, the second of which was supplemented with 0.2% Triton X-100 (MP Biomedicals), and followed by three washes with 1x PBS. Sections were blocked with 1x PBS with 1% goat serum for 1 hour at room temperature and incubated in 1x PBS with 1% goat serum at 4C overnight with the primary antibody at the indicated dilution. The sections were then washed four times with 1x PBS and incubated with 1x PBS with 1% goat serum supplemented with the appropriate highly cross-absorbed Alexa Fluor 594 and 488 dye conjugated secondary antibodies (Life Technologies Inc.) at the indicated dilution. Sections were washed three times in 1x PBS followed by one wash with 1x PBS supplemented with DAPI (Thermo Scientific) at a final concentration of 0.5 ug/mL. Sections were washed in 1x PBS, glycerol and glass cover slips were added, and slides were sealed with clear nail polish.

Statistical analysis and computer software.

All statistical analyses and graphics presented were performed by using GraphPad Prism version 5.04 for Windows (GraphPad Software Inc.). All figures were created by using Adobe Photoshop CS5 extended version 12.0.3 X64 (Adobe Systems Inc.).

3.3 Results:

NS1 proteins from different influenza A viral strains exhibit varying levels of SUMOylation. Previous studies had characterized the SUMOylation of NS1 from the A/ Puerto Rico/8/1934 [H1N1] strain of influenza, therefore, we sought to determine the SUMOylation of NS1 proteins from other influenza A viral strains (**Table 3.1**). SUMOylated forms of NS1 were detected for all influenza viral proteins (**Figure 3.1**). The A/Brevig Mission/1/1918 [H1N1] influenza strain had the appearance of several new SUMOylated bands in contrast to a single form for all other NS1 proteins. SUMOylated NS1 was quantified as compared to non-SUMOylated NS1 and it showed that all influenza viral proteins, except for the A/Brevig Mission/1/1918 [H1N1] NS1, had less than 4% of SUMOylated NS1, making the non-SUMOylated NS1 the dominant form (**Figure 3.2**). Conversely, the A/Brevig Mission/1/1918 [H1N1] influenza strain had more than 81% of SUMOylated NS1, making the SUMOylated NS1 the dominant form **(Figure 3.2**).

SUMOylated NS1 proteins are able to trigger an increase in cellular SUMOylation. Previous studies using SUMOylatable and non-SUMOylatable NS1 proteins from the A/Puerto Rico/8/1934 [H1N1] influenza A strain showed that an increase in cellular SUMOylation was only triggered by the SUMOylatable form of NS1. In order to determine if the SUMOylation of NS1 has an effect on the increase in cellular SUMOylation, NS1 proteins from different influenza A viral strains were tested. Influenza NS1 viral proteins that have higher levels of SUMOylation are able to trigger the increase in cellular SUMOylation more effectively (**Figure 3.3**). The NS1 proteins from

the A/WSN/1933 [H1N1] and A/Brevig Mission/1/1918 [H1N1] were able to trigger the highest increases in cellular SUMOylation.

Influenza infections *ex vivo* and *in vivo* exhibit a global increase in cellular SUMOylation. An increase in cellular SUMOylation had been observed upon infection using immortalized cell lines. Therefore, in order to determine whether an increase in cellular SUMOylation could be triggered in primary cells, bone marrow derived dendritic cells (BMDCs) were infected with the A/WSN/1933 influenza virus. Both A549 cells and BMDCs exhibited a global increase in cellular SUMOylation characterized by the appearance of new SUMOylated bands at 40, 52, and 70 kDa when compared to the mock-infected samples (**Figure 3.4A**). It is demonstrated in **Figure 3.4B** that A549 cells and BMDCs have increased levels of SUMO1 production upon infection with the A/WSN/1933 influenza virus. In order to determine whether an increase in cellular SUMOylation occurred during infections in an animal model, DBA/2J mice were infected with either the WSN/T7T7[NS1~NS2] or WSN/T7T7[NS1K70AK219A~NS2] influenza viruses. Lung tissue from mice infected with WSN/T7T7[NS1~NS2] also had the appearance of new low molecular weight bands, between 25 and 37 kDa, and high molecular weight bands, between 75 and 100 kDa, as compared to the mock-infected lung tissue (**Figure 3.4C and 3.4D**). Lung tissue from mice infected with WSN/T7T7[NS1K70AK219A~NS2] was tested, however, did not produce new molecular weight bands characteristic of a global increase in cellular SUMOylation (data not shown).

Increases in cellular SUMOylation are observed during influenza A viral infection in an animal model. To further examine the significance of NS1 SUMOylation on influenza viral infection, we evaluated changes in cellular SUMOylation from infected mice at day 6 post-infection Lung tissue harvested from animals infected with the WSN/T7T7[NS1~NS2] virus showed increases in cellular SUMOylation (**Figure 3.5**) as compared to animals infected with the WSN/T7T7[NS1K70AK219A~NS2] virus (**Figure 3.6**). Similar results were obtained for all animals within each group.

Additionally, in order to determine whether the increase in cellular SUMOylation is a characteristic shared among different influenza viruses, five groups of four DBA/2J mice were intranasally infected with 1 x 10^6 PFU/mL with either A/WSN/33, A/Puerto Rico/8/1934, A/Hong Kong/1968 (X31), A/Guinea Fowl/Hong Kong/WF10/1999 (WF10) strains of influenza virus or PBS as a control (**Figure 3.7**). Mice were euthanized at hours 0, 6, 12, 24, and 48 post-infection and lungs and trachea were harvested. All animals infected with the influenza A viruses exhibited increases in cellular SUMOylation as compared to mock infected tissues (**Figure 3.8**).

Infections with Vaccinia virus and Lymphocytic choriomeningitis virus results in an increase in cellular SUMOylation. Previous studies have demonstrated that influenza A viral infection is able to trigger an increase in cellular SUMOylation, however, it is unknown whether this increase in cellular SUMOylation occurs upon infection with other viruses. In order to determine the ability of vaccinia virus and lymphocytic choriomeningitis virus (referred to as LCMV hereafter) trigger an increase in cellular SUMOylation, samples infected with either virus were tested. Infection with

vaccinia virus showed increases in SUMOylation in the high molecular weight region as compared to non-infected Vero cells **(Figure 3.9**). Three different strains of LCMV were used: armstrong (ARM; non-pathogenic strain), armstrong-clone 13 (clone 13; chronic infection), and WE (pathogenic strain). In addition, a viral vaccine candidate for Lassa hemorrhagic fever (ML29) was included. The LCMV ARM and clone 13 strain infected samples showed increases in cellular SUMOylation in the high molecular weight region at both 48 and 72 hpi (**Figure 3.9**). In contrast, the pathogenic LCMV WE strain showed increases in cellular SUMOylation at 48 hpi, however, SUMOylation levels decreased by 72 hpi (**Figure 3.9**). The ML29 vaccine candidate treated samples showed an increase in cellular SUMOylation in the high molecular weight region at both 48 and 72 hpi as compared to the non-infected Vero cells (**Figure 3.9**).

To determine differences in SUMOylation, we divided the high molecular weight region into four areas as identified in **Figure 3.10A** (yellow boxes). The intensity of each area was quantified to determine the intensity of SUMO as compared to GAPDH, which was used as a loading control (**Figure 3.10B**). There was no significant differences between the samples in rows one, two, or four as compared to the non-infected Vero cells. However, the quantification of row three showed dramatic increased levels of SUMOylation in the LCMV ARM and clone 13 infected samples at 72 hpi as compared to all other samples (**Figure 3.10B**). In addition, quantification of row three showed slight increases in SUMOylation in Vero cells and ML29 treated cells and decreases in SUMOylation in vaccinia virus and LCMV WE infected cells between 48 and 72 hpi (**Figure 3.10B**).

In order to determine whether these changes in cellular SUMOylation were due to differences in levels in Ubc9, we quantified the intensity of Ubc9 as compared to GAPDH and found that there were no significant differences between any of the samples (**Figure 3.11**). To better resolve the high molecular weight region, we ran a gel containing a lower percentage of acrylamide which revealed the presence of two new SUMOylated bands just above 50 kD (**Figure 3.12**). These two bands appear in all samples except for the Vero cells.

Table 3.1. Influenza A viral strains used in studies

Influenza A viral strain	Abbreviation used	Modifications	Figure referenced
A/Puerto Rico/8/1934 [H1N1]	PR8	none	**Figure 3.1 - Figure 3.3; Figure 3.8**
A/WSN/1933 [H1N1]	WSN	none	**Figure 3.1 - Figure 3.3; Figure 3.8**
A/Memphis/31/1998 [H3N2]	Memphis	none	**Figure 3.1 - Figure 3.3**
A/Guinea Fowl/Hong Kong/WF10/1999 [H9N2]	WF10	none	**Figure 3.3; Figure 3.8**
A/Aichi/2/1968 [H3N2]	X31	none	**Figure 3.8**
A/Zhejiang/DTID-ZJU01/2013 [H7N9]	ZJU	none	**Figure 3.1 - Figure 3.3**
A/Brevig Mission/1/1918 [H1N1]	BM	none	**Figure 3.1 - Figure 3.3**
A/Brevig Mission/1/1918 [H1N1]	BM K227S/R	K227S or R mutation in NS1	**Figure 3.1 - Figure 3.3**

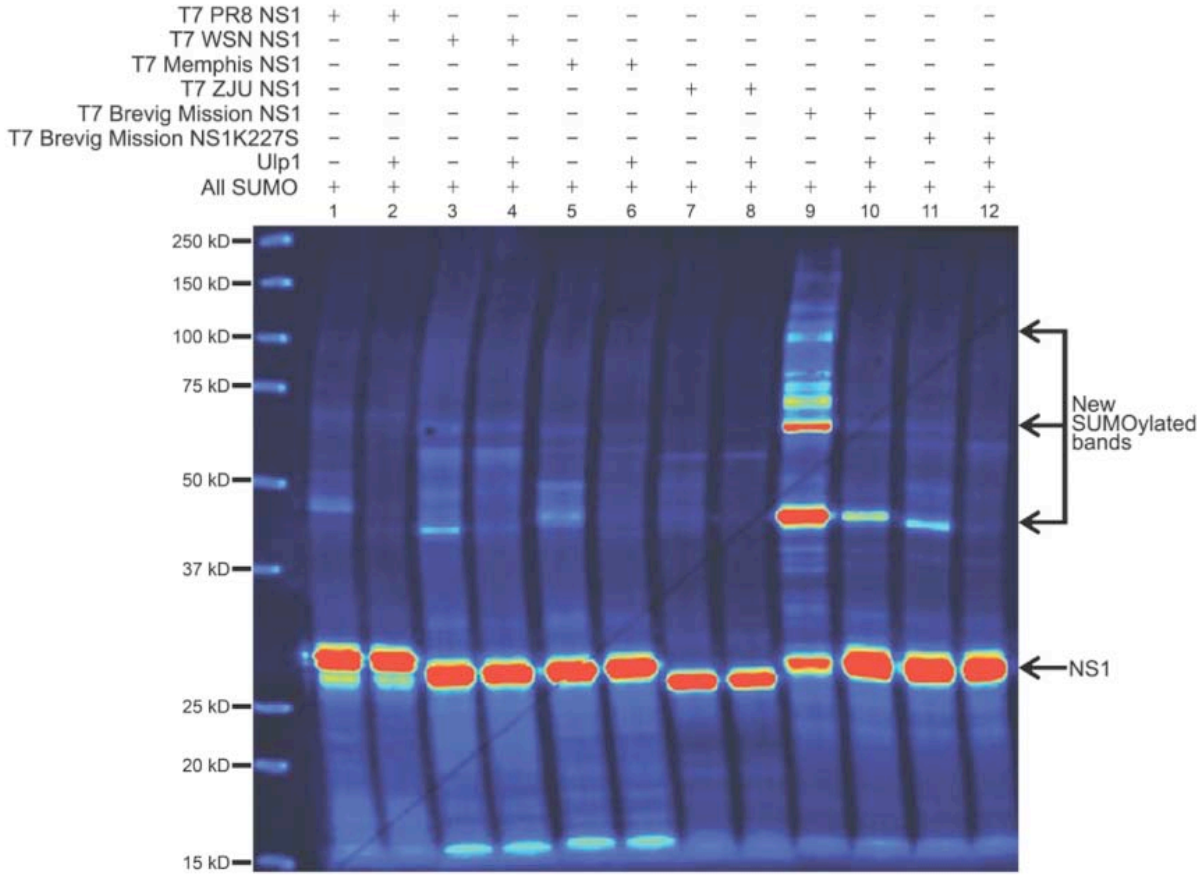

Figure 3.1. NS1 proteins from different influenza A viruses exhibit varying levels of SUMOylation. Mammalian expression plasmids encoding the NS1 proteins from different influenza A viruses were used as the template for a TNT coupled transcription/translation reaction. An *in-vitro* SUMOylation reaction was performed and samples were incubated with (+) or without (-) the SUMO protease, Ulp1, as indicated. The resulting SUMOylation profile for the NS1 proteins are shown above. The new SUMOylated NS1 bands are indicated by the arrows.

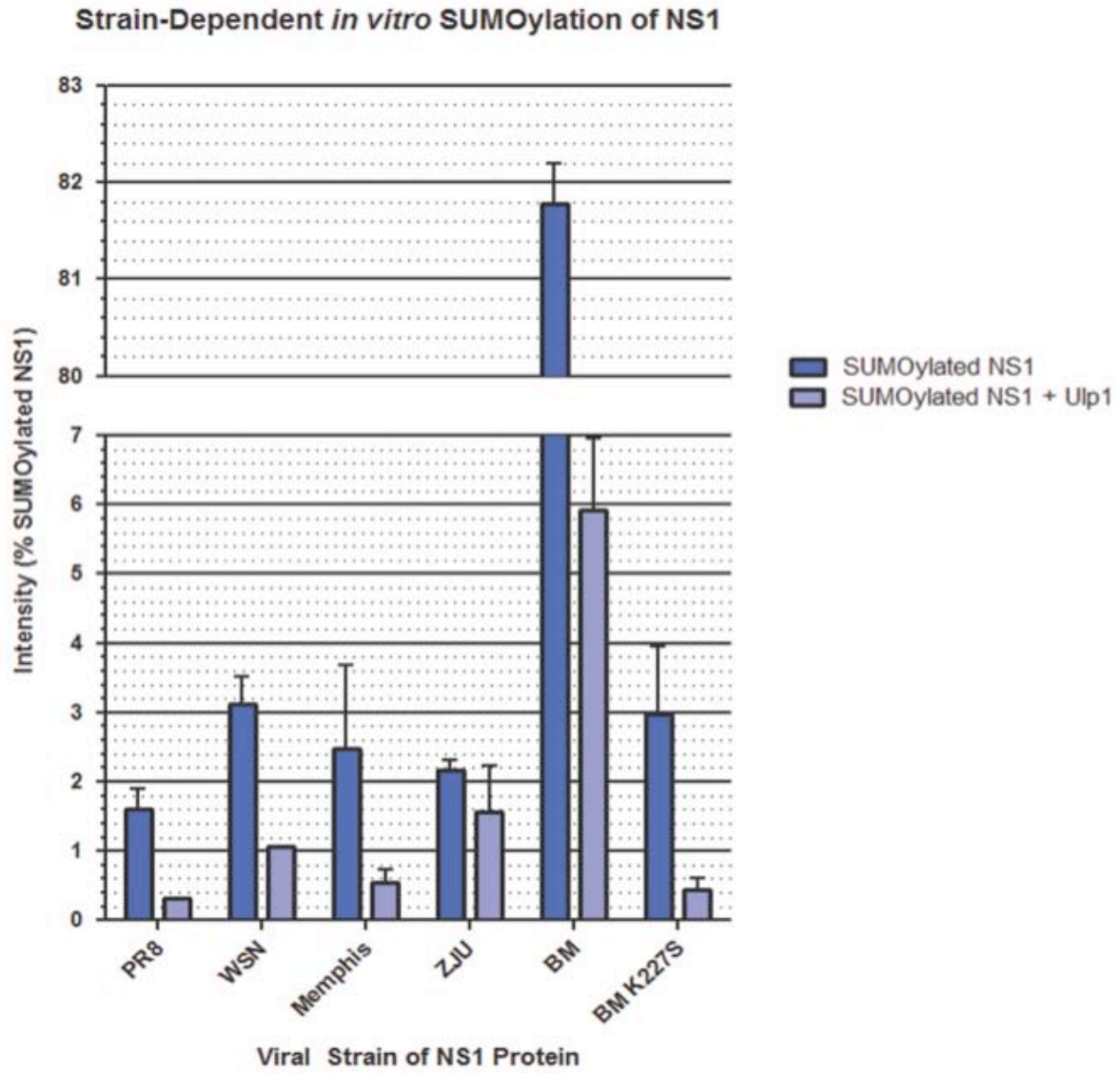

Figure 3.2. Quantification of NS1 SUMOylation from different influenza A viruses. Mammalian expression plasmids encoding the NS1 proteins from different influenza A viruses were used as the template for a TNT coupled transcription/ translation reaction followed by an *in-vitro* SUMOylation reaction. Samples were incubated with (+) or without (-) the SUMO protease, Ulp1, as indicated. The quantification of the resulting SUMOylation profile for the NS1 proteins is shown above.

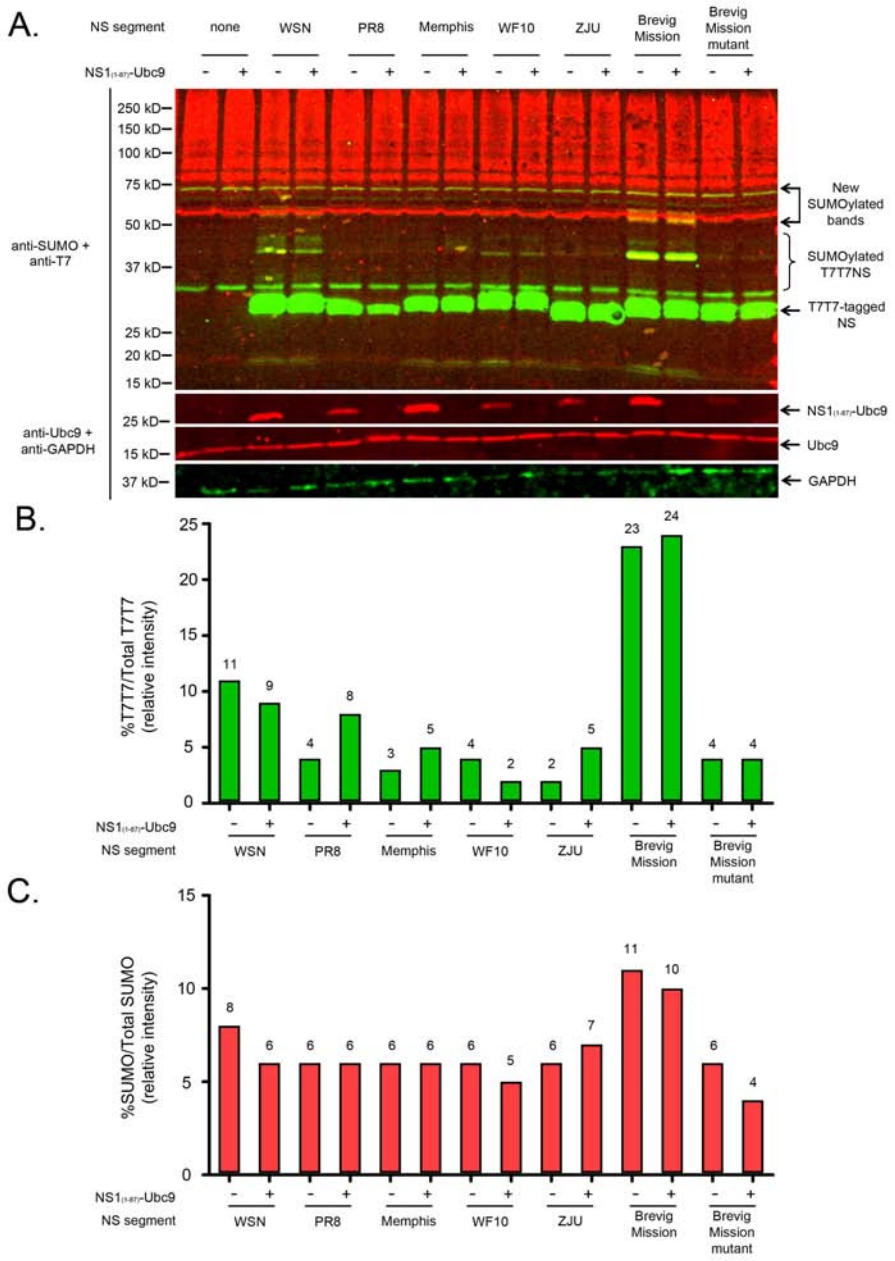

Figure 3.3. SUMOylated NS1 proteins are able to trigger an increase in cellular SUMOylation. (A) HEK293FT cells were transfected with the indicated mammalian expression plasmids encoding the NS1 proteins from A/WSN/33 [H1N1], A/Puerto Rico/8/1934 [H1N1], A/Memphis/31/1998 [H3N2], A/Guinea Fowl/Hong Kong/ WF10/1999 [H9N2], A/Zhejiang/DTID-ZJU01/2013 [H7N9], and A/Brevig Mission/ 1/1918 [H1N1], including a SUMOylatable and non-SUMOylatable form. Samples were analyzed by SDS-PAGE and immunoblotting using anti-SUMO1 MAb, anti-T7 MAb, anti-Ubc9 MAb, and anti-GAPDH MAb. (B) Quantification of SUMOylated T7T7NS (between 37 kD and 75 kD) as relative intensity to total T7T7 per lane. (C) Quantification of SUMO1 (between 37 kD and 75 kD) as relative intensity to total SUMO1 per lane. MAb: monoclonal antibody.

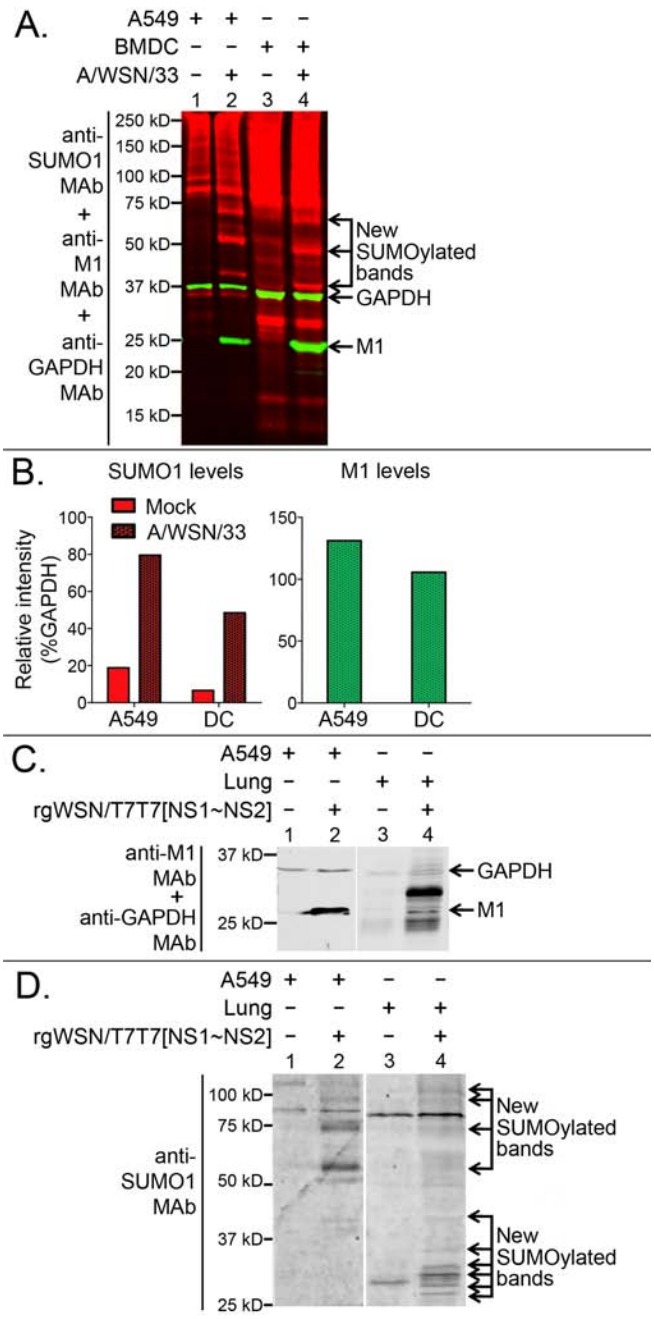

Figure 3.4. Influenza infections *ex vivo* and *in vivo* exhibit a global increase in cellular SUMOylation. A549 cells or bone marrow derived dendritic cells (BMDC) were either mock-infected or infected with A/WSN/33. (A) anti-SUMO1, anti-M1 and anti-GAPDH MAb. (B) Quantification of SUMO1 and M1 relative intensity as compared to GAPDH levels in A549 cells or BMDC. DBA/2J mice and A549 cells were either mock-infected or infected with WSN/T7T7[NS1~NS2]. Lung tissue and cell extracts, respectively, were analyzed by SDS-PAGE using (C) anti-M1 and anti-GAPDH mouse MAb and (D) anti-SUMO1 rabbit MAb. New SUMOylated bands are indicated by the arrows. MAb: monoclonal antibody.

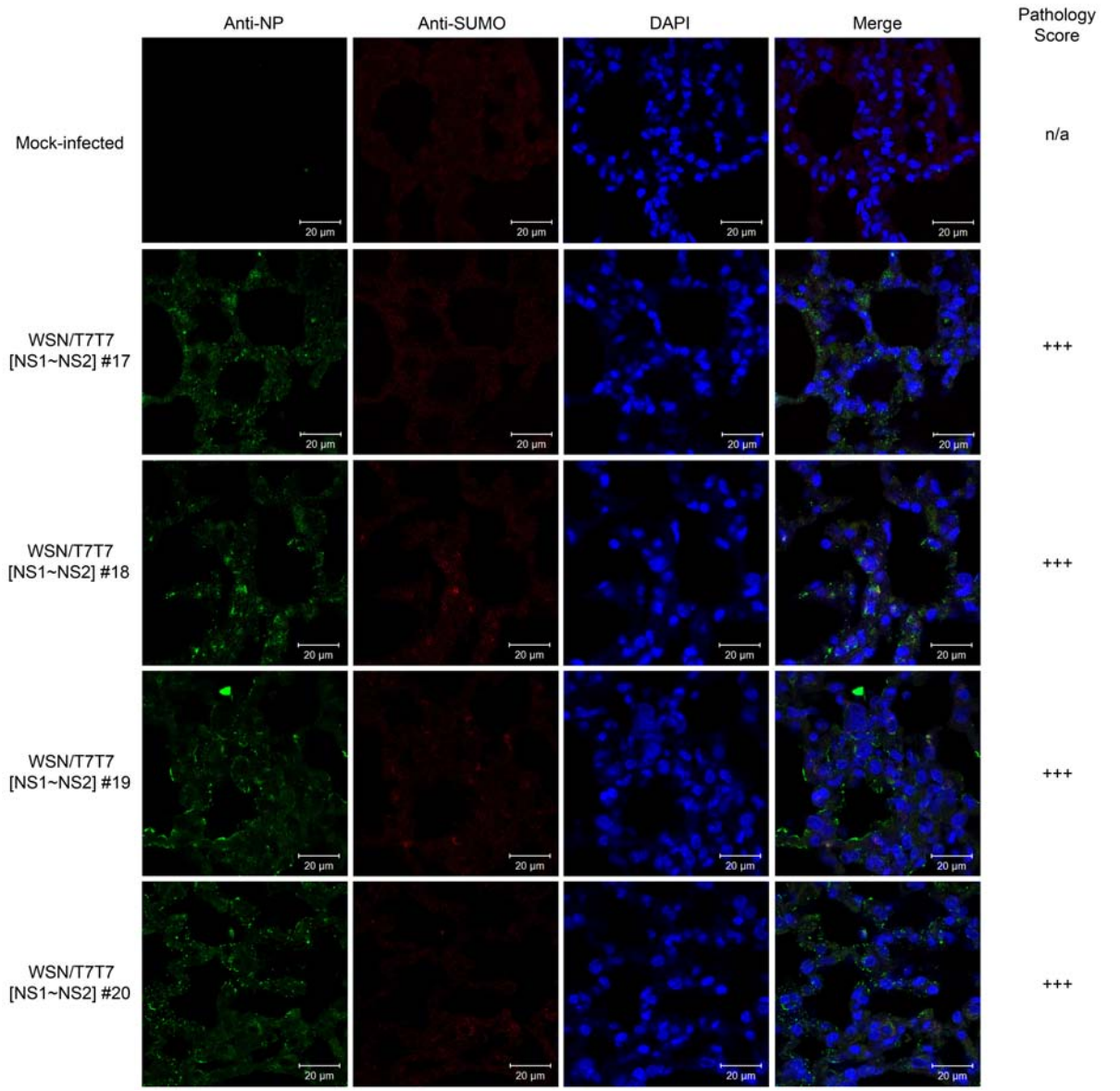

Figure 3.5. Animals infected with WSN/T7T7[NS1~NS2] virus exhibit increases in cellular SUMOylation. 5-6 week old female DBA/2J mice were inoculated with one of the inocula indicated. At the indicated times post-infection, four animals per inoculation group were sacrificed and the organs were harvested for immunohistochemistry analysis. Lung tissue was fixed in formalin, embedded in paraffin, sectioned, and fixed onto microscope slides. Slides were processed and stained with DAPI (blue), anti-SUMO1 MAb (red), and anti-NP PAb (green). Images were taken using confocal microscope. MAb: monoclonal antibody. PAb: polyclonal antibody.

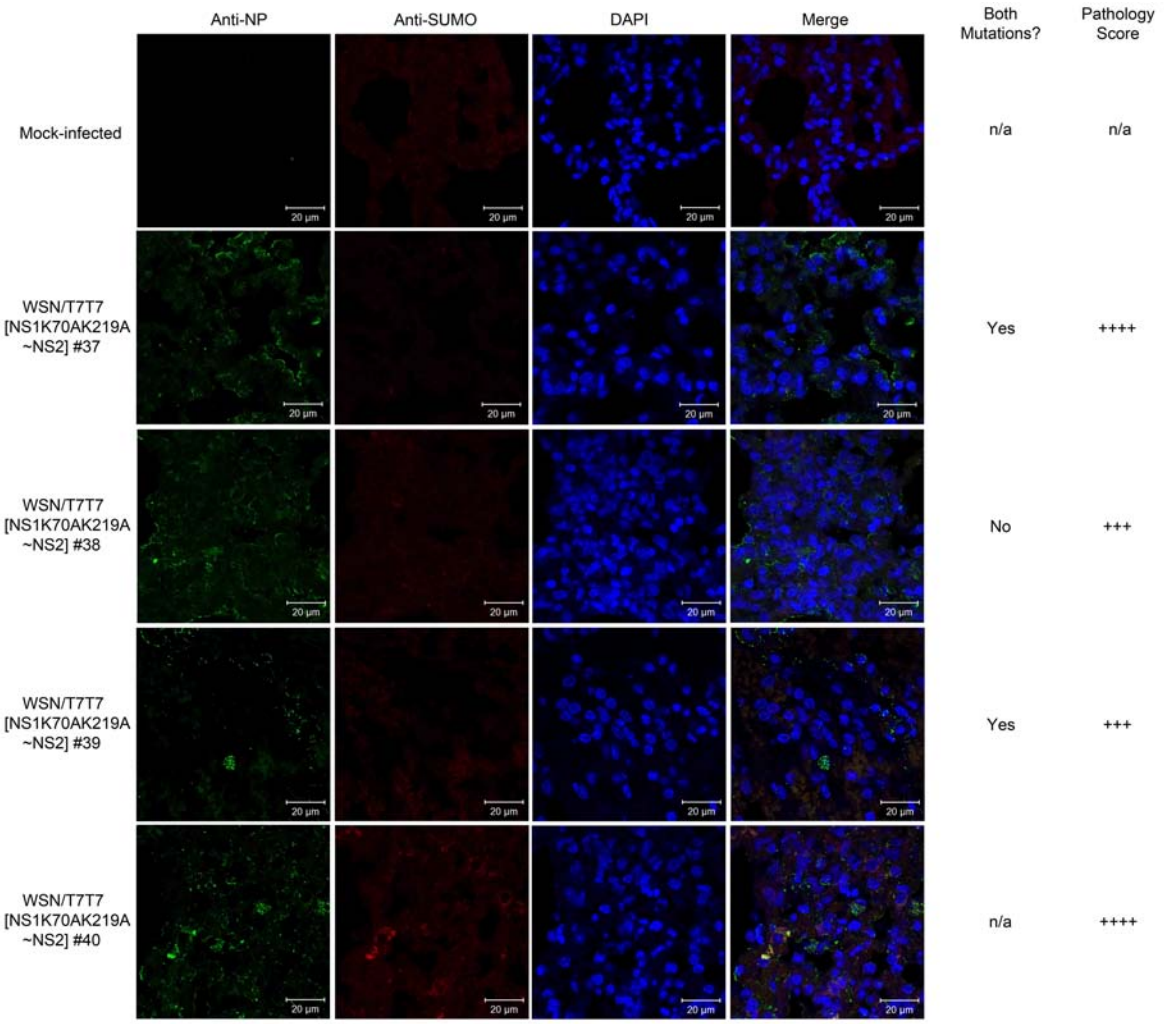

Figure 3.6. Animals infected with WSN/T7T7[NS1K70AK219A~NS2] virus do not exhibit increases in cellular SUMOylation. 5-6 week old female DBA/2J mice were inoculated with one of the inocula indicated. At the indicated times post-infection, four animals per inoculation group were sacrificed and the organs were harvested for immunohistochemistry analysis. Lung tissue was fixed in formalin, embedded in paraffin, sectioned, and fixed onto microscope slides. Slides were processed and stained with DAPI (blue), anti-SUMO1 MAb (red), and anti-NP PAb (green). Images were taken using confocal microscope. MAb: monoclonal antibody. PAb: polyclonal antibody.

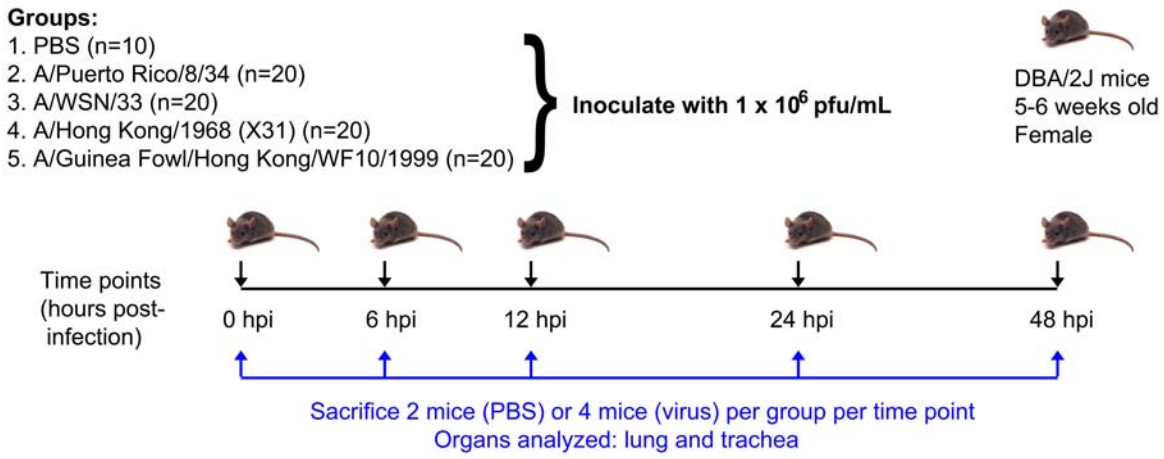

Figure 3.7. Overall experimental approach. 5-6 week old female DBA/2J mice were inoculated with one of the inocula indicated. At the indicated times post-infection, four animals per inoculation group were sacrificed and the organs were harvested for immunohistochemistry analysis.

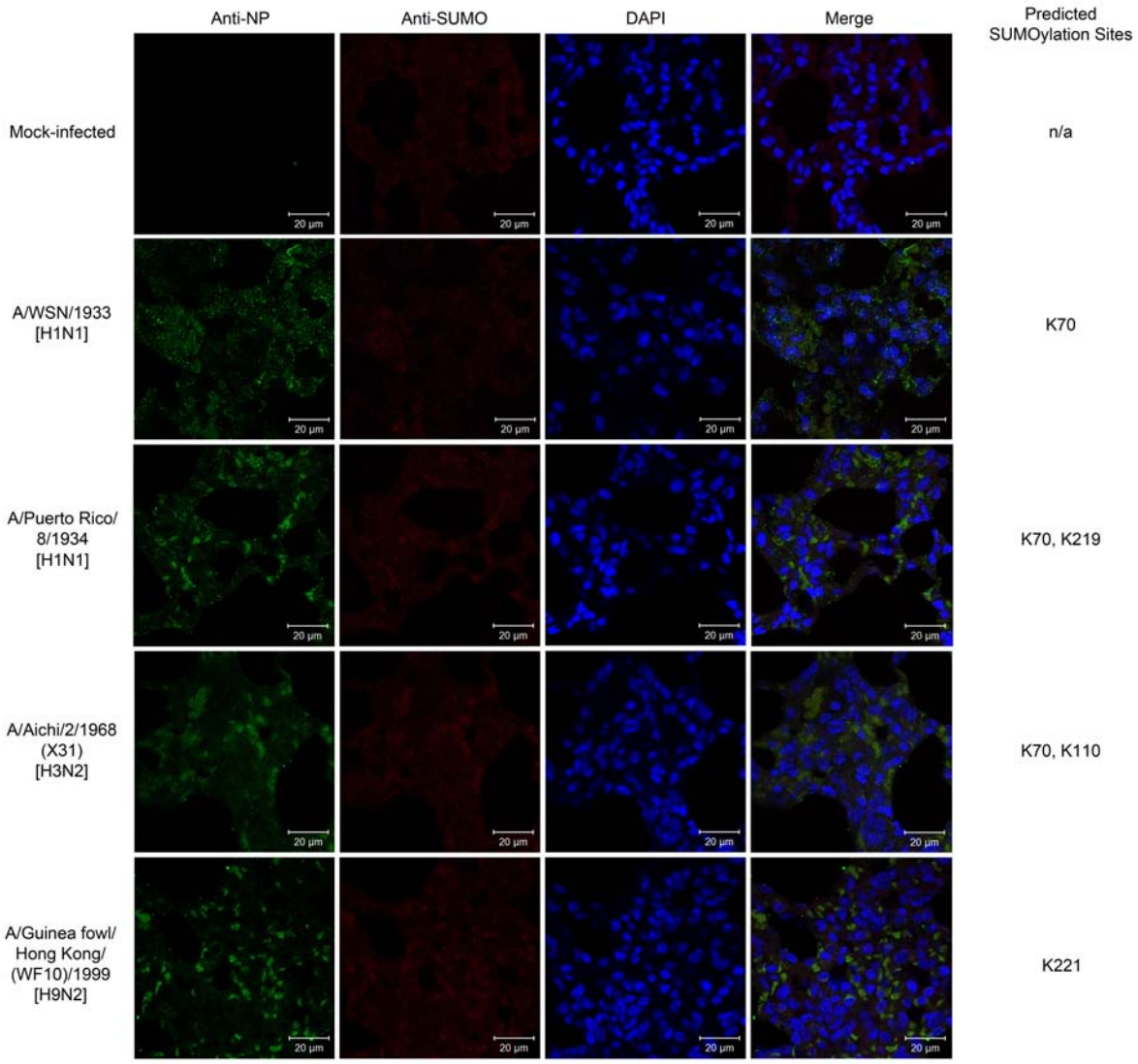

Figure 3.8. Animals infected with different influenza A viruses exhibit increases in cellular SUMOylation albeit to different extents. 5-6 week old female DBA/2J mice were inoculated with one of the inocula indicated. At the indicated times post-infection, four animals per inoculation group were sacrificed and the organs were harvested for immunohistochemistry analysis. Lung tissue was fixed in formalin, embedded in paraffin, sectioned, and fixed onto microscope slides. Slides were processed and stained with DAPI (blue), anti-SUMO1 MAb (red), and anti-NP PAb (green). Images were taken using confocal microscope. MAb: monoclonal antibody. PAb: polyclonal antibody. Representative images from each group are presented.

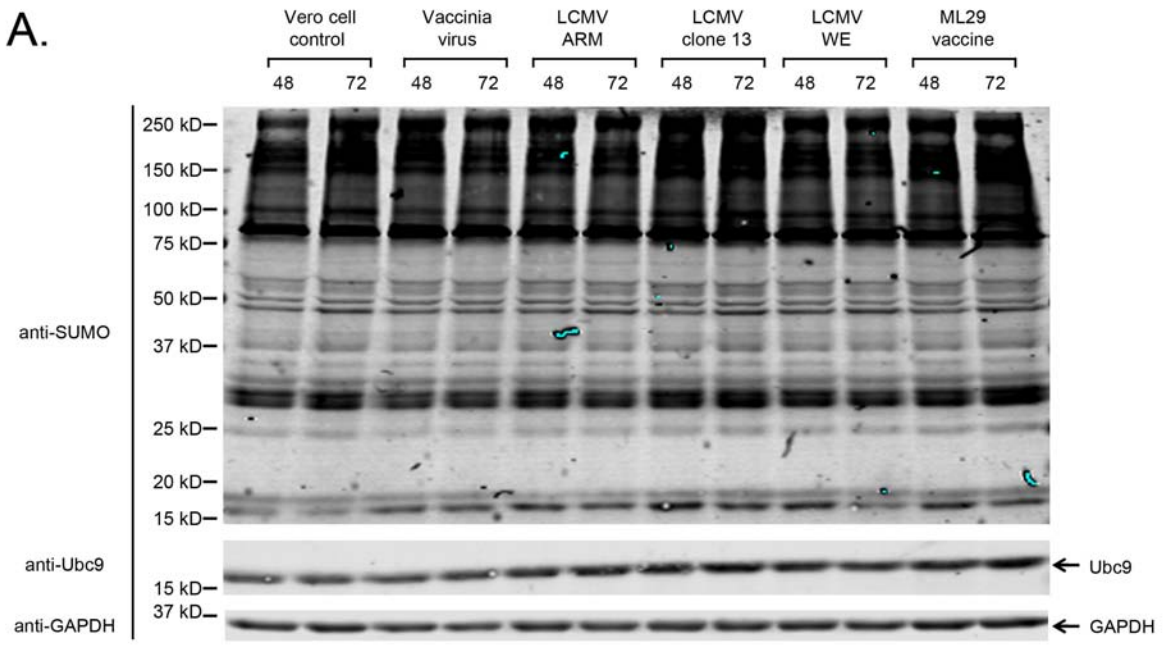

Figure 3.9. Infections with Vaccinia virus and LCMV results in an increase in cellular SUMOylation. VERO cells were infected with Vaccinia virus and LCMV. Cell extracts were collected at 48 and 72 hours post-infection and analyzed by SDS-PAGE (10% acrylamide) and immunoblotting using anti-SUMO1 MAb, anti-Ubc9 MAb, and anti-GAPDH MAb. MAb: monoclonal antibody.

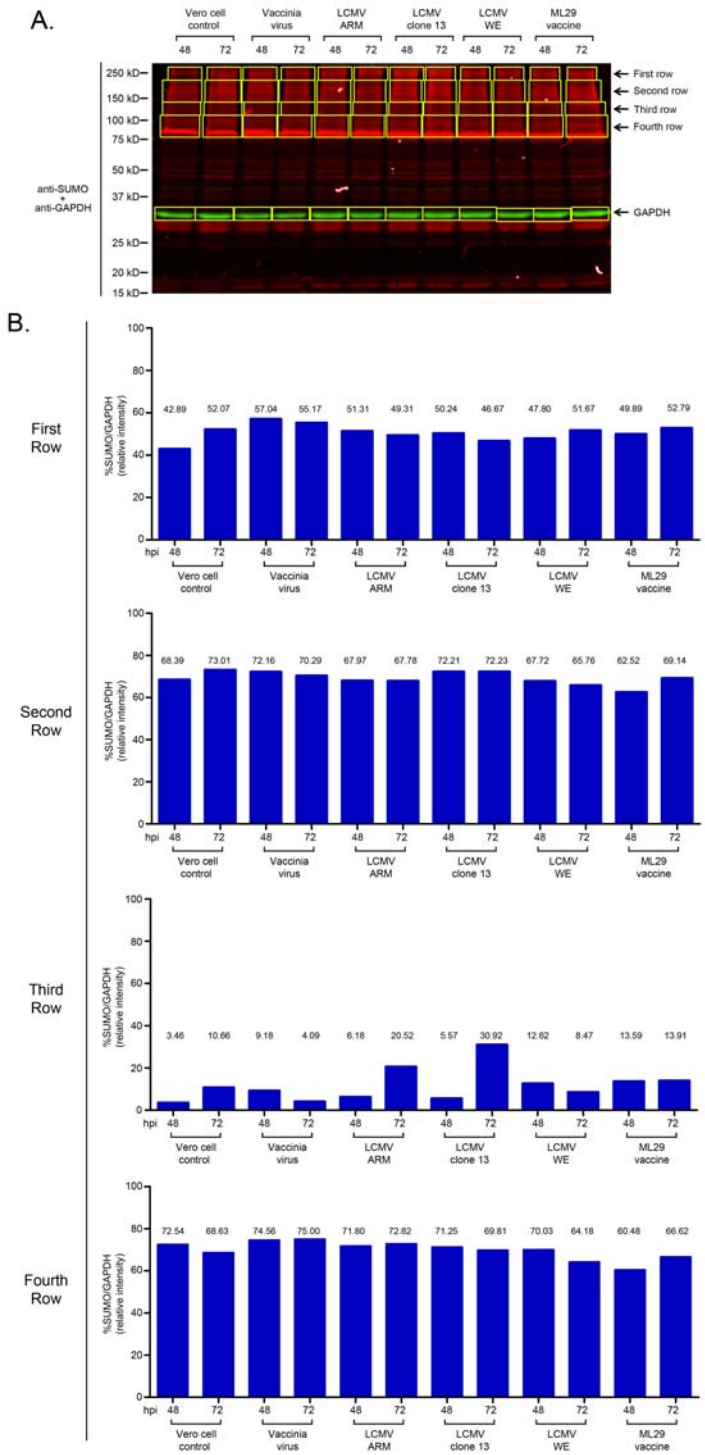

Figure 3.10. Infection with LCMV results in an increase in cellular SUMOylation within the 125 to 150 kD range. (A) VERO cells were infected with Vaccinia virus and LCMV, collected, and analyzed by SDS-PAGE (10% acrylamide) and immunoblotting using anti-SUMO1 MAb, anti-Ubc9 MAb, and anti-GAPDH MAb. The high molecular weight region was divided into four regions (yellow boxes). (B) Quantification of each of the four regions. MAb: monoclonal antibody.

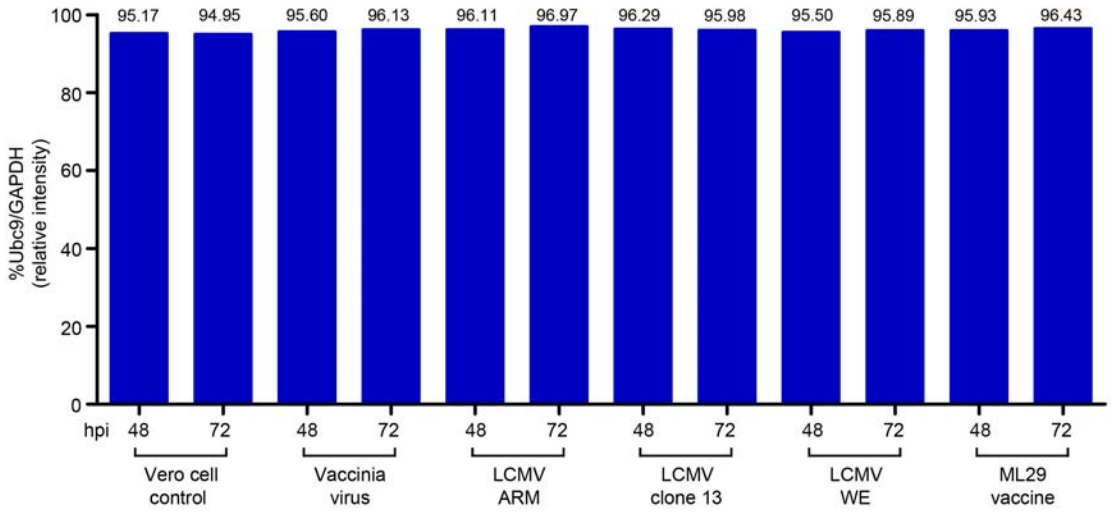

Figure 3.11. Increases in cellular SUMOylation during LCMV infection are not due to changes in the level of SUMO conjugating enzyme Ubc9. VERO cells were infected with Vaccinia virus and LCMV, collected, and analyzed by SDS-PAGE (10% acrylamide) and immunoblotting using anti-Ubc9 MAb and anti-GAPDH MAb. The relative intensity of Ubc9 for each sample was quantified as shown in the graph above (blue bars). MAb: monoclonal antibody.

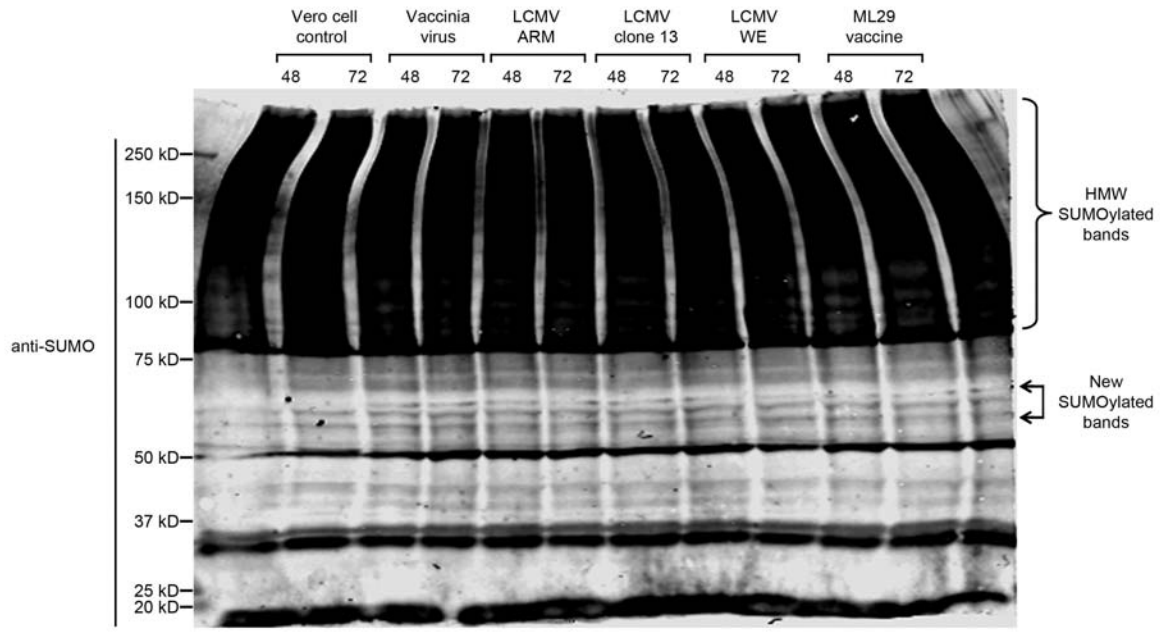

Figure 3.12. Infection with Vaccinia virus and LCMV results in the appearance of two new SUMOylated bands. VERO cells were infected with Vaccinia virus and LCMV. Cell extracts were collected at 48 and 72 hours post-infection and analyzed by SDS-PAGE (6% acrylamide) and immunoblotting using anti-SUMO1 MAb. MAb: monoclonal antibody.

3.4 Discussion:

Previous studies relating to the role of SUMOylation have characterized the increase in SUMOylation upon infection with different influenza A viral strains (Pal, Santos et al. 2011). Despite the ongoing research related to the interplay between the increase in cellular SUMOylation and viral infection, this is the first and only study that investigates increases in cellular SUMOylation upon influenza A viral infection in an animal model. Here, we evaluated the effect of NS1 SUMOylation on the increase in cellular SUMOylation and studies performed *in vitro,* tissue culture, and in an animal model showed that the ability of NS1 to be SUMOylated correlates to its ability to trigger an increase in cellular SUMOylation. We demonstrate that the global increase in cellular SUMOylation can be recapitulated in primary immune cells and in infected animal tissues, indicating that the observed increase is not specific to immortal cell lines. Furthermore, we show that an increase in cellular SUMOylation is also observed during viral infection with vaccinia virus and lymphocytic choriomeningitis virus. Overall, our results indicate that the increase in cellular SUMOylation is not limited to influenza A viral infection, but may be responsible for acting as a protection mechanism against viral infection.

Modulation of the cellular SUMOylation system has been shown to be a pathway that viruses exploit in order to promote viral replication and assembly, or to evade the host immune response (Flotho and Melchior 2013, Mattoscio, Segre et al. 2013). The chicken embryo lethal orphan (CELO) adenovirus protein, Gam1, is able to inhibit SUMOylation by interacting with and promoting the degradation of the E1 activating enzyme and enhancing viral replication (Boggio, Colombo et al. 2004, Boggio,

Passafaro et al. 2007). Thus, increasing SUMOylation with the cell would lead to an inhibition to viral replication. Our laboratory has shown that influenza A viral proteins are modified by the cellular SUMOylation system and that the influenza viral protein NS1 protein can trigger an increase in cellular SUMOylation (Pal, Rosas et al. 2010, Pal, Santos et al. 2011, Santos, Pal et al. 2013). We show here that this increase in cellular SUMOylation is directly related to the ability of NS1 to be SUMOylated.

Vaccinia virus is a member of the poxvirus family and contains a double stranded DNA genome. Vaccinia virus encodes two viral proteins, E3L and A40R, that are known targets of the cellular SUMOylation system (Palacios, Perez et al. 2005, Mattoscio, Segre et al. 2013). The E3L protein has been shown to be essential for virulence through its ability to bind DNA and double-stranded RNA (Marq, Hausmann et al. 2009) and transactivation activity of genes involved in apoptosis, the immune response, and viral pathogenesis (Kwon and Rich 2005, Gonzalez-Santamaria, Campagna et al. 2011). Moreover, the presence of a SIM is required for its stability and its SUMOylation, although, SUMO modification of the E3L protein negatively regulates its transactivation activity (Gonzalez-Santamaria, Campagna et al. 2011). The SUMO modification of the vaccinia virus protein A40R was shown to be required for its specific localization to the DNA replication sites within the cytoplasm and prevented its self-association (Palacios, Perez et al. 2005, Mattoscio, Segre et al. 2013). Our studies showed that upon viral infection with vaccinia virus there is an increase in cellular SUMOylation, possibly contributing to viral persistence and avoidance of the host immune response.

LCMV is a member of the *Arenaviridae* family and contains a negative-sense, single-stranded RNA genome. LCMV replicates in the cytoplasm and that its replication

can be diminished by increased expression of the PML-NBs that regulate cytokine signaling within the cell (Djavani, Rodas et al. 2001). Currently, there are no known LCMV viral proteins that are modified by SUMO. However, the increase in cellular SUMOylation upon viral infection suggests that LCMV may express at least one viral protein that is modified by SUMO. Similarly to influenza NS1 protein, the LCMV nucleoprotein (NP) is able to antagonize the host immune response by binding double-stranded RNA, as well as preventing the nuclear localization of NF-κB (Ortiz-Riano, Cheng et al. 2012). It is possible that the LCMV NP viral protein may be a target for SUMO modification.

Altogether, the data suggests that the increase in SUMOylation may be acting as a protection mechanism against viral infection by activating immune pathways and preventing apoptosis.

3.5 Acknowledgements:

I want to thank Dr. Daniel R. Perez and Ms. Johanna Lavigne (Department of Veterinary Medicine, University of Maryland-College Park, College Park, MD) for providing the mice, materials, and time necessary to complete the animal infections and for providing the reverse genetics systems for A/Puerto Rico/8/1934 [H1N1], A/Guinea Fowl/Hong Kong/WF10/99 [H9N2], and A/Memphis/14/1998 [H3N2]. I would like to thank Dr. Kristine Garza and Dr. Amanda Gonzalez (Department of Biological Sciences, The University of Texas at El Paso, El Paso, TX) for providing the bone marrow-derived dendritic cells. I would also like to thank Dr. John M. Quarles (Department of Microbial and Molecular Pathogenesis, College of Medicine, Texas A&M Health Sciences Center, College Station, TX) for providing the A/Puerto Rico/8/1934 [H1N1] influenza virus, and Dr. Yoshihiro Kawaoka (Department of Pathobiological Sciences, School of Veterinary Medicine, University of Wisconsin-Madison, Madison, WI) for providing the A/WSN/1933 [H1N1] 12-plasmid reverse genetics system. I would like to thank Dr. Armando Varela (Department of Biological Sciences, The University of Texas at El Paso, El Paso, TX) for his assistance with the confocal microscope. I would also like to thank Dr. Maria P. Salvato and Dr. Juan C. Zapata (Institute of Human Virology, University of Maryland, Baltimore, MD) for providing the LCMV and Vaccinia virus samples. This project was funded by grants from the National Institutes of General Medicine Sciences (NIH grant #1SC1AI098976 to GRA), Border Biomedical Research Center at UTEP (NIH-HIMHD-RCMI grant #8G12MD007592), and Center for Research on Influenza Pathogenesis (CRIP grant #HHSN266200700010C to DP). Katherine A. Meraz was supported by Graduate STEM Fellows in K-12 Education (GK-12) (NSF grant #NSF0947992).

CHAPTER 4: THE ARTIFICIAL SUMO LIGASE IS EFFECTIVELY EXPRESSED IN CELLS AND COULD ACT AS A POTENTIAL THERAPEUTIC AGAINST INFLUENZA A VIRAL INFECTION

4.1 Introduction:

Previous studies have indicated that increasing levels of any members of the SUMOylation pathway leads to a decrease in viral infection and, conversely, loss of SUMO modification leads to an increase in viral infection (Ribet and Cossart 2010, Hwang and Kalejta 2011). Our lab has demonstrated that altering the SUMOylation of NS1, either by increasing or decreasing, affects its ability to neutralize the host interferon immune response, however, has no effect on its stability or localization (Santos, Pal et al. 2013). Increasing the levels of NS1 SUMOylation was done using an $NS1_{1-87}$-Ubc9 artificial SUMO ligase. This interaction is mediated through NS1's ability to form homodimers. Although this data suggests that decreasing the SUMOylation of NS1 would decrease NS1's ability to neutralize IFN, based on the data from Chapter 1, viral infection with influenza viruses containing a non-SUMOylatable NS1 appear to have enhanced viral fitness and pathogenicity. This suggests that using the $NS1_{1-87}$-Ubc9 artificial SUMO ligase to enhance the SUMOylation of NS1 may diminish viral fitness and pathogenicity.

Many viruses interact with and exploit the SUMOylation system in order to promote viral replication and evade the host immune response (Mattoscio, Segre et al.

2013). Most viruses require SUMO modification in order to activate viral proteins for the recruitment of other viral or cellular factors or for its localization. However, similar to influenza virus, the Epstein-Barr virus encodes an immediate-early viral protein, Zta, which has been shown to be a target of SUMO modification. Zta SUMOylation decreases its transactivation of viral gene expression leading to the establishment of latentcy as opposed to lytic replication and, ultimately, repressing viral infection (Wimmer, Schreiner et al. 2012). We believe that use of the $NS1_{1-87}$-Ubc9 artificial SUMO ligase would allow us to modulate the SUMOylation of NS1 and possibly disrupt its antagonistic effect on the host immune response.

Furthermore, new technologies, including purified proteins and lentiviruses, are being utilized for the delivery of therapeutics for cancer therapy and viral infections (Hui, Yap et al. 2004, McKay, Patel et al. 2006, Patel, Giddings et al. 2013). The use of protein therapeutics is becoming more advantageous for several reasons: 1) their ability to perform specific functions that cannot be mimicked by other chemical compounds; 2) their action is less likely to interfere with biological processes; 3) the body produces many of the proteins that are being used as therapeutics; 4) they can provide effective replacement treatment for mutated or deleted genes; 5) the development and approval of protein therapeutics is faster than other chemical compounds; and 6) proteins are unique in form and function (Leader, Baca et al. 2008). The use of lentiviral vectors for delivery of therapeutics have become increasingly more popular due to their preferable integration pattern into the host genome (Farinelli, Capo et al. 2014). Previous retroviral vectors were prone to transcriptional activation of surrounding proto-oncogenes through their integration into enhancer and promoter regions, however, lentiviral vectors have

overcome this through their integration into actively transcribed genes (Farinelli, Capo et al. 2014).

Our lab has developed the artificial SUMO ligase, which is a fusion protein comprised of the first 87 amino acids from NS1 with the E2 conjugating enzyme, Ubc9, that is able to specifically enhance the SUMOylation of NS1. The objective of this chapter is to investigate whether the $NS1_{1-87}$-Ubc9 artificial SUMO ligase can be effectively expressed within cells and assess its effects on influenza viral infection. In order to investigate this, we used two methods to test the artificial SUMO ligase. First, the protein was purified through expression in a bacterial cell line followed by GST pulldowns. The purified protein would be used to transfect cell lines and test for its expression. In addition, the artificial SUMO ligase was inserted into a lentiviral vector which was then used to develop cell lines that would stably express the artificial SUMO ligase. The cell lines would be tested for the expression of the artificial SUMO ligase.

4.2 Materials and Methods:

Artificial SUMO ligase protein purification

To produce purified protein that can be used as a potential therapeutic, a plasmid was developed containing the NS1(R38AK41A)$_{1\text{-}87}$-Ubc9 artificial SUMO ligase in a GST expression vector that allowed for its expression in bacterial cells. The plasmid was transformed into BL21 competent bacterial cells and protein production was induced using isopropyl β-D-1-thiogalactopyranoside (IPTG). A GST pulldown was then performed in which glutathione-sepharose beads were used to capture GST fused proteins. The RNA binding domain within NS1 has been modified to contain two mutations within the RNA binding domain which allow the protein to maintain its tubular structure, however, remain in the soluble fraction during purification (Bornholdt and Prasad 2008).

Development of stably transduced cell lines

To produce lentiviruses that contain the ASL as a potential therapeutic, a plasmid was developed containing the NS1$_{1\text{-}87}$-Ubc9 artificial SUMO ligase in the pENTR1A expression vector. Using this plasmid, an *in vitro* recombination reaction was required to transfer the ASL cassette into the pLenti vector. Recombinant lentiviruses were produced by transfection of A549 and MDCK cells with the lentiviral vector system. A549 and MDCK cells transduced with the lentivirus were maintained in complete media supplemented with the antibiotic, zeocin.

GST-pulldown

A GST pulldown, using either GST-SUMO1 or GST-SUMO3, was performed in which glutathione-sepharose beads were used to capture GST fused proteins of interest. Glutathione-sepharose beads were centrifuged twice at 3,000 rpm for 1 minute, once with water and once with cold 1x PBS. The beads were then equilibrated with 1x PBS supplemented with either GST or GST-NS1 to make a 50% slurry. The reaction was then incubated at 4°C for 1 hour. The beads were washed with 1x PBS supplemented with 0.1% Tween 20 in the HulaMixer® Sample Mixer (Life Technologies) for 3 minutes. Samples were centrifuged at 3,000 rpm for 1 minute and the supernatant removed by the vacuum system. Samples were mixed with 4x sample buffer and analyzed by immunoblot.

Transient transfections

HEK293FT cells (Invitrogen Corp.) were seeded at a density of 5 x 10^5 cells/well into 6 well plates. The following day, cells were transfected by liposome-mediated transfection using 1 ug of CsCl-purified plasmids and 2 uL of TransIT-LT1 (Mirus Bio LLC, Madison, WI) per well, according to the manufacturer's recommendations. Cells were incubated at 37ºC in 5% CO_2 for 24 hours. Cell extracts were collected at 1 and 24 hours post-transfection and analyzed by SDS-PAGE followed by immunoblotting to determine transfection efficiency of the ASL. Culture supernatant was then discarded and 4x sample buffer and β-mercaptoethanol was added up to a final concentration of 10%, and the samples were boiled in a water bath for 3 minutes.

Transient transfections of purified protein

HEK293FT cells (Invitrogen Corp.), MDCK cell or A549 cells (ATCC) were seeded at a density of 5 x 10^5 cells/well into 6 well plates. The following day, cells were transfected with purified ASL protein at different concentrations using using the Xfect Protein Transfection Reagent (Clontech Laboratories Inc., Mountain View, CA), according to the manufacturer's recommendations. Cells were incubated at 37ºC in 5% CO_2. Cell extracts were collected at 1 and 24 hours post-transfection and analyzed by SDS-PAGE followed by immunoblotting to determine transfection efficiency of the ASL. Culture supernatant was then discarded and 4x sample buffer and β-mercaptoethanol was added up to a final concentration of 10%, and the samples were boiled in a water bath for 3 minutes.

Immunoblot analyses

Prior to SDS-PAGE analyses, all cell extracts generate were passed several times through a 29½ gauge needle to break down the genomic DNA released and to decrease the viscosity of the samples. β-mercaptoethanol was added up to a final concentration of 10%, and the samples were boiled in a water bath for 3 minutes. The samples were resolved by 10% SDS-PAGE gels made in-house and, subsequently, the proteins were transferred to Immobilon-FL (Millipore Corp., Bedford, MA) for use with IRDye-conjugated secondary antibodies (LI-COR Biosciences Inc., Lincoln, NE) and infrared fluorescence imaging.

Infrared fluorescence imaging

Immobilon-FL membranes (Millipore Corp.) were washed four times in 1x PBS, blocked with Odyssey Blocking Buffer (LI-COR Biosciences Inc.) for a minimum of 1 hour at room temperature, and incubated in Odyssey Blocking Buffer at 4°C overnight with the primary antibody at the indicated dilution. The membranes were then washed four times with 1x PBS, supplemented with 0.1% polysorbate 20 (Tween 20), and incubated with Odyssey Blocking Buffer with the appropriate highly cross-absorbed IRDye 800 CW- and IRDye 680 LT-conjugated secondary antibodies (LI-COR Biosciences Inc.) at the indicated dilution. The membranes were then washed four times with 1x PBS, supplemented with 0.1% Tween 20 and twice again with 1x PBS and scanned on an Odyssey CLx infrared imaging system (LI-COR Biosciences Inc.). Quantitative analyses of the images obtained was performed by using Odyssey Infrared Imaging System Application software version 3.0.29 (LI-COR Biosciences Inc.). Statistical analyses and graphics of the data generated were performed by using GraphPad Prism version 5.04 for Windows (GraphPad Software Inc., San Diego, CA).

Immunofluorescence assay of cultured cell lines

HEK293FT or HEK293A cells (Invitrogen Corp.) or MDCK cells (ATCC) were seeded at a density of 8 x 10^3 cells/well into 96 well plates. The following day, cells were transfected with the specified concentrations of purified ASL protein using the Xfect Protein Transfection Reagent (Clontech Laboratories Inc.), according to the manufacturer's recommendations. Cells were incubated at 37ºC in 5% CO_2 for 24 hours. The supernatant was then discarded and the cells were fixed with 4%

paraformaldehyde for 15 minutes at room temperature. The fixative was aspirated and the cells were rinsed three times with 1x PBS, blocked with 1x PBS supplemented with 1% goat serum for a minimum of 1 hour at room temperature, and incubated in 1x PBS supplemented with 1% goat serum at 4°C overnight with the primary antibody at the indicated dilution. The cells were then washed three times with 1x PBS, and incubated with 1x PBS supplemented with 1% goat serum with the appropriate highly cross-absorbed AlexaFluor 594 and AlexaFluor 488 fluorophore-conjugated secondary antibodies (LI-COR Biosciences Inc.) at the indicated dilution. Sections were washed three times in 1x PBS followed by one wash with 1x PBS supplemented with DAPI (Thermo Scientific) at a final concentration of 0.5 ug/mL. After 10 minutes, the cells were washed two additional times and analyzed using the confocal microscope.

Viral Infection

MDCK, MDCK-ASL, or HEK293A cells were plated into 96-well or 12 well plates at a density of 2.0 x 10^5 or 1.6 x 10^4 cells/well, respectively, in either 1x DMEM supplemented with 10% FBS (for MDCK and MDCK-ASL) or 10% Fetal Plex (for HEK293FT). The next day the cells were washed once with 1x DMEM, and a virus dilution prepared in 1x DMEM supplemented with 0.2% BSA was added to the cells and incubated with the cells at 37°C in 5% CO_2 for 24 hours (96-well) or for 1 hour (12-well). For the 96-well plate: 24 hours post-infection the plate was processed for analysis by immunofluorescence assay. For the 12-well plate: the supernatant was then removed and replaced with 1x DMEM supplemented with 1% TPCK-treated trypsin. A portion of the viral supernatants were collected at this time (0 hours post-infection), labeled, and

stored at -80°C. The plates were incubated at 37°C in 5% CO_2 for an additional 24 hours. Viral supernatants were collected at 24 hours post-infection, labeled, and stored at -80°C. Total cell extracts were collected in 4x sample buffer for analysis by SDS-PAGE.

$TCID_{50}$ to determine viral titers

MDCK cells were plated into 96-well plates at a density of 1.6 x 10^5 cells/well in 1x DMEM supplemented with 10% FBS and incubated at 37°C in 5% CO_2 until the cells formed a confluent monolayer. The cells were then washed once with 1x DMEM, and a virus dilution prepared in 1ml of 1x DMEM supplemented with 0.2% BSA was added to the cells and incubated with the cells at 37°C in 5% CO_2 for 3 days until cytopathic effects (CPE) were observed. 50 µL of the supernantants from $TCID_{50}$ plates were transferred to a 96-well V-bottom plate (Corning Incorporated Life Sciences). 50 µL of 0.5% turkey red blood cells (Lampire Biological Laboratories, Pipersville, PA) suspended in 1x PBS, were added to the V-bottom plate and gently tapped to mix. Plates were incubated at room temperature for 45 minutes. Plates were scored and viral titers were determined using the Reed-Muench method.

Statistical analysis and computer software.

All statistical analyses and graphics presented were performed by using GraphPad Prism version 5.04 for Windows (GraphPad Software Inc.). All figures were created by using Adobe Photoshop CS5 extended version 12.0.3 X64 (Adobe Systems Inc.).

4.3 Results:

Transfection of the purified protein form of the artificial SUMO ligase can be achieved in multiple cell lines. Previous studies had shown that modulation of NS1 SUMOylation affects its ability to neutralize the host IFN response (Santos, Pal et al. 2013). We have developed an novel tool, the artificial SUMO ligase (ASL), in order to specifically enhance the SUMOylation of NS1. To determine whether we can deliver the ASL purified protein into the cell, we transfected different cell lines with the protein and then analyzed for its presence at different times post-transfection. We were able to detect the ASL in transfected HEK293FT, MDCK, and A549 cells (**Figure 4.1**).

The purified protein form of the artificial SUMO ligase is located in the cytoplasm of transfected cells. In order to determine whether the protein was being delivered into the cells and not simply remaining stuck at the plasma membrane, immunofluorescence assays were performed. HEK293FT cells were transfected with different concentrations of ASL protein and its localization was determined by confocal microscope. Cells transfected with 0.1 or 0.4 µg/µL of the ASL protein showed mostly cytoplasmic localization (**Figure 4.2**). Conversely, cells transfected with 1.0 or 4.0 µg/µL of the ASL protein showed mostly extracellular localization (**Figure 4.2**).

Transfection with purified GST or GST-ASL results in decreased viral replication. In order to determine the effect of the transfected purified ASL during influenza viral infection, MDCK cells were either not transfected or transfected with 0.4 µg/µL either purified GST-ASL, or GST as a control, and subsequently infected with A/

Puerto Rico/8/1934 [H1N1] influenza virus at an MOI of 0.5. Total cell extracts were analyzed by immunoblot and viral supernatants were quantified by $TCID_{50}$. Although the exogenous GST or GST-ASL could not be detected by immunoblot (**Figure 4.3A**), cells transfected either with GST or GST-ASL resulted in substantially lower viral titers as compared to non-transfected cells (**Figure 4.3B**).

The artificial SUMO ligase is expressed at low levels in transduced cells. As an alternative delivery method of the ASL protein, a lentivirus was developed and used to transduce two different cell lines, MDCK and A549. Stably transduced cell lines were selected for zeocin antibiotic resistance and maintained in complete medium supplemented with zeocin. To determine whether the ASL is expressed in transduced cells, cells from each of the cell lines were collected and analyzed for the presence of the ASL. Both MDCK and A549 cell lines expressed the ASL (**Figure 4.4A**). The expression of the ASL protein was quantified as compared to the intensity of GAPDH and showed that the intensity of the ASL in MDCK cells was found to be approximately 1.4% and 1.8% of the intensity measured for GAPDH in MDCK and A549 cells, respectively (**Figure 4.4B**).

The artificial SUMO ligase is expressed within the cytoplasm of transfected cells. In order to determine the location of transduced ASL, HEK293A cells were transfected with a plasmid expressing the ASL and its localization was determined by confocal microscope. Cells transfected with the ASL protein showed both nuclear and cytoplasmic localization (**Figure 4.5**).

Plasmid transfection with HA-Ubc9 or artificial SUMO ligase ($NS1_{(1-87)}$-Ubc9) results in decreased viral infection. To determine how expression of the artificial SUMO ligase affects viral infection, HEK293A cells were either not transfected or transfected with either the plasmid encoding the ASL, or $NS1_{(1-87)}$, HA-Ubc9 or an empty plasmid as controls, and subsequently infected with A/Puerto Rico/8/1934 [H1N1] influenza virus at an MOI of 5. Although infected cells were observed in every sample (**Figure 4.6**), there were slightly fewer infected cells in samples transfected with the ASL.

Expression of the artificial SUMO ligase increases upon viral infection and results in higher viral titers. In order to determine how the expression of the ASL affects influenza viral infection, we infected either MDCK cells or the stably transduced MDCK-ASL cells with A/Puerto Rico/8/1934 [H1N1] influenza virus at an MOI of 0.5. Total cell extracts were collected and analyzed by SDS-PAGE. Immunoblot analysis showed that the ASL protein and the influenza late viral protein, M1, was detectable at 24 hours post-infection in MDCK-ASL, however, was not detectable in infected MDCK cells (**Figure 4.7A**). The expression of the ASL protein was quantified as compared to the intensity of GAPDH and showed that the intensity of the ASL in MDCK-ASL cells was found to be approximately 21% of the intensity measured for GAPDH in MDCK-ASL cells (**Figure 4.7B, left panel**). The expression of the M1 viral protein was quantified as compared to the intensity of GAPDH and showed that the intensity was found to be approximately 0% and 2% of the intensity measured for GAPDH in MDCK and MDCK-ASL cells, respectively (**Figure 4.7B, right panel**). Viral supernatants were

quantified by $TCID_{50}$. Stably transduced MDCK-ASL cells had increased levels of viral titers as compared to non-transduced MDCK cells at both 0 and 24 hours post-infection (**Figure 4.7C**).

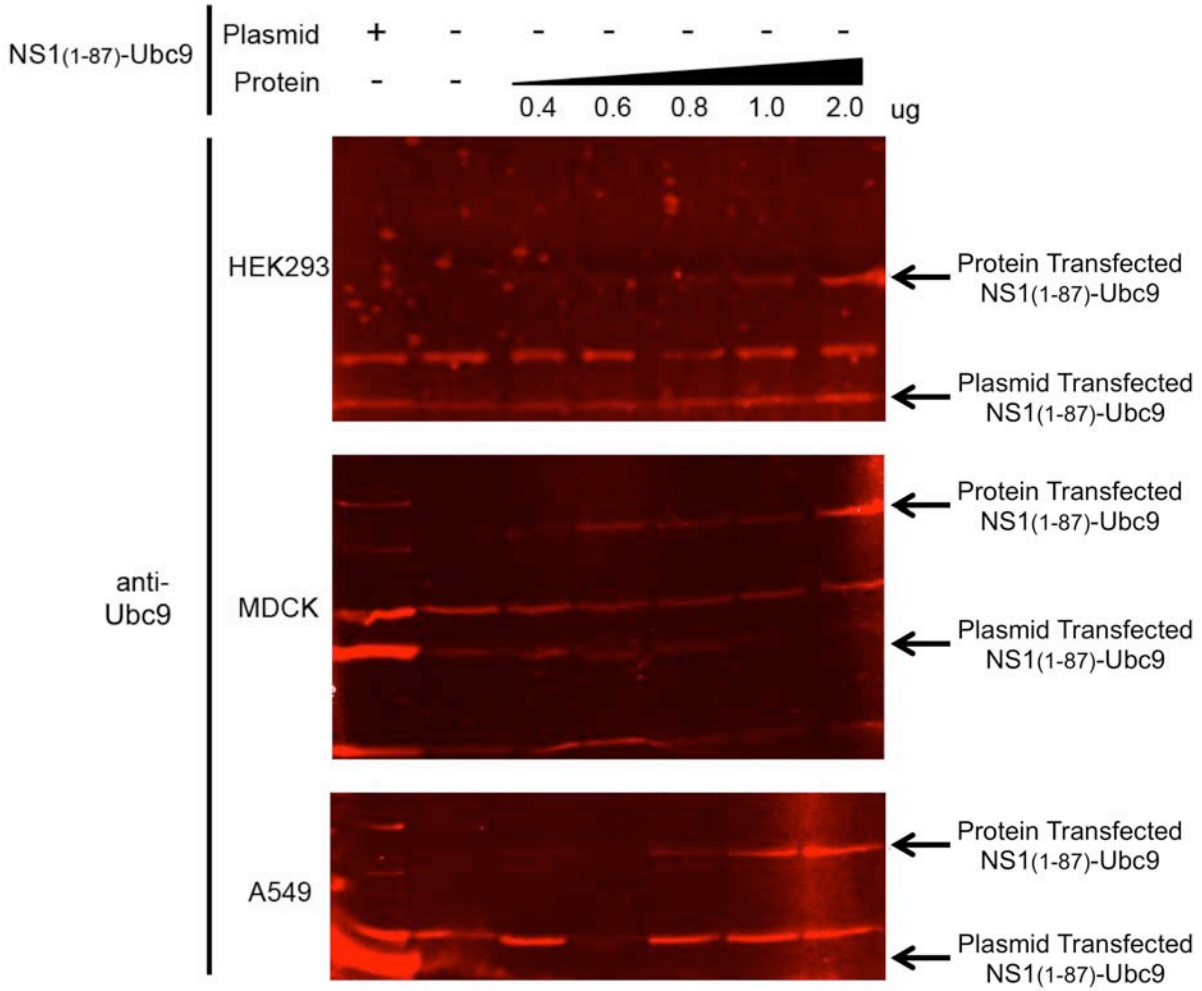

Figure 4.1. Transfection of the purified protein form of the artificial SUMO ligase can be achieved in multiple cell lines. HEK293FT, MDCK, and A549 cells were transfected with the plasmid encoding the ASL or with purified ASL protein. Samples were analyzed by SDS-PAGE and immunoblotting using anti-Ubc9 MAb. MAb: monoclonal antibody.

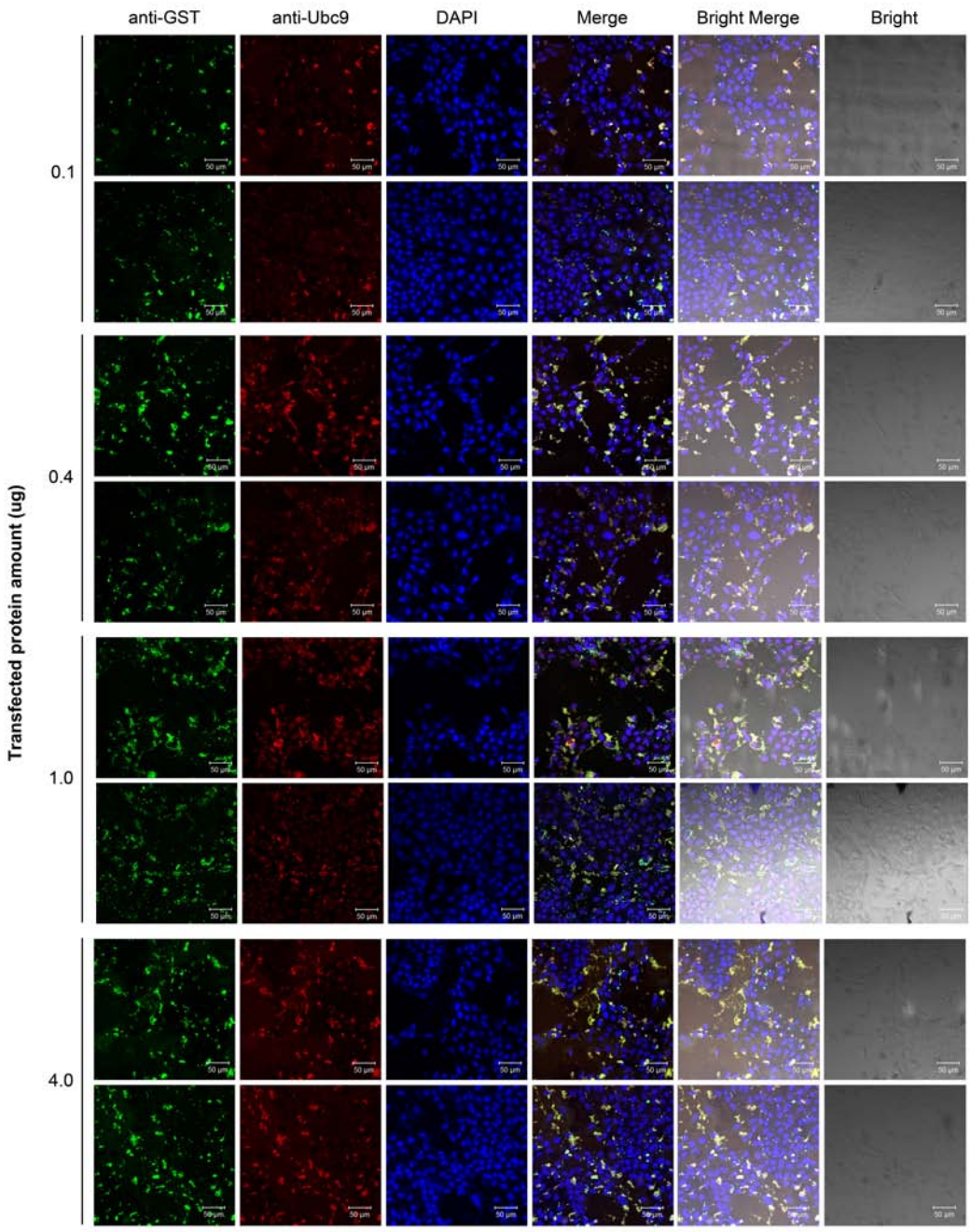

Figure 4.2. The purified protein form of the artificial SUMO ligase is located in the cytoplasm of transfected cells. HEK293FT cells were harvested for immunofluorescence analysis. Cells were fixed in paraformaldehyde and were processed and stained with DAPI (blue), anti-Ubc9 MAb (red), and anti-GST MAb (green). Images were taken using confocal microscope. MAb: monoclonal antibody.

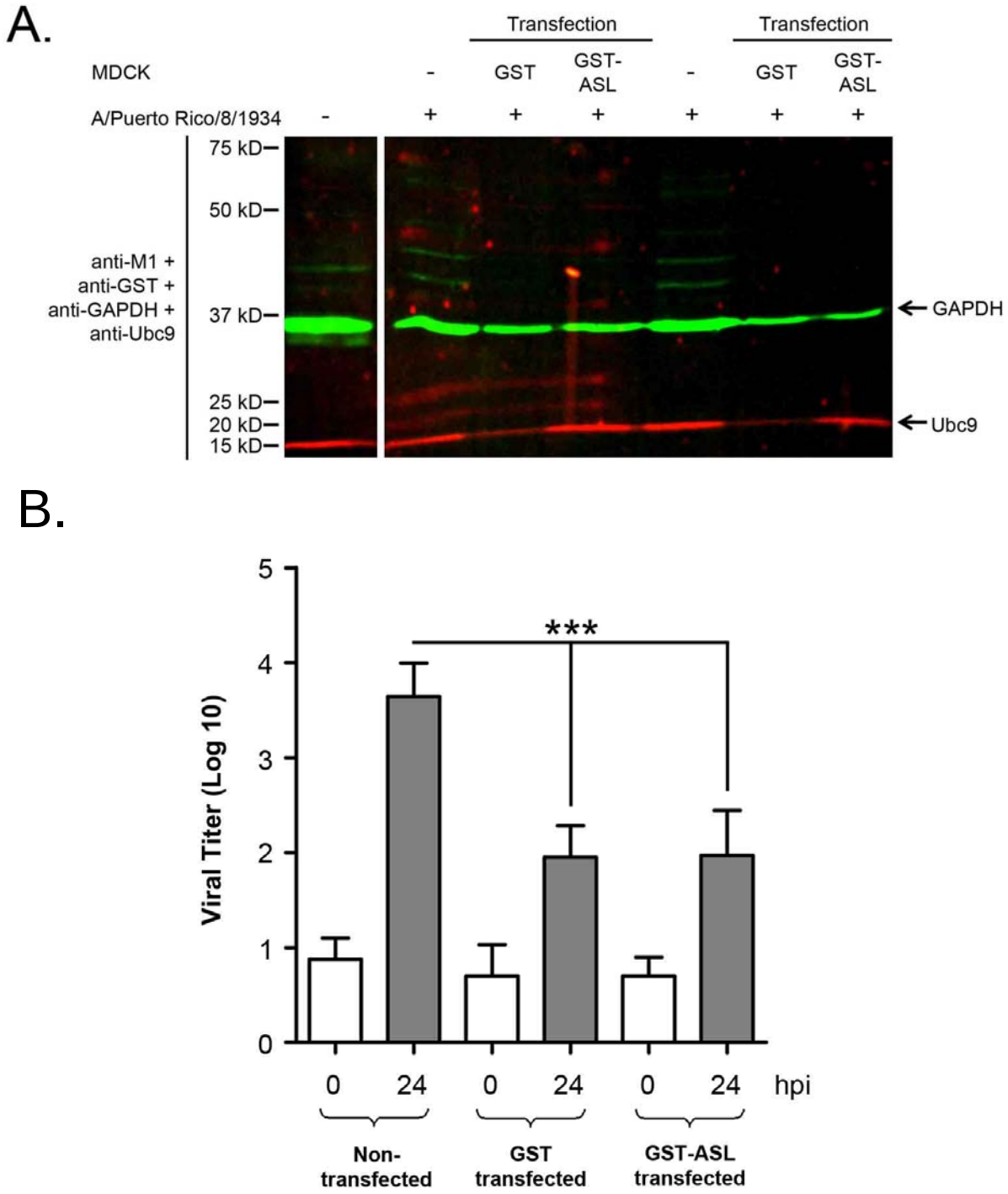

Figure 4.3. Transfection with purified GST or GST-ASL results in decreased viral replication. MDCK cells were transfected with either purified GST or GST-ASL and infected with A/Puerto Rico/8/1934. (A) Samples were analyzed by SDS-PAGE and immunoblotting using anti-M1, anti-GST MAb, anti-GAPDH MAb, and anti-Ubc9. (B) Quantification of viral titers was performed by $TCID_{50}$. Error bars indicate standard deviation. ***, P<0.0001. MAb: monoclonal antibody.

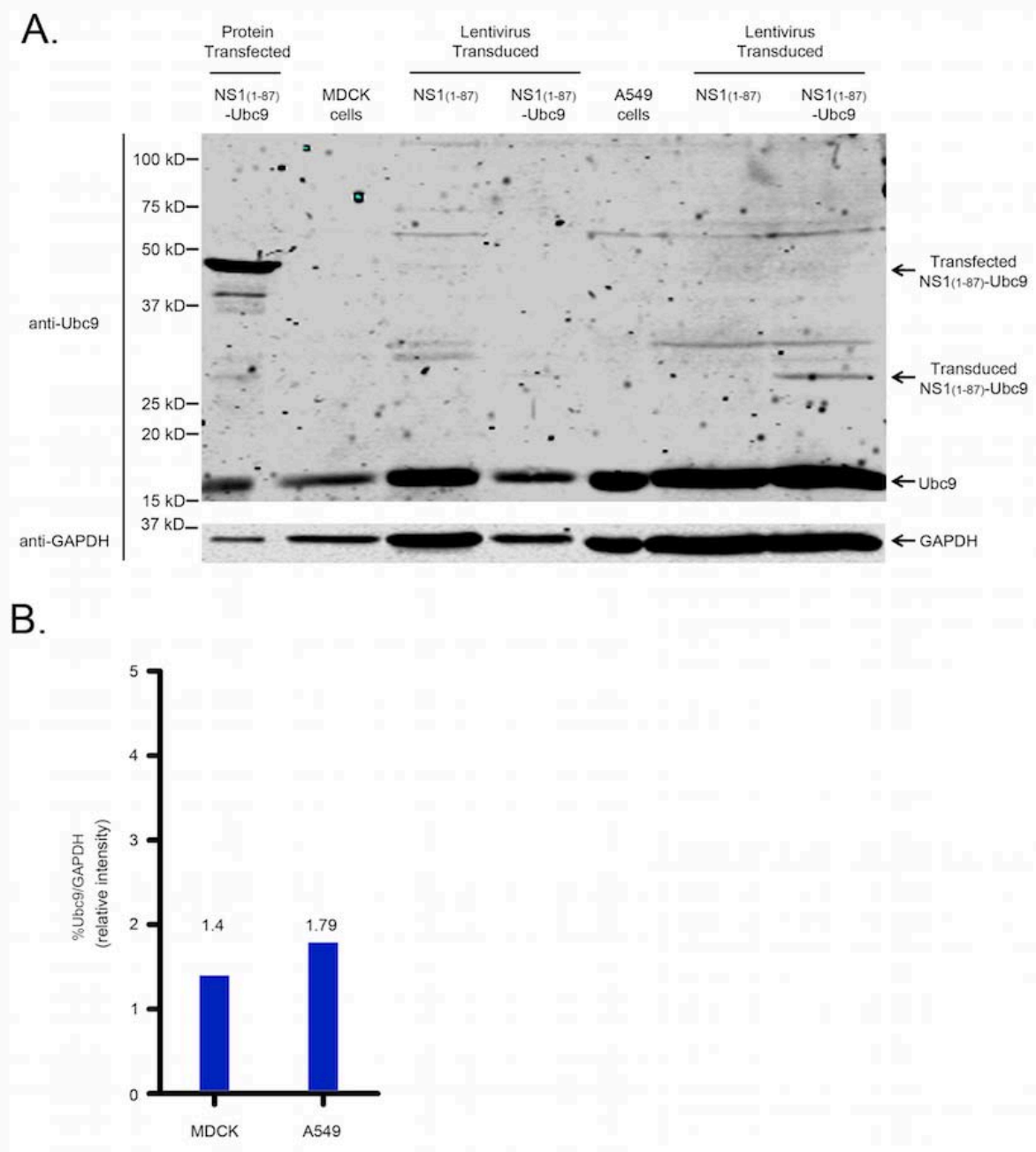

Figure 4.4. The artificial SUMO ligase is expressed at low levels in transduced, non-infected cells. MDCK and A549 cells were transduced using a lentiviral vector containing the ASL. (A) Samples were analyzed by SDS-PAGE and immunoblotting using anti-Ubc9 MAb and anti-GAPDH MAb. (B) Quantification of the transduced ASL as relative intensity to GAPDH. MAb: monoclonal antibody.

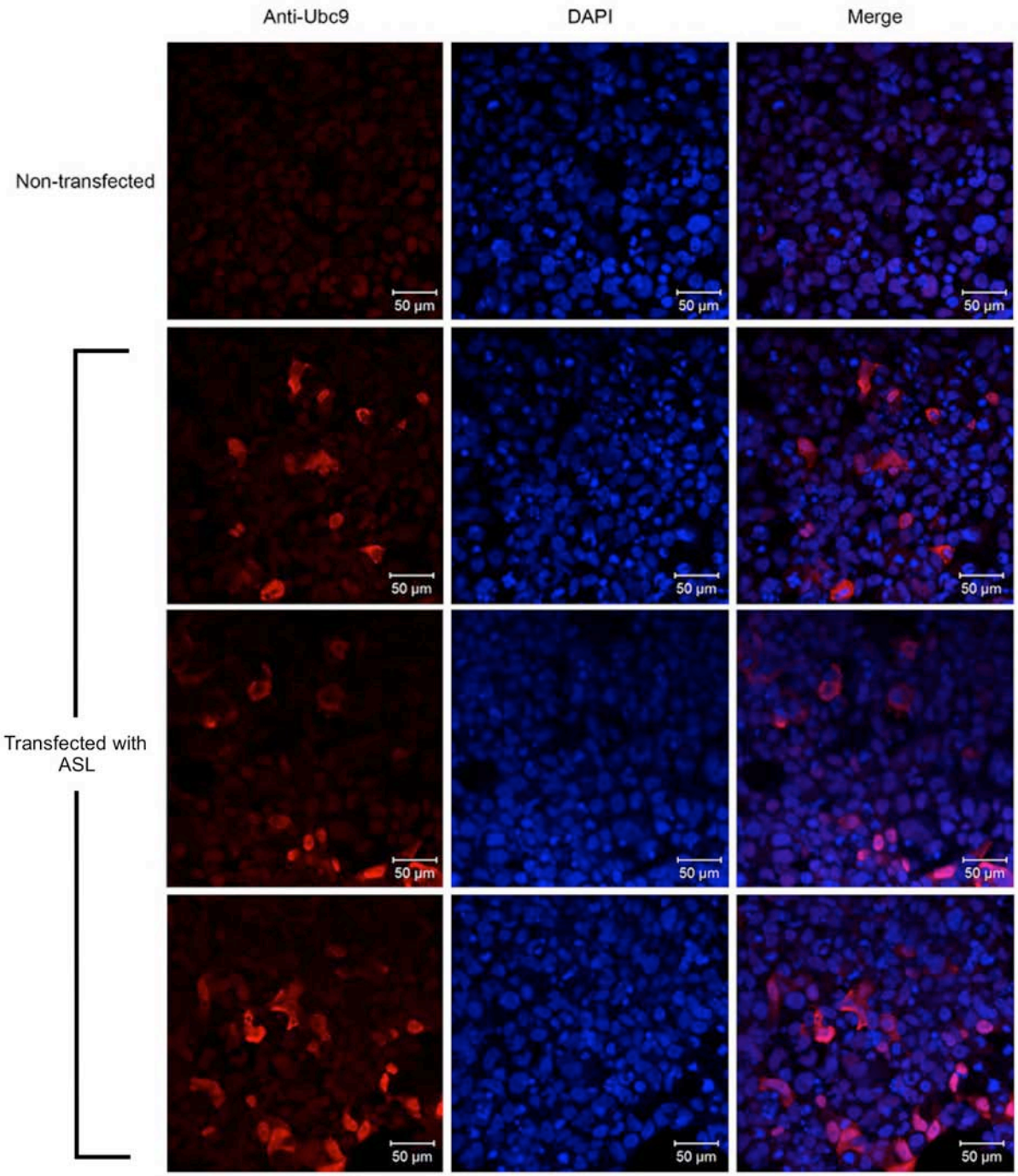

Figure 4.5. The artificial SUMO ligase is expressed within the nucleus and cytoplasm of transfected cells. HEK293A cells were not transfected or transfected with a plasmid that encodes the ASL. Samples were analyzed by immunofluorescence assay using anti-Ubc9. MAb: monoclonal antibody.

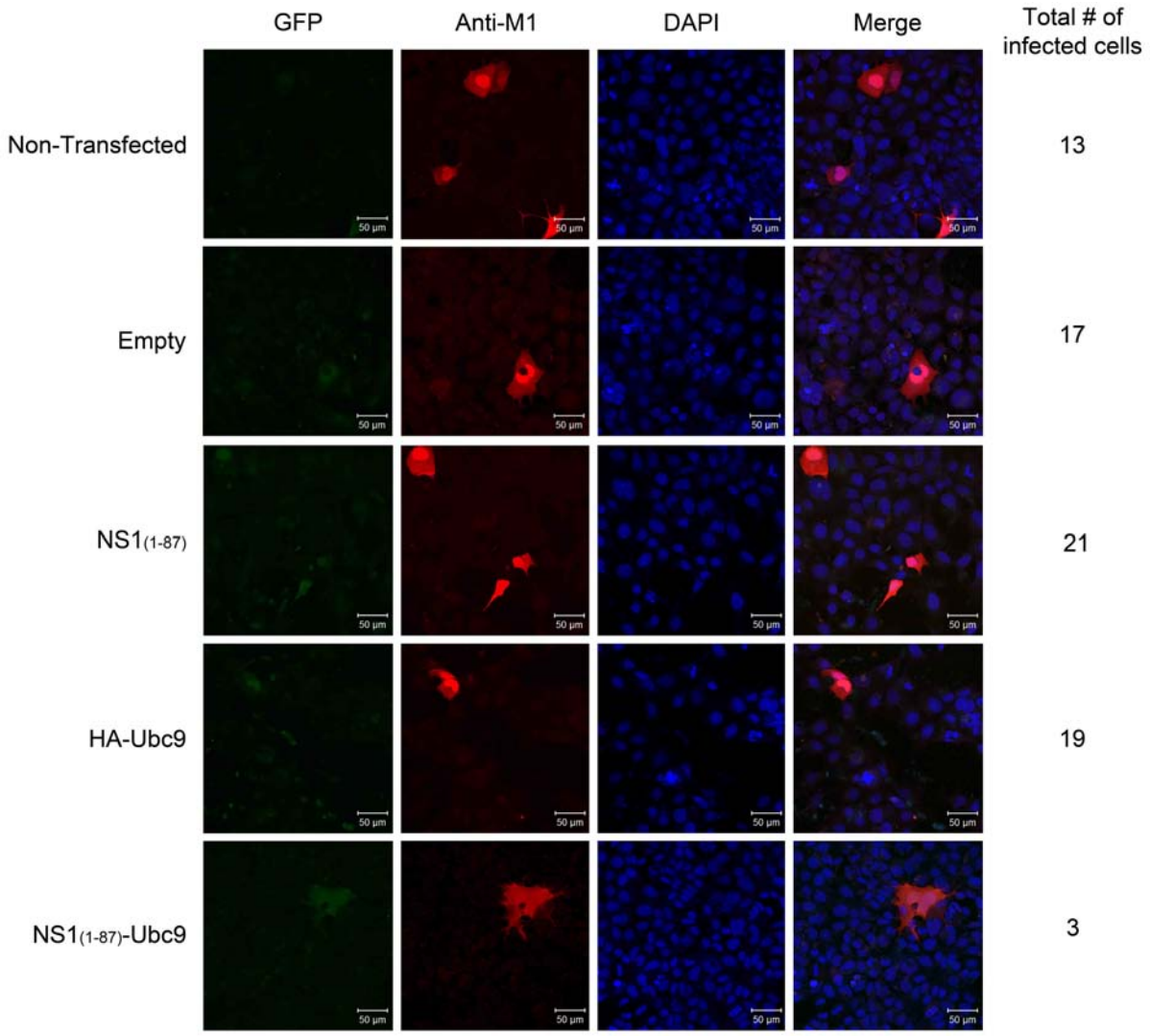

Figure 4.6. Plasmid transfection with HA-Ubc9 or artificial SUMO ligase (NS1$_{(1-87)}$-Ubc9) results in decreased viral infection. HEK293A cells were not transfected or transfected with either a plasmid that encodes an empty vector, NS1$_{(1-87)}$, HA-Ubc9, or the ASL. 24 hours post-transfection samples were infected with A/Puerto Rico/8/1934 influenza virus. 24 hours post-infection, samples were analyzed by immunofluorescence assay using anti-M1 and GFP. MAb: monoclonal antibody.

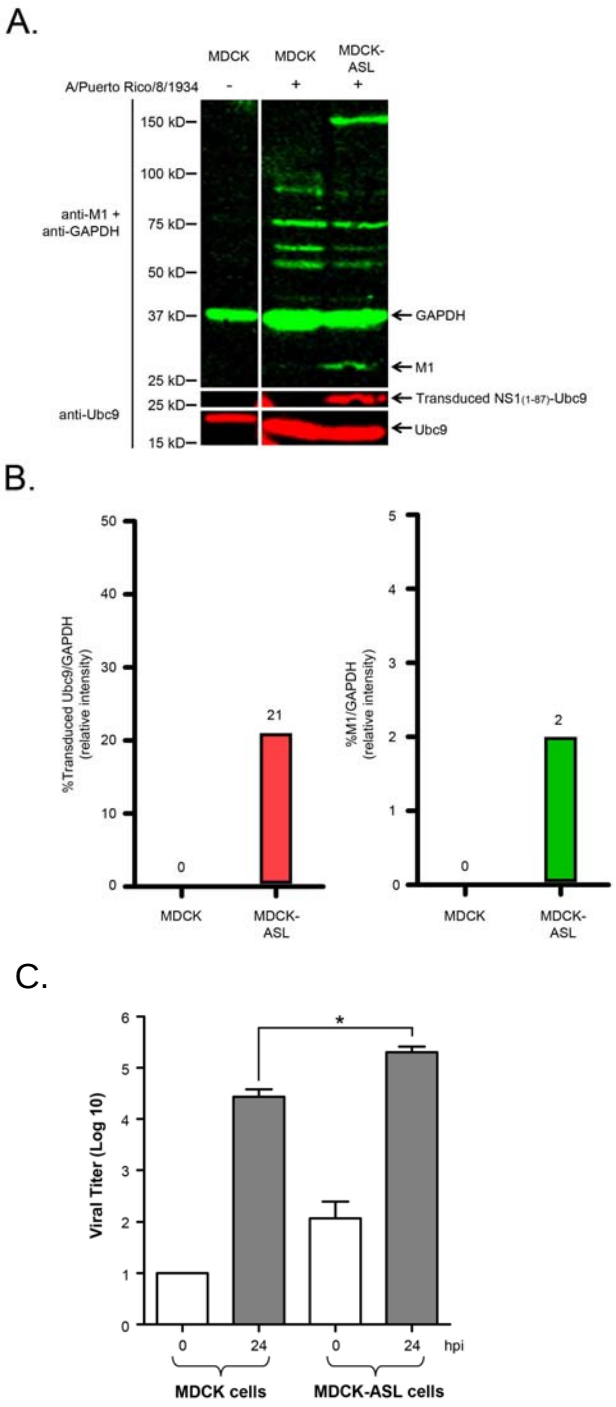

Figure 4.7. Expression of the artificial SUMO ligase increases upon viral infection and results in higher viral titers. MDCK and MDCK-ASL cells were infected with A/Puerto Rico/8/1934. (A) Samples were analyzed by SDS-PAGE and immunoblotting using anti-M1 MAb, anti-GAPDH MAb, and anti-Ubc9. (B) Quantification of the transduced ASL (left panel) and M1 (right panel) as relative intensity to GAPDH. (C) Quantification of viral titers was performed by $TCID_{50}$. Error bars indicate standard deviation. *, $P<0.05$. MAb: monoclonal antibody.

4.4 Discussion:

Previous studies relating to the use of the $NS1_{1-87}$-Ubc9 artificial SUMO ligase showed that increasing NS1 SUMOylation decreased its ability to neutralize the host IFN response (Santos, Pal et al. 2013). Despite the ongoing research related to the effect of NS1 SUMOylation on viral infection, this is the first and only study that investigates whether the $NS1_{1-87}$-Ubc9 artificial SUMO ligase can be effectively expressed within cells and be considered as a novel treatment against influenza viral infection. We demonstrate that the $NS1_{1-87}$-Ubc9 artificial SUMO ligase in the purified protein form can be effectively transfected into different cell lines. Furthermore, we show that the protein form of the $NS1_{1-87}$-Ubc9 artificial SUMO ligase locates to the cytoplasm of transfected cells which could potentially interact with the cytoplasmic fraction of NS1. In addition, we show that the $NS1_{1-87}$-Ubc9 artificial SUMO ligase can be constitutively expressed in stably transduced cells produced by lentiviral transduction, albeit at substantially lower levels, and that its expression is both nuclear and cytoplasmic. The transduced ASL could potentially interact with both the nuclear and cytoplasmic fractions of NS1 regulating its function. Overall, our results indicate that the two methods used to deliver the $NS1_{1-87}$-Ubc9 artificial SUMO ligase are effective.

Infections performed in purified protein-transfected cells resulted in lower viral titers as compared to non-transfected cells. Although the GST and GST-ASL transfected cells had very similar titers, the data suggests that the transfection itself may be inhibiting viral infection. This would be a reasonable explanation considering previous studies demonstrating that transfection reagents can induce IFN and IFN-stimulated genes (Li, Boyanapalli et al. 1998). In addition, infections performed in plasmid-

transfected cells resulted in a markedly reduced number of infected cells in both HA-Ubc9 and ASL transfected samples as compared to $NS1_{(1-87)}$, empty, or non-transfected samples. The data obtained from transfecting HA-Ubc9 is in agreement with previous experiments performed in our lab demonstrating that over-expression of Ubc9 prevents viral infection (Melendez et al., manuscript in preparation). This data suggests that expression of the ASL is effective at limiting viral infection.

In contrast, infections performed in the stably transduced MDCK-ASL cell line resulted in higher expression of the ASL protein and increased viral titers as compared to MDCK infected cells. Previously, we observed low levels of ASL protein in non-infected samples, however, the expression of the ASL protein was induced during viral infection. In terms of viral titers, the difference in viral titers at 24 hours post-infection may be due to the abundance of virus at 0 hours post-infection. If this difference is accounted for, the viral titer of the MDCK-ASL cells would be lower than that of the MDCK cells, further supporting the ASL at limiting viral infection.

Most viral proteins have been shown to be activated upon SUMO modification and may regulate their activity during viral infection. The E1B-55K protein encoded by adenoviruses is a target for SUMO modification and acts as a SUMO-1 specific E3 ligase to promote viral replication (Mattoscio, Segre et al. 2013). Similarly, the K-bZip protein encoded by Kaposi's sarcoma associated herpesvirus is a target for SUMOylation and acts as a SUMO-2/3 specific E3 ligase in order to regulate the cell cycle and apoptosis (Mattoscio, Segre et al. 2013). In addition, viral proteins encoded by vaccinia virus, bovine and human papillomavirus, and cytomegalovirus that regulate viral replication or viral capsid assembly and are all targets for the SUMOylation system

appear to require this modification to exert their function (Boggio and Chiocca 2006, Mattoscio, Segre et al. 2013). Although the influenza NS1 protein does not require SUMO modification to antagonize the host immune response, previous studies have demonstrated that altering its levels of SUMOylation have negative effects on its function and have provided some insight on how influenza viruses are able to interact with the SUMOylation system (Pal, Santos et al. 2011). Therefore, finding viral targets that are not only SUMO targets, but also play a role in the manipulation of the cellular SUMOylation system could lead to potential targets for a new generation of therapeutics.

4.5 Acknowledgements:

I would like to thank Dr. John M. Quarles (Department of Microbial and Molecular Pathogenesis, College of Medicine, Texas A&M Health Sciences Center, College Station, TX) for providing the A/Puerto Rico/8/1934 [H1N1] influenza virus, and Dr. Yoshihiro Kawaoka (Department of Pathobiological Sciences, School of Veterinary Medicine, University of Wisconsin-Madison, Madison, WI) for providing the A/WSN/1933 [H1N1] 12-plasmid reverse genetics system used to develop the WSN/T7T7[NS1~NS2] and WSN/T7T7[NS1K70AK219A~NS2] viruses. I would like to thank Dr. Armando Varela (Department of Biological Sciences, The University of Texas at El Paso, El Paso, TX) for his assistance with the confocal microscope. I would also like to thank Dr. Manuel Llano and Mr. Luis Valdez (Department of Biological Sciences, The University of Texas at El Paso, El Paso, TX) for developing the lentivirus and stably transduced cell lines. This project was funded by grants from the National Institutes of General Medicine Sciences (NIH grant #1SC1AI098976 to GRA) and Border Biomedical Research Center at UTEP (NIH-HIMHD-RCMI grant #8G12MD007592). Katherine A. Meraz was supported by Graduate STEM Fellows in K-12 Education (GK-12) (NSF grant #NSF0947992).

CHAPTER 5: FINAL CONCLUSIONS AND FUTURE DIRECTIONS

5.1 Overview and Final Conclusions:

The focus of the first part of this dissertation was to investigate the relevance of NS1 SUMOylation during influenza A viral infection. Our laboratory has shown that influenza A viral proteins are modified by the cellular SUMOylation system and that the influenza viral protein NS1 protein can trigger an increase in cellular SUMOylation (Pal, Rosas et al. 2010, Pal, Santos et al. 2011, Santos, Pal et al. 2013). Furthermore, we identified K70 and K219 as the two main SUMOylation sites within NS1 (Santos, Pal et al. 2013). Here, we evaluated the effects of mutations affecting NS1 SUMOylation in both a tissue culture and a mouse model of influenza infection. We found that compared to a virus carrying a SUMOylatable NS1 protein, infection with a virus containing a non-SUMOylatable NS1 resulted in the increase of clinical symptoms, morbidity, and mortality. Furthermore, we showed that inhibition of NS1 SUMOylation enabled viral replication in a broad range of organs as well as increase the pathology of influenza viral infection. Previous studies had suggested that NS1 SUMOylation regulated protein stability (Xu, Klenk et al. 2011), however, the enhanced infection with viruses containing a non-SUMOylatable NS1 favor a model in which NS1 SUMOylation regulates NS1's ability to interact with other cellular factors. Overall, our results indicated that a virus carrying a non-SUMOylatable NS1 exhibits increased viral pathogenicity as compared to an otherwise identical virus carrying a SUMOylatable NS1.

In the second part of this dissertation, we evaluated the effect of NS1 SUMOylation and its ability to trigger the increase in cellular SUMOylation. Our studies performed *in vitro,* tissue culture, and in an animal model showed that the ability of NS1 to be SUMOylated correlates to its ability to trigger an increase in cellular SUMOylation. We demonstrated that the global increase in cellular SUMOylation could be recapitulated in primary immune cells and in infected animal tissues. These results indicate that the observed increase is not specific to immortal cell lines and may be relevant for influenza viral infections in animals. Moreover, we show that this increase in cellular SUMOylation is directly related to the ability of NS1 to be SUMOylated. Furthermore, we also observed an increase in cellular SUMOylation during viral infection with vaccinia virus and lymphocytic choriomeningitis virus. Overall, our results indicate that the increase in cellular SUMOylation is not limited to influenza A viral infection, but may be relevant for other viral infections. It is possible that the increase in cellular SUMOylation is responsible for acting as a protection mechanism against viral infection.

It is known that some viruses exploit the cellular SUMOylation system in order to promote viral replication and assembly, or to evade the host immune response (Flotho and Melchior 2013, Mattoscio, Segre et al. 2013). Thus, altering the activity of the cellular SUMOylation system may inhibit viral replication. Our lab previously demonstrated that altering the SUMOylation of NS1, either by increasing it or decreasing it, affects its ability to neutralize the host interferon immune response, but exerts no effect on its stability or localization (Santos, Pal et al. 2013). However, infections with viruses containing NS1‘s that were non-SUMOylatable in animals enhanced viral fitness and

pathogenicity. Therefore, our laboratory has developed an artificial SUMO ligase that has been shown to specifically enhance NS1 SUMOylation during influenza viral infection (Santos, Pal et al. 2013). The function of the $NS1_{1-87}$-Ubc9 artificial SUMO ligase is mediated through NS1's ability to form homodimers. Our data suggests that using the $NS1_{1-87}$-Ubc9 artificial SUMO ligase to enhance the SUMOylation of NS1 may diminish viral fitness and pathogenicity.

Therefore, in the third part of this dissertation, we investigated whether the $NS1_{1-87}$-Ubc9 artificial SUMO ligase could be effectively expressed within cells and be considered as a novel treatment against influenza viral infection. We demonstrated that the $NS1_{1-87}$-Ubc9 artificial SUMO ligase in the purified protein form can be effectively transfected into different cell lines and that it locates to the cytoplasm of transfected cells. In addition, we show that the $NS1_{1-87}$-Ubc9 artificial SUMO ligase can be expressed in lentivirus transduced cells. Our results indicate that the two methods used to deliver the $NS1_{1-87}$-Ubc9 artificial SUMO ligase are effective.

Overall, our results from this dissertation suggest that NS1 SUMOylation may act as a good predictor of viral pathogenicity and that the increase in cellular SUMOylation is triggered to enhance the SUMOylation of cellular factors in order to promote cell proliferation and prevent apoptosis. We believe that use of the $NS1_{1-87}$-Ubc9 artificial SUMO ligase will be an effective treatment against influenza A viral infection by decreasing NS1's ability to antagonize the host immune response.

5.2 Future directions:

In this study, we have characterized the relevance of NS1 SUMOylation on viral infection. However, we have failed to test the relevance of the other influenza viral proteins that are modified by SUMO during influenza viral infection. Further studies would be required to determine the relevance of SUMOylation for the other influenza viral proteins. Furthermore, it would be important to determine the relevance of NS1 SUMOylation in different strains of influenza (i.e. high pathogenic versus low pathogenic).

In studies looking at the increase in cellular SUMOylation, we found that the SUMOylatable NS1 is able to trigger the increase in cellular SUMOylation whereas the non-SUMOylatable NS1 is not. However, it is unknown why this difference exists. It is possible that the non-SUMOylatable NS1 is able to exert its functions through its two putative SIMs. The two SIMs may allow NS1 to function either through a new set of protein-protein interactions or through the activation and regulation of its transcriptional initiation activity allowing for rapid replication in an attempt to overcome the host immune response. SIM deficient viruses (**Table 5.1**) would provide further insight on the relevance of NS1 SUMOylation during viral infection.

In addition, we observed increases in cellular SUMOylation upon infection with vaccinia virus and LCMV. If the increase in cellular SUMOylation is dependent upon the SUMOylation of one of its viral proteins, it would further support the relevance of SUMOylation in viral infections. In addition, it may provide evidence of potential targets for drug development.

The results here provide initial insights into the use of the $NS1_{1-87}$-Ubc9 artificial SUMO ligase as a potential therapeutic against influenza viral infection. In order to validate it as a potential therapeutic against influenza A virus, further studies investigating its ability to decrease viral infection in both tissue culture and an animal model need to be performed.

Table 5.1. Properties of plasmids developed and their modifications

Plasmids	T7T7 tag	Other modifications
1. pcDNA3/Pol2/T7T7[NS1L144AI145A]	Yes	mutations in SIM1
2. pcDNA3/Pol2/T7T7[NS1K70L144AI145AK219A]	Yes	mutations in SIM1; SUMOylation deficient
3. pcDNA3/Pol2/T7T7[NS1V178AV180A]	Yes	mutations in SIM2
4. pcDNA3/Pol2/T7T7[NS1K70AV178AV180AK219A]	Yes	mutations in SIM2; SUMOylation deficient
5. pcDNA3/Pol2/T7T7[NS1L144AI145AV178AV180A]	Yes	mutations in SIM1/SIM2
6. pcDNA3/Pol2/T7T7[NS1K70AL144AI145AV178AV180AK219A]	Yes	mutations in SIM1/SIM2; SUMOylation deficient

REFERENCES

1. Akira, S. and H. Hemmi (2003). "Recognition of pathogen-associated molecular patterns by TLR family." Immunol Lett **85**(2): 85-95.
2. Angel, M., J. B. Kimble, L. Pena, H. Wan and D. R. Perez (2013). "In Vivo Selection of H1N2 Influenza Virus Reassortants in the Ferret Model." J Virol **87**(6): 3277-3283.
3. Arranz, R., R. Coloma, F. J. Chichon, J. J. Conesa, J. L. Carrascosa, J. M. Valpuesta, J. Ortin and J. Martin-Benito (2012). "The structure of native influenza virion ribonucleoproteins." Science **338**(6114): 1634-1637.
4. Backstrom Winquist, E., S. Abdurahman, A. Tranell, S. Lindstrom, S. Tingsborg and S. Schwartz (2012). "Inefficient splicing of segment 7 and 8 mRNAs is an inherent property of influenza virus A/Brevig Mission/1918/1 (H1N1) that causes elevated expression of NS1 protein." Virology **422**(1): 46-58.
5. Baskin, C. R., H. Bielefeldt-Ohmann, T. M. Tumpey, P. J. Sabourin, J. P. Long, A. Garcia-Sastre, A. E. Tolnay, R. Albrecht, J. A. Pyles, P. H. Olson, L. D. Aicher, E. R. Rosenzweig, K. Murali-Krishna, E. A. Clark, M. S. Kotur, J. L. Fornek, S. Proll, R. E. Palermo, C. L. Sabourin and M. G. Katze (2009). "Early and sustained innate immune response defines pathology and death in nonhuman primates infected by highly pathogenic influenza virus." Proc Natl Acad Sci U S A **106**(9): 3455-3460.
6. Begitt, A., M. Droescher, K. P. Knobeloch and U. Vinkemeier (2011). "SUMO conjugation of STAT1 protects cells from hyperresponsiveness to IFNgamma." Blood **118**(4): 1002-1007.

7. Bekes, M. and M. Drag (2012). "Trojan horse strategies used by pathogens to influence the small ubiquitin-like modifier (SUMO) system of host eukaryotic cells." J Innate Immun **4**(2): 159-167.
8. Bennett, R. L., Y. Pan, J. Christian, T. Hui and W. S. May, Jr. (2012). "The RAX/PACT-PKR stress response pathway promotes p53 sumoylation and activation, leading to G(1) arrest." Cell Cycle **11**(2): 407-417.
9. Boddy, M. N., K. Howe, L. D. Etkin, E. Solomon and P. S. Freemont (1996). "PIC 1, a novel ubiquitin-like protein which interacts with the PML component of a multiprotein complex that is disrupted in acute promyelocytic leukaemia." Oncogene **13**(5): 971-982.
10. Boggio, R. and S. Chiocca (2006). "Viruses and sumoylation: recent highlights." Curr Opin Microbiol **9**(4): 430-436.
11. Boggio, R., R. Colombo, R. T. Hay, G. F. Draetta and S. Chiocca (2004). "A mechanism for inhibiting the SUMO pathway." Mol Cell **16**(4): 549-561.
12. Boggio, R., A. Passafaro and S. Chiocca (2007). "Targeting SUMO E1 to ubiquitin ligases: a viral strategy to counteract sumoylation." J Biol Chem **282**(21): 15376-15382.
13. Bornholdt, Z. A. and B. V. Prasad (2008). "X-ray structure of NS1 from a highly pathogenic H5N1 influenza virus." Nature **456**(7224): 985-988.
14. Bosch, F. X., W. Garten, H. D. Klenk and R. Rott (1981). "Proteolytic cleavage of influenza virus hemagglutinins: primary structure of the connecting peptide between HA1 and HA2 determines proteolytic cleavability and pathogenicity of Avian influenza viruses." Virology **113**(2): 725-735.

15. Bosch, F. X., M. Orlich, H. D. Klenk and R. Rott (1979). "The structure of the hemagglutinin, a determinant for the pathogenicity of influenza viruses." Virology **95**(1): 197-207.
16. Braun, L., D. Cannella, A. M. Pinheiro, S. Kieffer, H. Belrhali, J. Garin and M. A. Hakimi (2009). "The small ubiquitin-like modifier (SUMO)-conjugating system of Toxoplasma gondii." Int J Parasitol **39**(1): 81-90.
17. Brincks, E. L., T. A. Kucaba, K. L. Legge and T. S. Griffith (2008). "Influenza-induced expression of functional tumor necrosis factor-related apoptosis-inducing ligand on human peripheral blood mononuclear cells." Hum Immunol **69**(10): 634-646.
18. Brooke, C. B., W. L. Ince, J. Wrammert, R. Ahmed, P. C. Wilson, J. R. Bennink and J. W. Yewdell (2013). "Most influenza a virions fail to express at least one essential viral protein." J Virol **87**(6): 3155-3162.
19. Brown, D. M. (2010). "Cytolytic CD4 cells: Direct mediators in infectious disease and malignancy." Cell Immunol **262**(2): 89-95.
20. Brown, D. M., A. M. Dilzer, D. L. Meents and S. L. Swain (2006). "CD4 T cell-mediated protection from lethal influenza: perforin and antibody-mediated mechanisms give a one-two punch." J Immunol **177**(5): 2888-2898.
21. Brown, D. M., E. Roman and S. L. Swain (2004). "CD4 T cell responses to influenza infection." Semin Immunol **16**(3): 171-177.
22. Chan, C. H., K. L. Lin, Y. Chan, Y. L. Wang, Y. T. Chi, H. L. Tu, H. K. Shieh and W. T. Liu (2006). "Amplification of the entire genome of influenza A virus H1N1 and

H3N2 subtypes by reverse-transcription polymerase chain reaction." J Virol Methods **136**(1-2): 38-43.

23. Chua, M. A., S. Schmid, J. T. Perez, R. A. Langlois and B. R. Tenoever (2013). "Influenza A virus utilizes suboptimal splicing to coordinate the timing of infection." Cell Rep **3**(1): 23-29.

24. Citro, S. and S. Chiocca (2010). "Listeria monocytogenes: a bacterial pathogen to hit on the SUMO pathway." Cell Res **20**(7): 738-740.

25. Das, K., J. M. Aramini, L. C. Ma, R. M. Krug and E. Arnold (2010). "Structures of influenza A proteins and insights into antiviral drug targets." Nat Struct Mol Biol **17**(5): 530-538.

26. de Vries, W., J. Haasnoot, R. Fouchier, P. de Haan and B. Berkhout (2009). "Differential RNA silencing suppression activity of NS1 proteins from different influenza A virus strains." J Gen Virol **90**(Pt 8): 1916-1922.

27. Di Pietro, A., A. Kajaste-Rudnitski, A. Oteiza, L. Nicora, G. J. Towers, N. Mechti and E. Vicenzi (2013). "TRIM22 Inhibits Influenza A Virus Infection by Targeting the Viral Nucleoprotein for Degradation." J Virol.

28. Dias, A., D. Bouvier, T. Crepin, A. A. McCarthy, D. J. Hart, F. Baudin, S. Cusack and R. W. Ruigrok (2009). "The cap-snatching endonuclease of influenza virus polymerase resides in the PA subunit." Nature **458**(7240): 914-918.

29. Djavani, M., J. Rodas, I. S. Lukashevich, D. Horejsh, P. P. Pandolfi, K. L. Borden and M. S. Salvato (2001). "Role of the promyelocytic leukemia protein PML in the interferon sensitivity of lymphocytic choriomeningitis virus." J Virol **75**(13): 6204-6208.

30. Drag, M. and G. S. Salvesen (2008). "DeSUMOylating enzymes--SENPs." IUBMB Life **60**(11): 734-742.

31. Dundon, W. G. and I. Capua (2009). "A Closer Look at the NS1 of Influenza Virus." Viruses **1**(3): 1057-1072.

32. Ehrhardt, C. and S. Ludwig (2009). "A new player in a deadly game: influenza viruses and the PI3K/Akt signalling pathway." Cell Microbiol **11**(6): 863-871.

33. Everett, R. D., C. Boutell and B. G. Hale (2013). "Interplay between viruses and host sumoylation pathways." Nat Rev Microbiol **11**(6): 400-411.

34. Farinelli, G., V. Capo, S. Scaramuzza and A. Aiuti (2014). "Lentiviral vectors for the treatment of primary immunodeficiencies." J Inherit Metab Dis.

35. Fauci, A. S. and F. S. Collins (2012). "Benefits and risks of influenza research: lessons learned." Science **336**(6088): 1522-1523.

36. Flotho, A. and F. Melchior (2013). "Sumoylation: a regulatory protein modification in health and disease." Annu Rev Biochem **82**: 357-385.

37. Furuya, Y., J. Chan, M. Regner, M. Lobigs, A. Koskinen, T. Kok, J. Manavis, P. Li, A. Mullbacher and M. Alsharifi (2010). "Cytotoxic T cells are the predominant players providing cross-protective immunity induced by {gamma}-irradiated influenza A viruses." J Virol **84**(9): 4212-4221.

38. Gannage, M. and C. Munz (2009). "Autophagy in MHC class II presentation of endogenous antigens." Curr Top Microbiol Immunol **335**: 123-140.

39. Garcia-Sastre, A. (2011). "Induction and evasion of type I interferon responses by influenza viruses." Virus Res **162**(1-2): 12-18.

40. Garcia-Sastre, A., R. K. Durbin, H. Zheng, P. Palese, R. Gertner, D. E. Levy and J. E. Durbin (1998). "The role of interferon in influenza virus tissue tropism." J Virol **72**(11): 8550-8558.

41. Garcia-Sastre, A., A. Egorov, D. Matassov, S. Brandt, D. E. Levy, J. E. Durbin, P. Palese and T. Muster (1998). "Influenza A virus lacking the NS1 gene replicates in interferon-deficient systems." Virology **252**(2): 324-330.

42. Garten, W., F. X. Bosch, D. Linder, R. Rott and H. D. Klenk (1981). "Proteolytic activation of the influenza virus hemagglutinin: The structure of the cleavage site and the enzymes involved in cleavage." Virology **115**(2): 361-374.

43. Ge, X., V. Tan, P. L. Bollyky, N. E. Standifer, E. A. James and W. W. Kwok (2010). "Assessment of seasonal influenza A virus-specific CD4 T-cell responses to 2009 pandemic H1N1 swine-origin influenza A virus." J Virol **84**(7): 3312-3319.

44. Geiss-Friedlander, R. and F. Melchior (2007). "Concepts in sumoylation: a decade on." Nat Rev Mol Cell Biol **8**(12): 947-956.

45. Gill, G. (2005). "Something about SUMO inhibits transcription." Curr Opin Genet Dev **15**(5): 536-541.

46. Glass, M. and R. D. Everett (2013). "Components of promyelocytic leukemia nuclear bodies (ND10) act cooperatively to repress herpesvirus infection." J Virol **87**(4): 2174-2185.

47. Gong, L., T. Kamitani, K. Fujise, L. S. Caskey and E. T. Yeh (1997). "Preferential interaction of sentrin with a ubiquitin-conjugating enzyme, Ubc9." J Biol Chem **272**(45): 28198-28201.

48. Gonzalez-Santamaria, J., M. Campagna, M. A. Garcia, L. Marcos-Villar, D. Gonzalez, P. Gallego, F. Lopitz-Otsoa, S. Guerra, M. S. Rodriguez, M. Esteban and C. Rivas (2011). "Regulation of vaccinia virus E3 protein by small ubiquitin-like modifier proteins." J Virol **85**(24): 12890-12900.

49. Gotch, F., J. Rothbard, K. Howland, A. Townsend and A. McMichael (1987). "Cytotoxic T lymphocytes recognize a fragment of influenza virus matrix protein in association with HLA-A2." Nature **326**(6116): 881-882.

50. Goubau, D., S. Deddouche and E. S. C. Reis (2013). "Cytosolic sensing of viruses." Immunity **38**(5): 855-869.

51. Guan, Y., A. Farooqui, H. Zhu, W. Dong, J. Wang and D. J. Kelvin (2013). "H7N9 Incident, immune status, the elderly and a warning of an influenza pandemic." J Infect Dev Ctries **7**(4): 302-307.

52. Hagemeier, S. R., S. J. Dickerson, Q. Meng, X. Yu, J. E. Mertz and S. C. Kenney (2010). "Sumoylation of the Epstein-Barr virus BZLF1 protein inhibits its transcriptional activity and is regulated by the virus-encoded protein kinase." J Virol **84**(9): 4383-4394.

53. Hale, B. G., R. E. Randall, J. Ortin and D. Jackson (2008). "The multifunctional NS1 protein of influenza A viruses." J Gen Virol **89**(Pt 10): 2359-2376.

54. Hale, B. G., J. Steel, R. A. Medina, B. Manicassamy, J. Ye, D. Hickman, R. Hai, M. Schmolke, A. C. Lowen, D. R. Perez and A. Garcia-Sastre (2010). "Inefficient control of host gene expression by the 2009 pandemic H1N1 influenza A virus NS1 protein." J Virol **84**(14): 6909-6922.

55. Hannoun, Z., S. Greenhough, E. Jaffray, R. T. Hay and D. C. Hay (2010). "Post-translational modification by SUMO." Toxicology **278**(3): 288-293.

56. Hatta, Y., K. Hershberger, K. Shinya, S. C. Proll, R. R. Dubielzig, M. Hatta, M. G. Katze, Y. Kawaoka and M. Suresh (2010). "Viral replication rate regulates clinical outcome and CD8 T cell responses during highly pathogenic H5N1 influenza virus infection in mice." PLoS Pathog **6**(10).

57. Hayman, A., S. Comely, A. Lackenby, S. Murphy, J. McCauley, S. Goodbourn and W. Barclay (2006). "Variation in the ability of human influenza A viruses to induce and inhibit the IFN-beta pathway." Virology **347**(1): 52-64.

58. Hecker, C. M., M. Rabiller, K. Haglund, P. Bayer and I. Dikic (2006). "Specification of SUMO1- and SUMO2-interacting motifs." J Biol Chem **281**(23): 16117-16127.

59. Herfst, S., E. J. Schrauwen, M. Linster, S. Chutinimitkul, E. de Wit, V. J. Munster, E. M. Sorrell, T. M. Bestebroer, D. F. Burke, D. J. Smith, G. F. Rimmelzwaan, A. D. Osterhaus and R. A. Fouchier (2012). "Airborne transmission of influenza A/H5N1 virus between ferrets." Science **336**(6088): 1534-1541.

60. Hoffmann, E., J. Stech, Y. Guan, R. G. Webster and D. R. Perez (2001). "Universal primer set for the full-length amplification of all influenza A viruses." Arch Virol **146**(12): 2275-2289.

61. Hui, E. K., E. M. Yap, D. S. An, I. S. Chen and D. P. Nayak (2004). "Inhibition of influenza virus matrix (M1) protein expression and virus replication by U6 promoter-driven and lentivirus-mediated delivery of siRNA." J Gen Virol **85**(Pt 7): 1877-1884.

62. Hwang, J. and R. F. Kalejta (2011). "In vivo analysis of protein sumoylation induced by a viral protein: Detection of HCMV pp71-induced Daxx sumoylation." Methods **55**(2): 160-165.

63. Ibricevic, A., A. Pekosz, M. J. Walter, C. Newby, J. T. Battaile, E. G. Brown, M. J. Holtzman and S. L. Brody (2006). "Influenza virus receptor specificity and cell tropism in mouse and human airway epithelial cells." J Virol **80**(15): 7469-7480.

64. Jackson, D., M. J. Hossain, D. Hickman, D. R. Perez and R. A. Lamb (2008). "A new influenza virus virulence determinant: the NS1 protein four C-terminal residues modulate pathogenicity." Proc Natl Acad Sci U S A **105**(11): 4381-4386.

65. Jiang, T. J., J. Y. Zhang, W. G. Li, Y. X. Xie, X. W. Zhang, Y. Wang, L. Jin, F. S. Wang and M. Zhao (2010). "Preferential loss of Th17 cells is associated with CD4 T cell activation in patients with 2009 pandemic H1N1 swine-origin influenza A infection." Clin Immunol **137**(3): 303-310.

66. Jiang, W., Q. Wang, S. Chen, S. Gao, L. Song, P. Liu and W. Huang (2013). "Influenza A Virus NS1 Induces G0/G1 Cell Cycle Arrest by Inhibiting the Expression and Activity of RhoA Protein." J Virol **87**(6): 3039-3052.

67. Kageyama, T., S. Fujisaki, E. Takashita, H. Xu, S. Yamada, Y. Uchida, G. Neumann, T. Saito, Y. Kawaoka and M. Tashiro (2013). "Genetic analysis of novel avian A(H7N9) influenza viruses isolated from patients in China, February to April 2013." Euro Surveill **18**(15).

68. Kawai, T. and S. Akira (2006). "Innate immune recognition of viral infection." Nat Immunol **7**(2): 131-137.

69. Kawaoka, Y., S. Krauss and R. G. Webster (1989). "Avian-to-human transmission of the PB1 gene of influenza A viruses in the 1957 and 1968 pandemics." J Virol **63**(11): 4603-4608.

70. Kobinger, G. P., I. Meunier, A. Patel, S. Pillet, J. Gren, S. Stebner, A. Leung, J. L. Neufeld, D. Kobasa and V. von Messling (2010). "Assessment of the efficacy of commercially available and candidate vaccines against a pandemic H1N1 2009 virus." J Infect Dis **201**(7): 1000-1006.

71. Kochs, G., A. Garcia-Sastre and L. Martinez-Sobrido (2007). "Multiple anti-interferon actions of the influenza A virus NS1 protein." J Virol **81**(13): 7011-7021.

72. Koudstaal, W., M. H. Koldijk, J. P. Brakenhoff, L. A. Cornelissen, G. J. Weverling, R. H. Friesen and J. Goudsmit (2009). "Pre- and postexposure use of human monoclonal antibody against H5N1 and H1N1 influenza virus in mice: viable alternative to oseltamivir." J Infect Dis **200**(12): 1870-1873.

73. Krug, R. M. (2006). "Virology. Clues to the virulence of H5N1 viruses in humans." Science **311**(5767): 1562-1563.

74. Krug, R. M. and J. M. Aramini (2009). "Emerging antiviral targets for influenza A virus." Trends Pharmacol Sci **30**(6): 269-277.

75. Kubota, T., M. Matsuoka, T. H. Chang, P. Tailor, T. Sasaki, M. Tashiro, A. Kato and K. Ozato (2008). "Virus infection triggers SUMOylation of IRF3 and IRF7, leading to the negative regulation of type I interferon gene expression." J Biol Chem **283**(37): 25660-25670.

76. Kuchipudi, S. V., S. P. Dunham, R. Nelli, G. A. White, V. J. Coward, M. J. Slomka, I. H. Brown and K. C. Chang (2011). "Rapid death of duck cells infected with influenza: a potential mechanism for host resistance to H5N1." Immunol Cell Biol.

77. Kuiken, T., J. van den Brand, D. van Riel, M. Pantin-Jackwood and D. E. Swayne (2010). "Comparative pathology of select agent influenza a virus infections." Vet Pathol **47**(5): 893-914.

78. Kumar, H., T. Kawai and S. Akira (2011). "Pathogen recognition by the innate immune system." Int Rev Immunol **30**(1): 16-34.

79. Kuo, R. L., C. Zhao, M. Malur and R. M. Krug (2010). "Influenza A virus strains that circulate in humans differ in the ability of their NS1 proteins to block the activation of IRF3 and interferon-beta transcription." Virology **408**(2): 146-158.

80. Kurokawa, M., A. H. Koyama, S. Yasuoka and A. Adachi (1999). "Influenza virus overcomes apoptosis by rapid multiplication." Int J Mol Med **3**(5): 527-530.

81. Kwon, J. A. and A. Rich (2005). "Biological function of the vaccinia virus Z-DNA-binding protein E3L: gene transactivation and antiapoptotic activity in HeLa cells." Proc Natl Acad Sci U S A **102**(36): 12759-12764.

82. Lamb, J. R. and N. Green (1983). "Analysis of the antigen specificity of influenza haemagglutinin-immune human T lymphocyte clones: identification of an immunodominant region for T cells." Immunology **50**(4): 659-666.

83. Lapenta, V., P. Chiurazzi, P. van der Spek, A. Pizzuti, F. Hanaoka and C. Brahe (1997). "SMT3A, a human homologue of the S. cerevisiae SMT3 gene, maps

to chromosome 21qter and defines a novel gene family." Genomics **40**(2): 362-366.

84. Le Page, C., P. Genin, M. G. Baines and J. Hiscott (2000). "Interferon activation and innate immunity." Rev Immunogenet **2**(3): 374-386.

85. Leader, B., Q. J. Baca and D. E. Golan (2008). "Protein therapeutics: a summary and pharmacological classification." Nat Rev Drug Discov **7**(1): 21-39.

86. Li, T., R. Santockyte, R. F. Shen, E. Tekle, G. Wang, D. C. Yang and P. B. Chock (2006). "Expression of SUMO-2/3 induced senescence through p53- and pRB-mediated pathways." J Biol Chem **281**(47): 36221-36227.

87. Li, W. X., H. Li, R. Lu, F. Li, M. Dus, P. Atkinson, E. W. Brydon, K. L. Johnson, A. Garcia-Sastre, L. A. Ball, P. Palese and S. W. Ding (2004). "Interferon antagonist proteins of influenza and vaccinia viruses are suppressors of RNA silencing." Proc Natl Acad Sci U S A **101**(5): 1350-1355.

88. Li, X. L., M. Boyanapalli, X. Weihua, D. V. Kalvakolanu and B. A. Hassel (1998). "Induction of interferon synthesis and activation of interferon-stimulated genes by liposomal transfection reagents." J Interferon Cytokine Res **18**(11): 947-952.

89. Li, Y., D. H. Anderson, Q. Liu and Y. Zhou (2008). "Mechanism of influenza A virus NS1 protein interaction with the p85beta, but not the p85alpha, subunit of phosphatidylinositol 3-kinase (PI3K) and up-regulation of PI3K activity." J Biol Chem **283**(34): 23397-23409.

90. Li, Y., Y. Yamakita and R. M. Krug (1998). "Regulation of a nuclear export signal by an adjacent inhibitory sequence: the effector domain of the influenza virus NS1 protein." Proc Natl Acad Sci U S A **95**(9): 4864-4869.

91. Liu, X., Q. Wang, W. Chen and C. Wang (2013). "Dynamic regulation of innate immunity by ubiquitin and ubiquitin-like proteins." Cytokine Growth Factor Rev.

92. Lowen, A. C., S. Mubareka, J. Steel and P. Palese (2007). "Influenza virus transmission is dependent on relative humidity and temperature." PLoS Pathog **3**(10): 1470-1476.

93. Maines, T. R., J. A. Belser, K. M. Gustin, N. van Hoeven, H. Zeng, N. Svitek, V. von Messling, J. M. Katz and T. M. Tumpey (2012). "Local innate immune responses and influenza virus transmission and virulence in ferrets." J Infect Dis **205**(3): 474-485.

94. Man, J. H., H. Y. Li, P. J. Zhang, T. Zhou, K. He, X. Pan, B. Liang, A. L. Li, J. Zhao, W. L. Gong, B. F. Jin, Q. Xia, M. Yu, B. F. Shen and X. M. Zhang (2006). "PIAS3 induction of PRB sumoylation represses PRB transactivation by destabilizing its retention in the nucleus." Nucleic Acids Res **34**(19): 5552-5566.

95. Marq, J. B., S. Hausmann, J. Luban, D. Kolakofsky and D. Garcin (2009). "The double-stranded RNA binding domain of the vaccinia virus E3L protein inhibits both RNA- and DNA-induced activation of interferon beta." J Biol Chem **284**(38): 25471-25478.

96. Masurel, N. (1969). "Serological characteristics of a "new" serotype of influenza A virus: the Hong Kong strain." Bull World Health Organ **41**(3): 461-468.

97. Mattoscio, D., C. V. Segre and S. Chiocca (2013). "Viral manipulation of cellular protein conjugation pathways: The SUMO lesson." World J Virol **2**(2): 79-90.

98. Matunis, M. J., E. Coutavas and G. Blobel (1996). "A novel ubiquitin-like modification modulates the partitioning of the Ran-GTPase-activating protein RanGAP1 between the cytosol and the nuclear pore complex." J Cell Biol **135**(6 Pt 1): 1457-1470.

99. McKay, T., M. Patel, R. J. Pickles, L. G. Johnson and J. C. Olsen (2006). "Influenza M2 envelope protein augments avian influenza hemagglutinin pseudotyping of lentiviral vectors." Gene Ther **13**(8): 715-724.

100. McKinstry, K. K., T. M. Strutt and S. L. Swain (2011). "Hallmarks of CD4 T cell immunity against influenza." J Intern Med **269**(5): 507-518.

101. Merrill, J. C., T. A. Melhuish, M. H. Kagey, S. H. Yang, A. D. Sharrocks and D. Wotton (2010). "A role for non-covalent SUMO interaction motifs in Pc2/CBX4 E3 activity." PLoS One **5**(1): e8794.

102. Meulmeester, E., M. Kunze, H. H. Hsiao, H. Urlaub and F. Melchior (2008). "Mechanism and consequences for paralog-specific sumoylation of ubiquitin-specific protease 25." Mol Cell **30**(5): 610-619.

103. Meunier, I., C. Embury-Hyatt, S. Stebner, M. Gray, N. Bastien, Y. Li, F. Plummer, G. P. Kobinger and V. von Messling (2012). "Virulence differences of closely related pandemic 2009 H1N1 isolates correlate with increased inflammatory responses in ferrets." Virology **422**(1): 125-131.

104.Meunier, I. and V. von Messling (2011). "NS1-mediated delay of type I interferon induction contributes to influenza A virulence in ferrets." J Gen Virol **92**(Pt 7): 1635-1644.

105.Moscona, A. (2009). "Global transmission of oseltamivir-resistant influenza." N Engl J Med **360**(10): 953-956.

106.Mubareka, S., A. C. Lowen, J. Steel, A. L. Coates, A. Garcia-Sastre and P. Palese (2009). "Transmission of influenza virus via aerosols and fomites in the guinea pig model." J Infect Dis **199**(6): 858-865.

107.Nayak, J. L., K. A. Richards, F. A. Chaves and A. J. Sant (2010). "Analyses of the specificity of CD4 T cells during the primary immune response to influenza virus reveals dramatic MHC-linked asymmetries in reactivity to individual viral proteins." Viral Immunol **23**(2): 169-180.

108.Neumann, G., K. Fujii, Y. Kino and Y. Kawaoka (2005). "An improved reverse genetics system for influenza A virus generation and its implications for vaccine production." Proc Natl Acad Sci U S A **102**(46): 16825-16829.

109.Neumann, G. and Y. Kawaoka (2002). "Generation of influenza A virus from cloned cDNAs--historical perspective and outlook for the new millenium." Rev Med Virol **12**(1): 13-30.

110.Neumann, G., T. Noda and Y. Kawaoka (2009). "Emergence and pandemic potential of swine-origin H1N1 influenza virus." Nature **459**(7249): 931-939.

111.Neumann, G., T. Watanabe, H. Ito, S. Watanabe, H. Goto, P. Gao, M. Hughes, D. R. Perez, R. Donis, E. Hoffmann, G. Hobom and Y. Kawaoka (1999).

"Generation of influenza A viruses entirely from cloned cDNAs." Proc Natl Acad Sci U S A **96**(16): 9345-9350.

112.Nicoll, A. and N. Danielsson (2013). "A novel reassortant avian influenza A(H7N9) virus in China - what are the implications for Europe." Euro Surveill **18**(15).

113.Octaviani, C. P., M. Ozawa, S. Yamada, H. Goto and Y. Kawaoka (2010). "High level of genetic compatibility between swine-origin H1N1 and highly pathogenic avian H5N1 influenza viruses." J Virol **84**(20): 10918-10922.

114.Onomoto, K., M. Jogi, J. S. Yoo, R. Narita, S. Morimoto, A. Takemura, S. Sambhara, A. Kawaguchi, S. Osari, K. Nagata, T. Matsumiya, H. Namiki, M. Yoneyama and T. Fujita (2012). "Critical role of an antiviral stress granule containing RIG-I and PKR in viral detection and innate immunity." PLoS One **7**(8): e43031.

115.Ortigoza, M. B., O. Dibben, J. Maamary, L. Martinez-Gil, V. H. Leyva-Grado, P. Abreu, Jr., J. Ayllon, P. Palese and M. L. Shaw (2012). "A novel small molecule inhibitor of influenza A viruses that targets polymerase function and indirectly induces interferon." PLoS Pathog **8**(4): e1002668.

116.Ortiz-Riano, E., B. Y. Cheng, J. C. de la Torre and L. Martinez-Sobrido (2012). "D471G mutation in LCMV-NP affects its ability to self-associate and results in a dominant negative effect in viral RNA synthesis." Viruses **4**(10): 2137-2161.

117.Ozawa, M. and Y. Kawaoka (2011). "Taming influenza viruses." Virus Res **162**(1-2): 8-11.

118.Pal, S., J. M. Rosas and G. Rosas-Acosta (2010). "Identification of the non-structural influenza A viral protein NS1A as a bona fide target of the Small

Ubiquitin-like MOdifier by the use of dicistronic expression constructs." J Virol Methods **163**(2): 498-504.

119.Pal, S., A. Santos, J. M. Rosas, J. Ortiz-Guzman and G. Rosas-Acosta (2011). "Influenza A virus interacts extensively with the cellular SUMOylation system during infection." Virus Res **158**(1-2): 12-27.

120.Pal, S. R., J. M.; Rosas-Acosta, G. (2010). "Identification of the non-structural influenza A viral protein NS1A as a bona fide target of the small ubiquitin-like modifier by the use of dicistronic expression constructs." J Virol Methods **163**(2): 498-504.

121.Palacios, S., L. H. Perez, S. Welsch, S. Schleich, K. Chmielarska, F. Melchior and J. K. Locker (2005). "Quantitative SUMO-1 modification of a vaccinia virus protein is required for its specific localization and prevents its self-association." Mol Biol Cell **16**(6): 2822-2835.

122.Patel, M., A. M. Giddings, J. Sechelski and J. C. Olsen (2013). "High efficiency gene transfer to airways of mice using influenza hemagglutinin pseudotyped lentiviral vectors." J Gene Med **15**(1): 51-62.

123.Pekosz, A., B. He and R. A. Lamb (1999). "Reverse genetics of negative-strand RNA viruses: closing the circle." Proc Natl Acad Sci U S A **96**(16): 8804-8806.

124.Pillet, S., D. Kobasa, I. Meunier, M. Gray, D. Laddy, D. B. Weiner, V. von Messling and G. P. Kobinger (2011). "Cellular immune response in the presence of protective antibody levels correlates with protection against 1918 influenza in ferrets." Vaccine **29**(39): 6793-6801.

125.Ploegh, H. L. (1998). "Viral Strategies of Immune Evasion." Science **280**(5361): 248-253.

126.Prevention, C. f. D. C. a. (2012, July 23, 2012). "Seasonal Influenza (Flu): Influenza Antiviral Drug Resistance." Retrieved March 18, 2013, 2013, from http://www.cdc.gov/flu/about/qa/antiviralresistance.htm.

127.Prevention, C. f. D. C. a. (2013, April 2, 2013). "Influenza A virus subtypes." Retrieved April 24, 2013, 2013, from http://www.cdc.gov/flu/avianflu/influenza-a-virus-subtypes.htm.

128.Rahim, M. N., M. Selman, P. J. Sauder, N. E. Forbes, W. Stecho, W. Xu, M. Lebar, E. G. Brown and K. M. Coombs (2013). "Generation and characterization of a new panel of broadly reactive anti-NS1 mAbs for detection of influenza A virus." J Gen Virol **94**(Pt 3): 593-605.

129.Ran, Z., Y. Chen, H. Shen, X. Xiang, Q. Liu, B. Bawa, W. Qi, L. Zhu, A. Young, J. Richt, W. Ma and F. Li (2013). "In vitro and in vivo replication of influenza A H1N1 WSN33 viruses with different M1 proteins." J Gen Virol **94**(Pt 4): 884-895.

130.Randall, R. E. and S. Goodbourn (2008). "Interferons and viruses: an interplay between induction, signalling, antiviral responses and virus countermeasures." J Gen Virol **89**(Pt 1): 1-47.

131.Ribet, D. and P. Cossart (2010). "Pathogen-mediated posttranslational modifications: A re-emerging field." Cell **143**(5): 694-702.

132.Ribet, D. and P. Cossart (2010). "SUMOylation and bacterial pathogens." Virulence **1**(6): 532-534.

133.Rosas-Acosta, G., M. A. Langereis, A. Deyrieux and V. G. Wilson (2005). "Proteins of the PIAS family enhance the sumoylation of the papillomavirus E1 protein." Virology **331**(1): 190-203.

134.Rossman, J. S. and R. A. Lamb (2009). "Autophagy, apoptosis, and the influenza virus M2 protein." Cell Host Microbe **6**(4): 299-300.

135.Salvatore, M., C. F. Basler, J. P. Parisien, C. M. Horvath, S. Bourmakina, H. Zheng, T. Muster, P. Palese and A. Garcia-Sastre (2002). "Effects of influenza A virus NS1 protein on protein expression: the NS1 protein enhances translation and is not required for shutoff of host protein synthesis." J Virol **76**(3): 1206-1212.

136.Samji, T. (2009). "Influenza A: understanding the viral life cycle." Yale J Biol Med **82**(4): 153-159.

137.Santiago, A., D. Li, L. Y. Zhao, A. Godsey and D. Liao (2013). "p53 SUMOylation promotes its nuclear export by facilitating its release from the nuclear export receptor CRM1." Mol Biol Cell **24**(17): 2739-2752.

138.Santos, A., S. Pal, J. Chacon, K. Meraz, J. Gonzalez, K. Prieto and G. Rosas-Acosta (2013). "SUMOylation affects the interferon blocking activity of the influenza A nonstructural protein NS1 without affecting its stability or cellular localization." J Virol **87**(10): 5602-5620.

139.Sarge, K. D. and O. K. Park-Sarge (2009). "Sumoylation and human disease pathogenesis." Trends Biochem Sci **34**(4): 200-205.

140.Satterly, N., P. L. Tsai, J. van Deursen, D. R. Nussenzveig, Y. Wang, P. A. Faria, A. Levay, D. E. Levy and B. M. Fontoura (2007). "Influenza virus targets the

mRNA export machinery and the nuclear pore complex." Proc Natl Acad Sci U S A **104**(6): 1853-1858.

141. Schoenborn, J. R. and C. B. Wilson (2007). "Regulation of interferon-gamma during innate and adaptive immune responses." Adv Immunol **96**: 41-101.

142. Scholtissek, C., W. Rohde, V. Von Hoyningen and R. Rott (1978). "On the origin of the human influenza virus subtypes H2N2 and H3N2." Virology **87**(1): 13-20.

143. Scull, M. A. and C. M. Rice (2010). "A big role for small RNAs in influenza virus replication." Proc Natl Acad Sci U S A **107**(25): 11153-11154.

144. Selman, M. D., S. K.; Forbes, N. E.; Jia, J. J.; Brown, E. G (2012). "Adaptive mutation in influenza A virus non-structural gene is linked to host switching and induces a novel protein by alternative splicing." EMI **1**(42).

145. Shaw, M. L., K. L. Stone, C. M. Colangelo, E. E. Gulcicek and P. Palese (2008). "Cellular proteins in influenza virus particles." PLoS Pathog **4**(6): e1000085.

146. Shen, Y., X. Wang, L. Guo, Y. Qiu, X. Li, H. Yu, H. Xiang, G. Tong and Z. Ma (2009). "Influenza A virus induces p53 accumulation in a biphasic pattern." Biochem Biophys Res Commun **382**(2): 331-335.

147. Shen, Z., P. E. Pardington-Purtymun, J. C. Comeaux, R. K. Moyzis and D. J. Chen (1996). "UBL1, a human ubiquitin-like protein associating with human RAD51/RAD52 proteins." Genomics **36**(2): 271-279.

148. Skehel, J. J. and D. C. Wiley (2000). "Receptor binding and membrane fusion in virus entry: the influenza hemagglutinin." Annu Rev Biochem **69**: 531-569.

149.Song, J., L. K. Durrin, T. A. Wilkinson, T. G. Krontiris and Y. Chen (2004). "Identification of a SUMO-binding motif that recognizes SUMO-modified proteins." Proc Natl Acad Sci U S A **101**(40): 14373-14378.

150.Song, L., S. Bhattacharya, A. A. Yunus, C. D. Lima and C. Schindler (2006). "Stat1 and SUMO modification." Blood **108**(10): 3237-3244.

151.Soubies, S. M., T. W. Hoffmann, G. Croville, T. Larcher, M. Ledevin, D. Soubieux, P. Quere, J. L. Guerin, D. Marc and R. Volmer (2013). "Deletion of the C-terminal ESEV domain of NS1 does not affect the replication of a low-pathogenic avian influenza virus H7N1 in ducks and chickens." J Gen Virol **94**(Pt 1): 50-58.

152.Steidle, S., L. Martinez-Sobrido, M. Mordstein, S. Lienenklaus, A. Garcia-Sastre, P. Staheli and G. Kochs (2010). "Glycine 184 in nonstructural protein NS1 determines the virulence of influenza A virus strain PR8 without affecting the host interferon response." J Virol **84**(24): 12761-12770.

153.Steinhauer, D. A. S., J. J. (2002). "Genetics of Influenza Viruses." Annu Rev Genet **36**: 305-332.

154.Strutt, T. M., K. K. McKinstry and S. L. Swain (2009). "Functionally diverse subsets in CD4 T cell responses against influenza." J Clin Immunol **29**(2): 145-150.

155.Subbramanian, R. A., S. Basha, R. C. Brady, S. Hazenfeld, M. T. Shata and D. I. Bernstein (2010). "Age-related changes in magnitude and diversity of cross-reactive CD4+ T-cell responses to the novel pandemic H1N1 influenza hemagglutinin." Hum Immunol **71**(10): 957-963.

156.Surls, J., C. Nazarov-Stoica, M. Kehl, S. Casares and T. D. Brumeanu (2010). "Differential effect of CD4+Foxp3+ T-regulatory cells on the B and T helper cell responses to influenza virus vaccination." Vaccine **28**(45): 7319-7330.

157.Swanson, K. A., R. S. Kang, S. D. Stamenova, L. Hicke and I. Radhakrishnan (2003). "Solution structure of Vps27 UIM-ubiquitin complex important for endosomal sorting and receptor downregulation." EMBO J **22**(18): 4597-4606.

158.Talon, J., C. M. Horvath, R. Polley, C. F. Basler, T. Muster, P. Palese and A. Garcia-Sastre (2000). "Activation of interferon regulatory factor 3 is inhibited by the influenza A virus NS1 protein." J Virol **74**(17): 7989-7996.

159.Tang, Y., G. Zhong, L. Zhu, X. Liu, Y. Shan, H. Feng, Z. Bu, H. Chen and C. Wang (2010). "Herc5 attenuates influenza A virus by catalyzing ISGylation of viral NS1 protein." J Immunol **184**(10): 5777-5790.

160.Thomas, M., C. Kranjec, K. Nagasaka, G. Matlashewski and L. Banks (2011). "Analysis of the PDZ binding specificities of Influenza A virus NS1 proteins." Virol J **8**: 25.

161.Tisoncik, J. R., R. Billharz, S. Burmakina, S. E. Belisle, S. C. Proll, M. J. Korth, A. Garcia-Sastre and M. G. Katze (2011). "The NS1 protein of influenza A virus suppresses interferon-regulated activation of antigen-presentation and immune-proteasome pathways." J Gen Virol **92**(Pt 9): 2093-2104.

162.Tscherne, D. M. and A. Garcia-Sastre (2011). "Virulence determinants of pandemic influenza viruses." J Clin Invest **121**(1): 6-13.

163.Valkenburg, S. A., J. A. Rutigliano, A. H. Ellebedy, P. C. Doherty, P. G. Thomas and K. Kedzierska (2011). "Immunity to seasonal and pandemic influenza A viruses." Microbes Infect.

164.Wang, W. and R. M. Krug (1996). "The RNA-binding and effector domains of the viral NS1 protein are conserved to different extents among influenza A and B viruses." Virology **223**(1): 41-50.

165.Wilson, V. G. (2012). "Sumoylation at the Host-Pathogen Interface." Biomolecules **2**(2): 203-227.

166.Wilson, V. G. and D. Rangasamy (2001). "Intracellular targeting of proteins by sumoylation." Exp Cell Res **271**(1): 57-65.

167.Wimmer, P., S. Schreiner and T. Dobner (2012). "Human pathogens and the host cell SUMOylation system." J Virol **86**(2): 642-654.

168.Wu, C. Y., K. S. Jeng and M. M. Lai (2011). "The SUMOylation of matrix protein M1 modulates the assembly and morphogenesis of influenza A virus." J Virol **85**(13): 6618-6628.

169.Wu, Y. C., X. L. Bian, P. R. Heaton, A. F. Deyrieux and V. G. Wilson (2009). "Host cell sumoylation level influences papillomavirus E2 protein stability." Virology **387**(1): 176-183.

170.Wu, Y. C., A. A. Roark, X. L. Bian and V. G. Wilson (2008). "Modification of papillomavirus E2 proteins by the small ubiquitin-like modifier family members (SUMOs)." Virology **378**(2): 329-338.

171.Xu, J., H. A. Zhong, A. Madrahimov, T. Helikar and G. Lu (2013). "Molecular phylogeny and evolutionary dynamics of influenza A nonstructural (NS) gene." Infect Genet Evol.

172.Xu, K., C. Klenk, B. Liu, B. Keiner, J. Cheng, B. J. Zheng, L. Li, Q. Han, C. Wang, T. Li, Z. Chen, Y. Shu, J. Liu, H. D. Klenk and B. Sun (2011). "Modification of nonstructural protein 1 of influenza A virus by SUMO1." J Virol **85**(2): 1086-1098.

173.Xu, L. G., Y. Y. Wang, K. J. Han, L. Y. Li, Z. Zhai and H. B. Shu (2005). "VISA is an adapter protein required for virus-triggered IFN-beta signaling." Mol Cell **19**(6): 727-740.

174.Yang, W., H. Sheng, D. S. Warner and W. Paschen (2008). "Transient global cerebral ischemia induces a massive increase in protein sumoylation." J Cereb Blood Flow Metab **28**(2): 269-279.

175.Yewdell, J. W., J. R. Bennink, G. L. Smith and B. Moss (1985). "Influenza A virus nucleoprotein is a major target antigen for cross-reactive anti-influenza A virus cytotoxic T lymphocytes." Proc Natl Acad Sci U S A **82**(6): 1785-1789.

176.Youil, R., Q. Su, T. J. Toner, C. Szymkowiak, W. S. Kwan, B. Rubin, L. Petrukhin, I. Kiseleva, A. R. Shaw and D. DiStefano (2004). "Comparative study of influenza virus replication in Vero and MDCK cell lines." J Virol Methods **120**(1): 23-31.

APPENDIX A

List of Abbreviations

A549	adenocarcinomic human alveolar basal epithelial cells
ADP	adenosine diphosphate
Akt	protein kinase B; serine/threonine specific protein kinase
ASL	artificial SUMO ligase
ATF	activating transcription factor
ATP	adenosine triphosphate
BM	A/Brevig Mission/1/1918 [H1N1] influenza virus
BMDCs	bone marrow derived dendritic cells
BSA	bovine serum albumin
C57BL/6	mouse inbred strain
CELO	chick embryo lethal orphan
CK2	casein kinase II
CPE	cytopathic effects
CPSF30	cleavage and polyadenylation specificity factor 30 kDa subunit
CRD1	cysteine rich domain 1
Crk	adapter molecule; proto-oncogene
CrkL	adapter molecule; proto-oncogene
cRNA	complementary ribonucleic acid
DAPI	4’,6-diamidino-2-phenylindole
DBA/2J	mouse inbred strain
DMEM	Dulbecco’s modified eagle medium
DNA	deoxyribonucleic acid
dpi	days post-infection

dsDNA	double stranded deoxyribonucleic acid
dsRNA	double stranded ribonucleic acid
EBV	Epstein-Barr virus
ED	effector domain
EDTA	ethylenediaminetetraacetic acid
EF-2	elongation factor 2
eIF2α	eukaryotic initiation factor 2 alpha
env	envelope protein
FBS	fetal bovine serum
FDA	Food and Drug Administration
GAPDH	glyceraldehyde 3-phosphate dehydrogenase
GATA-1	globin transcription factor 1
GST	glutathione S-transferase
GTP	guanosine-5’-triphosphate
GTPase	hydrolase enzymes that act on guanosine triphosphate
H&E	hematoxylin and eosin
HA	hemagglutinin
HCMV	human cytomegalovirus
HDACs	histone deacetylases
HEK	human embryonic kidney cells
HHV6	human herpesvirus 6
HIV-1	human immunodeficiency virus 1
hpi	hours post-infection
HSF1	heat shock transcription factor 1
HSF46	heat shock transcription factor 46
HSV	herpes simplex virus
HTLV-1	human T-lymphotropic virus 1

HTNV	Hantaan river virus
ICP0	infected cell polypeptide 0
IE1	immediate early protein 1
IE2	immediate early protein 2
IFN	interferon
IL	interleukin
IPTG	isopropyl β-D-1-thiogalactopyranoside
IRF1	interferon regulatory factor 1
IRF3	interferon regulatory factor 3
IRF7	interferon regulatory factor 7
JAK	janus kinase
K-bZIP	Kaposi’s sarcoma-associated herpesvirus-basic region-leucine zipper
kDa	kilodalton
KSHV	Kaposi’s sarcoma-associated herpesvirus
LCMV	lymphocytic choriomeningitis virus
LGP2	laboratory of genetics and physiology 2
LLO	listeriolysin O
M1	matrix protein 1
M2	matrix protein 2
MAb	monoclonal antibody
MAPK	mitogen-activated protein kinase
MDA5	melanoma differentiation-associated protein 5
MDCK	Madin-Darby canine kidney cells
Memphis	A/Memphis/31/1998 [H3N2] influenza virus
mRNA	messanger ribonucleic acid
MuLV	Moloney murine leukemia virus

NA	neuraminidase
NBF	neutral phosphate buffered formalin
NF-κB	nuclear factor kappa-light-chain-enhancer of activated B cells
NP	nucleoprotein
NS1	non-structural protein 1
NS2/NEP	non-structural protein 2/nuclear export protein
NXF2	nuclear ribonucleic acid export factor 2
OAS	2’,5’ oligo A synthetase
ORF	open reading frame
PA	polymerase acidic
PAb	polyclonal antibody
PABPI	poly(A) binding protein I
PABPII	poly(A) binding protein II
PAMPs	pathogen-associated molecular patterns
PB1	polymerase basic protein 1
PB2	polymerase basic protein 2
PBS	phosphate buffer solution
PCR	polymerase chain reaction
PDZ	post-synaptic density protein (PSD95); Drosophila disc large tumor suppressor (Dlg-1); zonula occludens-1 protein (zo-1)
PFO	perfringolysin O
PFU	plaque forming units
PI3K	phosphatidylinositol 3-kinase
PIAS	protein inhibitor of activated signal transducer and activator of transcription
PKR	protein kinase R
PLO	pyolysin O

PML NBs	promyelocytic leukemia nuclear bodies
PR8	A/Puerto Rico/8/1934 [H1N1] influenza virus
PRRs	pattern recognition receptors
PV	papillomavirus
RanGAP	Ran GTPase activating protein
RBD	ribonucleic acid binding domain
RdRp	RNA dependent RNA polymerase
rER	rough endoplasmic reticulum
RhoA	Ras homolog gene family, member A
RIG-I	retinoic acid-inducible gene I
RLRs	RIG-I like receptors
RNA	ribonucleic acid
RPMI	Roswell Park Memorial Institute medium
RSAR	RNA-silencing antiviral response
RT-PCR	reverse transcription-polymerase chain reaction
SA	splicing acceptor
SAE1/2	SUMO activating enzyme subunit 1/ subunit 2
SARS	severe acute respiratory syndrome
SARS CoV	severe acute respiratory syndrome coronoavirus
SATB2	special AT-rich sequence-binding protein 2
SD	splicing donor
SDS-PAGE	sodium dodecyl sulfate polyacrylamide gel electrophoresis
SENP	sentrin-specific protease
SEOV	Seoul virus
SH2	Src homology 2 domain
SH3	Src homology 3 domain
SIM	SUMO interacting motif

STAT	signal transducer and activator of transcription
SUMO	small ubiquitin-like modifier
$TCID_{50}$	tissue culture infectious dose
TLRs	toll like receptors
TNFα	tumor necrosis factor alpha
TPCK	L-1-tosylamide-2-phenylethyl chloromethyl ketone
TRAIL	tumor necrosis factor-related apoptosis-inducing ligand
TRIM25	tripartite motif containing 25
TULV	Tula virus
Tween 20	polysorbate 20
UIM	ubiquitin interacting motif
UTR	untranslated region
VERO	African green monkey kidney cell line
vRNA	viral ribonucleic acid
vRNPs	viral ribonuceloproteins
VV	vaccinia virus
WF10	A/Guinea Fowl/Hong Kong/WF10/1999 [H9N2] influenza virus
WSN	A/Wilson Smith Neurotropic/1933 [H1N1] influenza virus
X31	A/Aichi/2/1968 [H3N2] influenza virus
ZJU	A/Zhejiang/DTID/ZJU01/2013 [H7N9] influenza virus

List of Developed Constructs

pPol1/WSN/T7T7NS-PR8	pcDNA3/Pol1/Pol2/T7NS-Brevig Mission
pPol1/WSN/T7T7NS(K70A)-PR8	pcDNA3/Pol1/Pol2/T7NS-Memphis
pPol1/WSN/T7T7NS(K219A)-PR8	pcDNA3/Pol1/Pol2/T7NS-Memphis
pPol1/WSN/T7T7NS(K70AK219A)-PR8	pcDNA3/Pol1/Pol2/T7NS(K227S)-Brevig Mission
pcDNA3/Pol2/NS1(R38AK41A)-Ubc9	pcDNA3/Pol1/Pol2/T7NS-ZJU
pcDNA3/Pol2/NS1(1-87)-Ubc9	pGEX4T1[NS1(R38AK41A)][Ubc9]
pcDNA3Pol1Pol2/NS1(1-87)R38AK41A-Ubc9	pGEX4T1[NS1(R38AK41AK70AK219A)]
pcDNA3PolIPolIIT7T7NS1K219E	pPol1/WSN/T7NS-Brevig Mission
pcDNA3/Pol2/NS1(1-87)(R38AK41A)-Ubc9	pPol1/WSN/T7NS(K227S)-Brevig Mission
pTE1[Adaptor]S1	pPol1/WSN/T7NS-ZJU
pTE1[NS1(1-87)-Ubc9]S1	pPol1/WSN/T7NS-Memphis
pcDNA3/Pol1/Pol2/T7T7NS1(R38AK41A)	pcDNA3/Pol2/T7NS-WSN
pcDNA3/Pol1/Pol2/T7T7NS1(R38AK41AK70AK219A)	pcDNA3/Pol2/T7NS-Memphis
pcDNA3/Pol1/Pol2/NS1(1-87)(R38AK41A)	pcDNA3/Pol2/T7NS-Brevig Mission
pPol1/WSN/PR8[T7T7NS(R38AK41A)]	pcDNA3/Pol2/T7NS(K227S)-Brevig Mission
pPol1/WSN/PR8[T7T7NS(R38AK41A)]-SplAccepMut	pcDNA3/Pol2/T7NS-ZJU
pcDNA3/Pol2/T7T7NS1 (K70AK219A)	pcDNA3/Pol2/T7T7NS-WSN
pcDNA3/Pol2/T7T7NS2	pPol1/WSN/T7T7NS-Brevig Mission
pcDNA3/Pol2/NS1(1-87)-Ubc9	pPol1/WSN/T7T7NS(K227S)-Brevig Mission
pcDNA3/Pol2/NS1(1-87)	pPol1/WSN/T7T7NS-ZJU
pcDNA3/Pol2/NS1(1-87) (R38AK41A)	pPol1/WSN/T7T7NS-Memphis
pcDNA3/Pol2/T7T7NS1 (R38AK41A)	pPol1/WSN/T7T7NS-WSN
pcDNA3/Pol2/T7T7NS1 (R38AK41AK70AK219A)	pPol1/WSN/T7T7NS-WF10
pENTR1a/[PR8 NS]	pPol1/WSN/T7NS-WF10
pENTR1a/[PR8 NS1(K70AK219A)~NS2]	pcDNA3/Pol2/T7NS-WF10
pcDNA5/FRT/TO/Alpha-synuclein(1-57)-HA-Ubc9	pcDNA3/Pol2/T7T7NS-Memphis
pcDNA5/FRT/TO/Alpha-synuclein(58-107)-HA-Ubc9	pcDNA3/Pol2/T7T7NS-Brevig Mission
pcDNA5/FRT/TO/Alpha-synuclein(108-140)-HA-Ubc9	pcDNA3/Pol2/T7T7NS(K227S)-Brevig Mission
pcDNA3/Pol2/T7T7NS1	pcDNA3/Pol2/T7T7NS-ZJU
pPol1/WSN/NS-SplAccptMut	pcDNA3/Pol2/T7T7NS-WF10
pPol1/WSN/T7T7NS(K219E)-PR8	
pPol1/WSN/T7T7NS1(K20AK219E)-PR8	
pPol1/WSN/T7T7NS1(R38AK41A)~EGFP	
pcDNA3/Pol1/Pol2/T7T7NS1(K219R)	
pcDNA3/Pol1/Pol2/BPV-E2(285-365)~Ubc9	
pcDNA5/FRT/TO/HA-Ubc9-HPV-E2(220-365)	
pcDNA3/Pol2/GST-T7NS1	
pcDNA3/Pol1/Pol2/T7NS-WSN	

Formula for Reed-Muench Method

$$I = \left\{ \frac{\text{\% of wells infected at dilution above 50\% - 50\%}}{\text{\% of wells infected at dilution above 50\% - \% wells infected at dilution below}} \right\}$$

$$\text{50\% endpoint titer} = 10^{\text{log total dilution above 50\% - (I x log h)}}$$

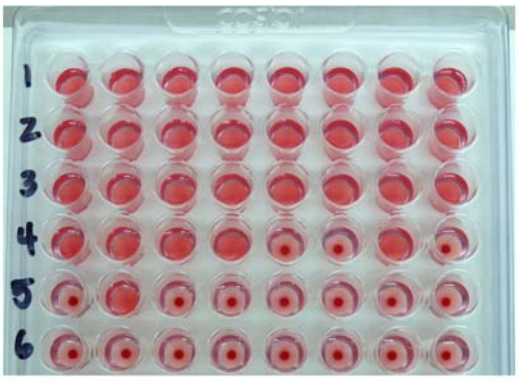

Dilution	10^{-1}	10^{-2}	10^{-3}	10^{-4}	10^{-5}	10^{-6}
Positives	8	8	8	5	1	0
Wells inoculated	8	8	8	8	8	8
% infected	100	100	100	62.5	12.5	0

$$I = [(62.5-50)/(62.5-12.5)] = 0.25$$

$$\text{50\% endpoint titer} = 10^{-4 - (0.25 \times 1)} = 10^{-4.25}$$

$$\text{Titer} = 1.95 \times 10^{5}$$

I = Interpolated value of the 50% endpoint
h = dilution factor

CURRICULUM VITA

Katherine Meraz was born on July 29, 1983 in El Paso, Texas. She graduated from Parkland High School, El Paso, Texas, in the spring of 2001 and entered The University of Texas at El Paso in the fall with the Lucille Stevens and Lawrence E. Baker Scholarships. While pursuing a bachelor's degree in microbiology, she was a member of the Marching Miner Band and participated in Women in Science and Engineering (WiSE). During the summer of 2001, she worked as an undergraduate researcher in the laboratory of Dr. Robert Webb. After receiving her bachelor's of science degree in the fall of 2004, she worked as a technician in the laboratory of Dr. Kyle L. Johnson. In the spring of 2006, Katherine accepted a position as a science teacher at Parkland High School, where she taught for four years and served as department chair for two of those years.

In the fall of 2010, she entered Graduate School at The University of Texas at El Paso (UTEP), El Paso, Texas, to work in the laboratory of Dr. German Rosas-Acosta. Her research has focused on the interaction between influenza A virus and the cellular SUMOylation system. She has worked as a teaching assistant and research assistant in the Department of Biological Sciences. From 2010 to 2011, she taught the General Microbiology laboratories. In the fall of 2012, she was awarded a fellowship from the National Science Foundation Graduate STEM Fellows in K-12 Education Program.

She has presented at the 2012 (poster) and 2013 (oral) American Society for Virology conferences, where both years she was the recipient of graduate travel grants, and at the First Annual Interdisciplinary Symposium: 21st Century Development in

Health Promoting Fields (2013). She has had her research presented at several other conferences, including the Sixth International Conference on SUMO, Ubiquitin, and UBL Proteins: Targets for Human Diseases (2012), Annual Biomedical Research Conference for Minority Students (ABRCMS) (2013), and Campus Office for Undergraduate Research Initiatives (COURI) Symposia (2014).

She has already published one peer-reviewed paper as a co-author and soon will publish at least two articles as first author and two as co-author. After graduation, she hopes to utilize her degree through the development of programs to enrich STEM teaching and learning within the El Paso border region.

Permanent Address: 11037 Wedge Ln.
El Paso, Texas 79934
USA

This dissertation was typed by Katherine Anne Meraz.